

**Double funneling in a mature forest
in coastal British Columbia:
Where does stemflow water go?**

by

Sheena Ann Spencer

B.Sc., Simon Fraser University, 2009

THESIS SUBMITTED IN PARTIAL FULFILLMENT OF THE
REQUIREMENTS FOR THE DEGREE OF
MASTER OF SCIENCE

in the

Department of Geography

Faculty of Environment

© **Sheena Ann Spencer 2012**

SIMON FRASER UNIVERSITY

Fall 2012

All rights reserved.

However, in accordance with the *Copyright Act of Canada*, this work may be reproduced, without authorization, under the conditions for "Fair Dealing." Therefore, limited reproduction of this work for the purposes of private study, research, criticism, review and news reporting is likely to be in accordance with the law, particularly if cited appropriately.

Approval

Name: Sheena A. Spencer
Degree: Master of Science (Geography)
Title of Thesis: *Double funneling in a mature forest in coastal British Columbia: Where does stemflow water go?*

Examining Committee: **Chair:** Dr. Eugene McCann
Associate Professor, Department of Geography
Simon Fraser University

Dr. Ilja van Meerveld
Senior Supervisor
Assistant Professor
Faculty of Earth and Life Sciences
VU University Amsterdam

Dr. Meg Krawchuk
Supervisor
Assistant Professor
Department of Geography
Simon Fraser University

Dr. Mark Johnson
Supervisor
Assistant Professor
Institute for Resources, Environment,
and Sustainability and Department of
Earth and Ocean Sciences
University of British Columbia

Dr. Margaret Schmidt
External Examiner
Associate Professor
Department of Geography
Simon Fraser University

Date Defended/Approved: November 13, 2012

Partial Copyright Licence



The author, whose copyright is declared on the title page of this work, has granted to Simon Fraser University the right to lend this thesis, project or extended essay to users of the Simon Fraser University Library, and to make partial or single copies only for such users or in response to a request from the library of any other university, or other educational institution, on its own behalf or for one of its users.

The author has further granted permission to Simon Fraser University to keep or make a digital copy for use in its circulating collection (currently available to the public at the "Institutional Repository" link of the SFU Library website (www.lib.sfu.ca) at <http://summit/sfu.ca> and, without changing the content, to translate the thesis/project or extended essays, if technically possible, to any medium or format for the purpose of preservation of the digital work.

The author has further agreed that permission for multiple copying of this work for scholarly purposes may be granted by either the author or the Dean of Graduate Studies.

It is understood that copying or publication of this work for financial gain shall not be allowed without the author's written permission.

Permission for public performance, or limited permission for private scholarly use, of any multimedia materials forming part of this work, may have been granted by the author. This information may be found on the separately catalogued multimedia material and in the signed Partial Copyright Licence.

While licensing SFU to permit the above uses, the author retains copyright in the thesis, project or extended essays, including the right to change the work for subsequent purposes, including editing and publishing the work in whole or in part, and licensing other parties, as the author may desire.

The original Partial Copyright Licence attesting to these terms, and signed by this author, may be found in the original bound copy of this work, retained in the Simon Fraser University Archive.

Simon Fraser University Library
Burnaby, British Columbia, Canada

revised Fall 2011

Abstract

Double funneling is the combination of the above ground process of stemflow initiation and the below ground infiltration of this water via macropores around tree roots. It affects soil moisture, nutrient dynamics, groundwater recharge, and plant water uptake. In this study, stemflow and soil moisture were measured and dye tracer experiments were conducted to better understand double funneling in a mature forest in coastal British Columbia, Canada. Stemflow accounted for 1% of gross incident precipitation and increased linearly with precipitation. Funneling ratios depended on tree size. Dye tracer experiments showed that stemflow infiltrated primarily along roots and was found more frequently at depth than at the soil surface. However, both stemflow and throughfall infiltrated to 6–14 cm above the bedrock. The side of the tree along which most of the stemflow flowed, influenced surface soil moisture dynamics around the tree.

Keywords: stemflow; double funneling; preferential flow; dye tracers; soil moisture dynamics; mature coastal forest

*To Grandma and Grandpa:
You are an inspiration to us all.
I love you both.*

Acknowledgements

First, I would like to thank my supervisor, Dr. Ilja van Meerveld, for pushing me when I needed to be pushed and for letting me run wild at times too. Although our coffee chats turned into Skype chats, I am grateful for your support and direction throughout this process.

Thanks to the Malcolm Knapp Research Forest staff, the SFU Geography department staff (in particular B-Jae Kelly and John Ng), and my research assistants (Jenn Melatini, Stephan Zimmermann, Jacquelyn Shrimmer, Penny Spencer, and Ryan Lewis) and all the others I was able to coax into coming to the field with me. Without all of you, this work would not have been possible.

A special thanks to my committee members, Dr. Mark Johnson and Dr. Meg Krawchuk, for their support and feedback on my thesis and to Dr. Nick Hedley for his help in the initial stages of this project. I would also like to thank Dr. Margaret Schmidt for her feedback on my thesis.

I would like to thank Dr. Owen Hertzman for his advice and friendship over the past 6 years. I am not sure if I would be where I am right now if it was not for your encouragement.

I would also like to thank my parents for the constant support and encouragement they have given me through the years and for telling me that there is no limit to what I can accomplish. More specifically, thank you for picking up the phone all the times I called stressed out or in need of a distraction.

I would like to thank my sisters and friends for putting up with me when I was in “hermit mode” and for sticking around through it all. The tea dates, movie nights, and nights out dancing were much needed after the long days spent at school or in the field, as were the countless bottles of wine we shared. Jacquelyn Shrimmer, Maureen Attard, and Ryan Bradley, thank you for keeping me sane in the caves of RCB. Our lunches and coffee

breaks were invaluable in completing my thesis. Chris Williams, thank you for supporting me and for giving me something to look forward to everyday.

Finally, I would like to acknowledge the Natural Sciences and Engineering Research Council of Canada for the Alexander Graham Bell Graduate Scholarship and Simon Fraser University for further financial support.

Table of Contents

| | |
|---|-----------|
| Approval..... | ii |
| Partial Copyright Licence | iii |
| Abstract..... | iv |
| Dedication..... | v |
| Acknowledgements..... | vi |
| Table of Contents..... | viii |
| List of Tables..... | x |
| List of Figures..... | xi |
| | |
| 1. Introduction | 1 |
| 1.1. Study site description | 4 |
| | |
| 2. Stemflow amount and timing in a mature forest in coastal BC | 9 |
| 2.1. Introduction | 9 |
| 2.2. Objectives | 13 |
| 2.2.1. Research questions | 13 |
| 2.2.2. Hypotheses..... | 14 |
| 2.3. Methods | 14 |
| 2.4. Data analysis..... | 19 |
| 2.4.1. Stemflow | 19 |
| 2.4.2. Division of data into events | 20 |
| 2.4.3. Lag times | 20 |
| 2.4.4. Cross correlation..... | 21 |
| 2.5. Results and discussion..... | 21 |
| 2.5.1. Stemflow amount | 21 |
| 2.5.1.1. Stemflow as a function of precipitation..... | 21 |
| 2.5.1.2. Stemflow funneling ratios as a function of tree size | 23 |
| 2.5.1.3. Total stemflow | 30 |
| 2.5.2. Stemflow timing and intensity..... | 32 |
| 2.5.2.1. Time series..... | 32 |
| 2.5.2.2. Start lag time and precipitation lag..... | 37 |
| 2.5.2.3. Centroid lag times..... | 40 |
| 2.5.2.4. Peak stemflow and precipitation intensities..... | 40 |
| 2.6. Conclusion | 42 |
| | |
| 3. Tracing stemflow flowpaths in the soil | 44 |
| 3.1. Introduction | 44 |
| 3.2. Objectives | 47 |
| 3.2.1. Research questions | 47 |
| 3.2.2. Hypotheses..... | 47 |
| 3.3. Methods and analysis..... | 48 |
| 3.4. Results | 52 |
| 3.4.1. Stemflow infiltration experiment 1..... | 52 |
| 3.4.2. Stemflow infiltration experiment 2..... | 52 |
| 3.4.3. Throughfall infiltration excavation | 53 |

| | | |
|-------------|---|------------|
| 3.5. | Discussion..... | 64 |
| 3.5.1. | Stemflow infiltration and flow pathways..... | 64 |
| 3.5.2. | Comparison of throughfall and stemflow infiltration..... | 67 |
| 3.6. | Conclusion..... | 68 |
| 4. | Surface soil moisture around hemlock trees..... | 70 |
| 4.1. | Introduction..... | 70 |
| 4.2. | Objectives..... | 74 |
| 4.2.1. | Research questions..... | 75 |
| 4.2.2. | Hypotheses..... | 75 |
| 4.3. | Methods..... | 75 |
| 4.4. | Analysis..... | 78 |
| 4.4.1. | Stemflow effects on soil moisture patterns..... | 78 |
| 4.4.1.1. | Proximity to tree..... | 78 |
| 4.4.1.2. | Slope effects..... | 78 |
| 4.4.1.3. | Mean difference..... | 78 |
| 4.4.2. | Throughfall effects on soil moisture patterns..... | 79 |
| 4.5. | Results..... | 80 |
| 4.5.1. | Watershed average soil moisture..... | 80 |
| 4.5.2. | Soil moisture patterns around individual trees..... | 80 |
| 4.5.2.1. | Tree 601..... | 80 |
| 4.5.2.2. | Tree 411..... | 81 |
| 4.5.2.3. | Tree 409..... | 82 |
| 4.5.3. | Throughfall effects on soil moisture patterns..... | 88 |
| 4.6. | Discussion..... | 88 |
| 4.6.1. | Stemflow effects on surface soil moisture patterns..... | 88 |
| 4.6.1.1. | Proximity to the tree..... | 88 |
| 4.6.1.2. | Slope effects..... | 89 |
| 4.6.2. | The effects of throughfall patterns on soil moisture..... | 90 |
| 4.7. | Conclusion..... | 92 |
| 5. | Conclusion..... | 94 |
| | References..... | 97 |
| | Appendices..... | 103 |
| Appendix A. | Matlab scripts..... | 104 |
| Appendix B. | Additional stemflow excavation figures..... | 117 |
| Appendix C. | Additional soil moisture figures..... | 121 |

List of Tables

| | |
|--|----|
| Table 2.1: Trees monitored for stemflow. Freezing temperatures and snow resulted in only a few useful events between mid November 2010 and February 2011 for all tipping buckets. For the location of the trees see Figure 2.1. | 17 |
| Table 4.1: Spearman rank correlation coefficient (r_s) for throughfall (TF) and soil moisture (Θ) change, and significance (p value) of the correlation for tree 409. None of the correlations were significant..... | 87 |

List of Figures

| | |
|---|----|
| Figure 1.1: Location of the MKRF. The red star indicates the location of the study site within MKRF..... | 6 |
| Figure 1.2: Distribution of tree species in the study site. Symbol size represents DBH..... | 7 |
| Figure 1.3: Species distribution in the study site; a) all trees, b) trees with a DBH less than 35 cm, c) trees with a DBH greater than or equal to 35 cm. Charts b) and c) do not include dead trees. | 8 |
| Figure 1.4: Monthly average precipitation (mm) and temperature (°C) at Haney, BC. Data from Environment Canada, 2012. | 8 |
| Figure 2.1: Location of trees for which stemflow was measured. Symbol size represents DBH. See Table 2.1 for the details of the measurement period. | 18 |
| Figure 2.2: Stemflow setup with the 19 litre container (Tree 306). | 19 |
| Figure 2.3: Stemflow as a function of precipitation for all trees that were studied. Stemflow volumes were standardized by dividing them by the basal area of the tree. Open symbol = water-collecting container data, closed symbol = tipping bucket data. All regression lines are statistically significant ($p < 0.05$). S = Stemflow (mm), P = Precipitation (mm). The black dashed line depicts change in stemflow axis, in which each group is organized due to tree size from top left to bottom right. For the location of the trees, see Figure 2.1. | 24 |
| Figure 2.4: Funneling ratios (unitless) as a function of event size for all monitored trees. Open symbol = water-collecting container data, closed symbol = tipping bucket data. The grey dashed line represents a funneling ratio of 1 (i.e. stemflow per unit basal area = precipitation). Trees are organized in the same order as Figure 2.3..... | 25 |
| Figure 2.5: Hemlock tree showing stemflow has reached the base of the tree but the stem surface is not entirely wet. Additional precipitation can be used to further fill bark water storage. | 26 |
| Figure 2.6: Funneling ratio (unitless) as a function of DBH (cm) for all species and events. The grey line represents a funneling ratio of 1. Funneling ratios increase with event size for each tree (black arrow indicates this general trend). | 30 |

Figure 2.7: Slopes of the relation between stemflow and precipitation (a in the equation $S=aP-b$; see Figure 2.3) as a function of DBH (cm). The equation of the best fit line is: $a=(6700*DBH)^{-2.35}$, $r^2 = 0.51$, $p = 0.0008$ 31

Figure 2.8: Stemflow (dashed line) and precipitation intensity (solid line) time series for 8 events for tree 403 (cedar; DBH = 31 cm). Optimized lag time is given in the top left corner for events for which the lag-optimized spearman rank correlation coefficient (r_s) was greater than 0.5. Total event precipitation is reported in top right corner. 33

Figure 2.9: Stemflow (dashed line) and precipitation intensity (solid line) time series for 8 events for tree 233 (Douglas fir; DBH = 34 cm). Optimized lag time is given in the top left corner for events for which the lag-optimized spearman rank correlation coefficient (r_s) was greater than 0.5. Total event precipitation is reported in top right corner. 34

Figure 2.10: Stemflow (dashed line) and precipitation intensity (solid line) time series for 8 events for tree 301 (Cedar; DBH = 30 cm). Optimized lag time is given in the top left corner for events for which the lag-optimized spearman rank correlation coefficient (r_s) was greater than 0.5. Total event precipitation is reported in top right corner. Note that this figure shows different events than Figure 2.8 and Figure 2.9. The tipping bucket for tree 301 malfunctioned during the period that measurements were taken at trees 233 and 403. However intensity data was collected for a longer period for this tree so that data is available for more events for this tree. 35

Figure 2.11: Optimized lag time (hours) for all trees monitored with tipping buckets. Upper box boundary = 75th percentile, black line in box = median, dashed black line in box = mean, lower box boundary = 25th percentile. 36

Figure 2.12: a) Start lag time for all trees monitored with tipping buckets. b) Precipitation amount required before stemflow begins. Circles outside boxes = outliers, upper whisker = 95th percentile, upper box boundary = 75th percentile, black line in box = median, dashed black line in box = mean, lower box boundary = 25th percentile, and lower whisker = 5th percentile. 39

Figure 2.13: Centroid lag time for all trees monitored with tipping buckets. Circles outside boxes = outliers, upper whisker = 95th percentile, upper box boundary = 75th percentile, black line in box = median, dashed black line in box = mean, lower box boundary = 25th percentile, and lower whisker = 5th percentile. 40

Figure 2.14: Peak stemflow intensity (mm/hr) as a function of peak precipitation intensity (mm/hr). The dashed line represents the 1:1 line. DBH is given in parentheses. 42

Figure 3.1: Locations of blue dye experiments. Red arrows show the direction in which the excavation occurred in. Stemflow excavation 2 (SIE 2) is oriented in the upslope/ downslope direction in relation to the stream, whereas stemflow excavation 1 (SIE 1) and throughfall excavation (TIE) are oriented perpendicular to the overall watershed slope. SM location = soil moisture measurement location..... 50

Figure 3.2: Large roots obstructed the view and limited the ability to automatically detect the locations of blue pixels. a) and b) are from SIE 1. b) Scale of wooden frame = 1m x 1m. c) is from SIE 2. 51

Figure 3.3: Diagrams drawn in Google Sketch-up for SIE 1. Yellow circles in a and b indicate where stemflow flowed laterally downslope beyond 50 cm from the tree. Red circles in c and d indicate maximum stemflow infiltration depth at 122 cm below the surface. Sites to the west of the tree are indicated by positive distances, while sites to the east of the tree are indicated by negative distances. The tree stem is located at x=0 cm, and indicated by the green arrow. See Appendix B Figure 5.1 for excavation layout..... 54

Figure 3.4: Stemflow water between roots and rocks, as well as along roots deeper into the soil at (a) -10 cm from the tree (scale skewed slightly due to camera angle) and (b) -30 cm from the tree for SIE 1; Frame is 1m x 1m..... 55

Figure 3.5: Percent blue dye as a function of depth and distance from the tree for SIE 1. Sites to the west of the tree are indicated by positive distances, while sites to the east of the tree are indicated by negative distances. The tree stem is located at x=0 m. The width of the excavation was 160 cm, except for excavations east of the tree (-10 cm, -20 cm, and -30 cm), for which the width was 140 cm, 120 cm, and 90 cm, respectively..... 56

Figure 3.6: Diagrams drawn in Google Sketch-up for SIE 2. Green arrow indicates tree location. Stemflow was confined within 60 cm of the tree. Flow generally occurred around tree roots and rocks. The red circle in e indicates the maximum stemflow infiltration depth at 77 cm. A negative distance represents an excavation profile on the east side of the tree. See Appendix B Figure 5.2 for excavation layout..... 57

Figure 3.7: Percent blue dye as a function of depth and distance from the tree for SIE 2. Sites to the west of the tree are indicated by positive distances, while sites to the east of the tree are indicated by negative distances. The tree stem is located at x=0 m. The width of the excavation was 200 cm, except for excavations on the east side of the tree (negative distances), for which the width was 100 cm. 58

Figure 3.8: Stemflow infiltrated along roots for SIE 2. Dye present in organic surface layer and along roots to depth. Scale of frame is 1 m x 0.3 m. 59

| | |
|---|----|
| Figure 3.9: Blue dye stains inside a decaying root (SIE 2). Stemflow water flowed laterally through the decaying root. | 59 |
| Figure 3.10: Stemflow water flows along roots and into the soil matrix along fine roots, or through the soil matrix in SIE 2. Orange box in (a) is zoomed in for (b). Yellow circles highlight light blue staining. | 60 |
| Figure 3.11: Throughfall infiltrated through the soil matrix and decreased steadily. See Appendix B Figure 5.3 for excavation layout. | 61 |
| Figure 3.12: Percent blue dye as a function of depth for TIE. Profile 1 is located the furthest upslope, while profile 6 is located the furthest downslope. The width of the excavation was 90 cm. | 62 |
| Figure 3.13: Lateral flow at 40 cm depth (at the yellow arrow) in TIE, profile 6. Scale distorted vertically. | 63 |
| Figure 3.14: a) Flow along a decayed root in profile 5 of the TIE, where the maximum infiltration occurred at 85 cm (outlined in orange). Scale distorted vertically. b) Close up of infiltration through decayed root and fine roots, into matrix below. | 63 |
| Figure 3.15: Decayed tree, active roots, and rocks directing vertical flow, TIE profile 2. | 64 |
| Figure 4.1: Soil moisture measurement locations. Tree trunks are indicated by green circles and are scaled by their DBH. UT = upslope transect; DWT = transect downslope in the watershed direction; DST = transect downslope towards the stream. Only the soil moisture measurements in the lower part of the watershed are shown (n = 16). | 77 |
| Figure 4.2: The mean difference for soil moisture (%) around tree 411 plotted as a function of rank. The error bar represents the standard deviation of the difference. Locations with a mean +/- one standard deviation above or below the mean were identified as “consistently wet” or “consistently dry”, respectively. | 79 |
| Figure 4.3: Average soil moisture below the trees compared to mean soil moisture in the lower watershed (n = 27). | 83 |
| Figure 4.4: Standard deviation of soil moisture as a function of average soil moisture for all trees and the lower watershed (n = 27). | 83 |
| Figure 4.5: Average soil moisture near the tree and away from the tree for each tree as a function of time. Blue solid line = soil moisture points within 60 cm of the tree. Red dashed line = soil moisture points more than 60 cm from the tree. Grey line = the difference between average soil moisture near the tree and away from the tree. * = statistically significant differences. | 84 |

| | |
|--|-----|
| Figure 4.6: Time series of precipitation and average soil moisture for each tree by slope position. (Statistically significant differences: * = for DWT; x = for DST; ● = for UT1/DT1; ○ = for UT2 and DT2) | 85 |
| Figure 4.7: Spatial patterns in soil moisture (circles) and throughfall (triangles) patterns for the 3 trees. Red circles (triangles) are locations where the mean difference plus one standard deviation was below zero, and are thus considered dry locations. Blue circles (triangles) are locations where the mean difference minus one standard deviation was above zero, and are thus considered wet locations. Green circles (triangles) are locations with soil moisture/throughfall around the mean. | 86 |
| Figure 5.1: Layout of stemflow infiltration experiment 1. Grid on soil profile = 10 cm x 10 cm. Width of excavation is 3 m. | 117 |
| Figure 5.2: Layout of stemflow infiltration experiment 2. Width of excavation is 3 m. | 117 |
| Figure 5.3: Layout of throughfall infiltration experiment. Width of excavation is 0.9 m. | 118 |
| Figure 5.4: Stemflow infiltrating along the large root, in a loose organic layer in SIE 2..... | 118 |
| Figure 5.5: Lateral flow along the confining clay layer (yellow arrows) in SIE 1. | 119 |
| Figure 5.6: Confined roots in SIE 2. (note: scale is distorted to right side of photo) | 119 |
| Figure 5.7: Fine roots in blue dye patches in TIE..... | 120 |
| Figure 5.8: Median soil moisture for each tree as a function of time. Blue solid line = soil moisture points within 60 cm of the tree. Red dashed line = soil moisture points more than 60 cm from the tree..... | 122 |
| Figure 5.9: Time series of median soil moisture for each tree by slope location. For tree 601, solid blue line is for most upslope oriented transect (UT1) and solid red line is for the most downslope oriented transect (DT1). | 123 |

1. Introduction

Precipitation is intercepted by the tree canopy and either evaporated, transmitted to the soil as throughfall, or transmitted to the base of the tree as stemflow. Stemflow was initially assumed to be insignificant in the forest water balance; however, it has now been shown that stemflow is often underestimated (Germer et al., 2010) and can contribute up to 20% of gross incident precipitation in some forests (Levia and Frost, 2003; Johnson and Lehmann, 2006). Although stemflow has received more attention in the recent decades, the double funneling by trees has received considerably less attention. Double funneling is the combination of the above ground process of stemflow initiation and the below ground process of infiltration of stemflow water via macropores around roots (Johnson and Lehmann, 2006). Macropores around tree roots allow stemflow water to infiltrate deeper and faster into the soil (Johnson and Lehmann, 2006; Liang et al., 2007; 2011).

Several studies have been conducted to determine the stemflow characteristics for a range of tree species (Levia and Frost, 2003). They have shown that stemflow must wet and exceed the surface water-holding capacity of leaves, branches and the stem before it can travel down the stem and reach the ground (Cape et al., 1991; Aboal et al., 1999; Germer et al., 2010). Aboal et al. (1999) showed for trees in a laurel forest on Tenerife that on average 2 mm of precipitation is required to wet the tree surfaces before stemflow occurs. After this initial wetting, stemflow increases linearly with precipitation (Levia and Frost, 2003; Johnson and Lehmann, 2006). Li et al. (2008) showed that for desert shrubs stemflow decreased when precipitation intensity was greater than 2

mm/hr. Levia et al. (2010) also showed for an American beech (*Fagus grandifolia*)-yellow poplar (*Liriodendron tulipifera*) forest that funneling ratios, which describe how much precipitation is concentrated as stemflow, decreased with increasing 5-minute precipitation intensity and suggested that this was due to the conversion of stemflow to throughfall via canopy drip. The amount of stemflow and how much drips off branches and leaves or remains on branches and stems depends on plant morphology, specifically leaf and branch morphology, branch angle, bark texture and the resulting bark water storage capacity (Voigt, 1960; Levia and Frost, 2003; Johnson and Lehmann, 2006; Levia et al., 2010). As a result, stemflow varies between and within species (Levia and Frost, 2003). However, it has also been shown that tree size can cause significant variation in the amount of stemflow (Germer et al., 2010).

Stemflow as a point source of water and solutes to the forest floor has important implications for groundwater recharge (Taniguchi et al., 1996), soil pH, soil nutrient status (Chang and Matzner, 2000; Hamden and Schmidt, 2012), and soil moisture dynamics (Li et al., 2008; Liang et al., 2011). Taniguchi et al. (1996), for example, studied stemflow in pine (*Pinus densiflora*) forests and found that although stemflow did not contribute a large volume of water to the forest floor, it contributed to a relatively large amount of groundwater recharge. Liang et al. (2011) compared soil moisture dynamics when stemflow occurred and when stemflow was removed from the system and found that stemflow increased soil moisture downslope of the base of a tree immediately after a storm. This can cause a localized saturated zone that is not present further away from the tree, where throughfall water infiltrates at the soil surface (Liang et al., 2011).

Often associated with the concentrated point source of precipitation is a micro-site of higher nutrient concentrations and lower pH (Gersper and Holowaychuk, 1971;

Chang and Matzner, 2000). Chang and Matzner (2000), for example, found that stemflow is enriched in nutrients and ions (especially H^+ , K^+ , and SO_4^{2-}) compared to throughfall and causes a localized pocket of acidic soils. Forest soil nutrient studies often obtain soil samples from the surface layers and relate results to stemflow, throughfall, evapotranspiration, and litter and bark fall patterns (Zinke, 1962; Gersper and Holowaychuk, 1971; Chang and Matzner, 2000; Hamden and Schmidt, 2012). Further studies are needed to determine if stemflow significantly influences surface soil moisture, and resultant soil chemistry, and does not mainly affect soil moisture at depth as the double funneling process suggests and other studies have shown (Gonzalez-Hidalgo and Bellot, 1997; Johnson and Lehmann, 2006; Li et al., 2009; Liang et al., 2011).

Previous studies have inferred stemflow water uptake by plants by determining the average rooting depth of active roots and the average depth of bypass flow. Chang and Matzner (2000) suggested that plants do not utilize stemflow because the majority of it bypasses the active roots. However, Li et al. (2009) showed that stemflow water primarily infiltrated around roots of a desert shrub with little interaction with the soil matrix, and was able to infiltrate deeper into the soil than throughfall. They therefore suggested stemflow is a moisture resource that is available for plant water uptake during dry periods when other soil moisture is not abundant.

The aim of this study was to examine the double funneling of stemflow to determine 1) how much stemflow occurs in a mature Western hemlock (*Tsuga heterophylla*)-Western red cedar (*Thuja plicata*) forest in British Columbia (BC), and 2) if it influences flow pathways and soil moisture dynamics around trees. It is important to gain a better understanding of stemflow and preferential flow from stemflow as it allows for a better understanding and conceptualization of subsurface flow pathways of water in

forest soils. This understanding of flow pathways can in turn improve our ecohydrological models and models for solute and contaminant transport in forested watersheds.

For this thesis, double funneling was separated into 3 parts: stemflow, infiltration of stemflow, and soil moisture dynamics. Chapter 2 focuses on the above ground processes involved in the double funneling process. Stemflow was measured in the Malcolm Knapp Research Forest (BC) to determine the amount of stemflow and the funneling ratios for this coastal forest, and how they vary between species, with tree size, and with precipitation amount. Peak stemflow intensity and stemflow timing were also examined in relation to peak precipitation intensity and precipitation timing. Chapter 3 focuses on the below ground distribution of stemflow water. Blue dye was applied to two hemlock trees and the soil surrounding the trees was subsequently excavated to determine where stemflow water goes once it reaches the ground. Flow pathways and infiltration depths were compared to a throughfall plot, where blue dye was applied to the surface of the soil. Chapter 4 links stemflow with surface soil moisture dynamics around three hemlock trees. Soil moisture was measured in the top 20 cm of the soil around the trees to determine if stemflow influences surface soil moisture dynamics.

1.1. Study site description

The study site is located in the Malcolm Knapp Research Forest (MKRF), approximately 60 km east of Vancouver, British Columbia (49°17'N, 122°36'W; Figure 1.1). The MKRF is located within the Coastal Western Hemlock biogeoclimatic zone. Annual precipitation ranges from approximately 2200 mm at the southern end to 3000 mm at the northern end of the research forest (MKRF, 2010a). The 0.9 ha study site is located near the middle of the MKRF at approximately 400 m above sea level. Soils are

Ferro-humic Podzols and Brunisols on glacial till and granodiorite bedrock (Chin, 2009; Wang et al., 2002) with an average soil depth less than a meter.

The study site was logged in the 1920's and burnt by a large forest fire in 1931. The forest was left to regenerate naturally; thus, the current forest is approximately 80 years old (MKRF, 2010b). The forest is a mixed species stand with approximately 550 trees per hectare and a total basal area of 51 m²/ha (Figure 1.2). Western red cedar (*Thuja plicata*; 41% of trees) and Western hemlock (*Tsuga heterophylla*; 40% of trees) are the primary tree species, although birch (*Betulaceae*), Douglas fir (*Pseudotsuga menziesii*) and vine maple (*Acer circinatum*) are also present in the study site (7%, 6%, and 3% of trees, respectively; Figure 1.3). Average (and median) diameter at breast height (DBH) per species is 31 cm (27 cm), 30 cm (30 cm), 22 cm (19 cm), 38 cm (32 cm), and 5 cm (5 cm) for cedar, hemlock, birch, Douglas fir, and maple, respectively (Figure 1.2).

Monthly total precipitation and average temperature during the study period (January 2010 to December 2011) at the MKRF weather station (Haney UBC RF Admin) at approximately 150 m above sea level are shown in Figure 1.4. July 2010 was an unusually dry month, with less than 1 mm of precipitation. Gross precipitation for 2010 and 2011 was 2035 mm and 1989 mm, respectively; the long term average precipitation was 2194 mm. A previous study at this site of 53 events from September 2007 to May 2009 showed that the average interception loss was 15% of the gross precipitation (Chin, 2009). Interception varied with precipitation amount, such that more interception occurred for smaller precipitation events (<20 mm) (Chin, 2009). Assuming an average interception loss of 15 %, net precipitation in 2010 and 2011 was 1729 mm and 1691 mm, respectively.

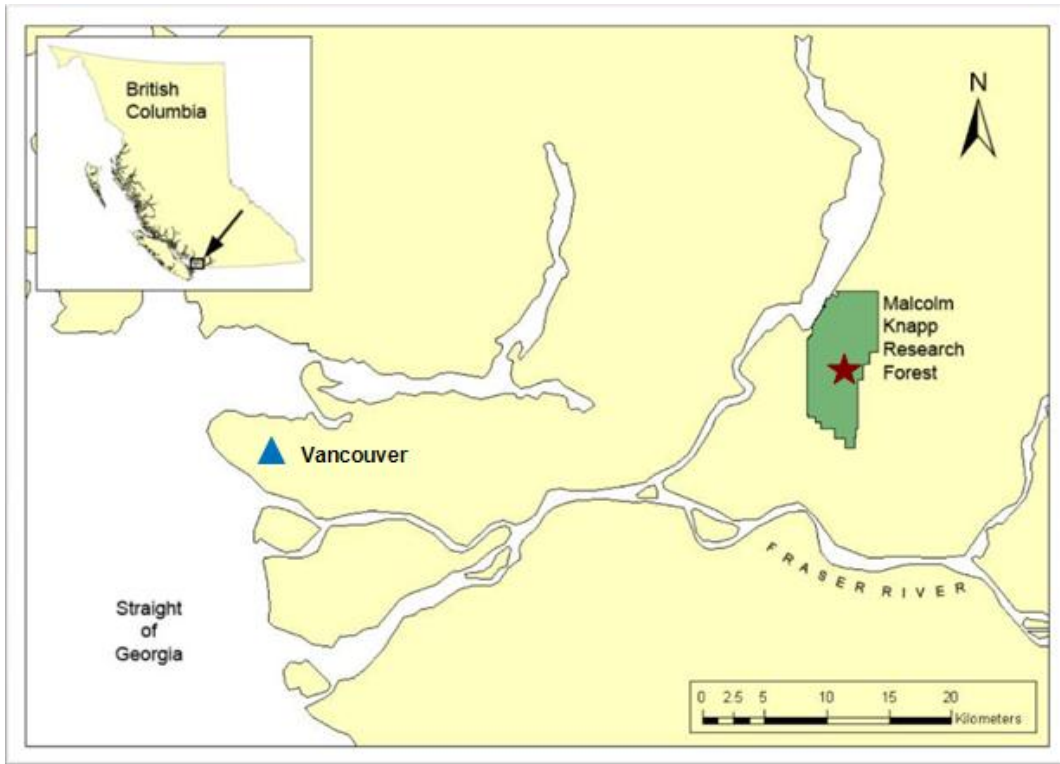


Figure 1.1: Location of the MKRF. The red star indicates the location of the study site within MKRF.

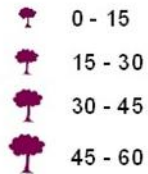
Legend

Tree Species and DBH (cm2)

Cedar



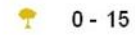
Birch



Douglas Fir



Maple



Hemlock



— Stream

Contour interval = 2 m

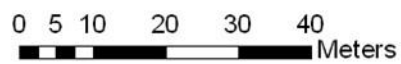


Figure 1.2: Distribution of tree species in the study site. Symbol size represents DBH.

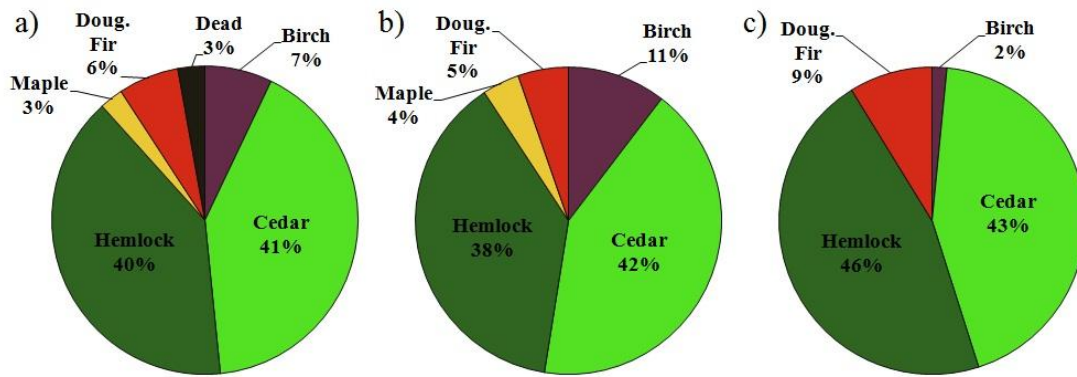


Figure 1.3: Species distribution in the study site; a) all trees, b) trees with a DBH less than 35 cm, c) trees with a DBH greater than or equal to 35 cm. Charts b) and c) do not include dead trees.

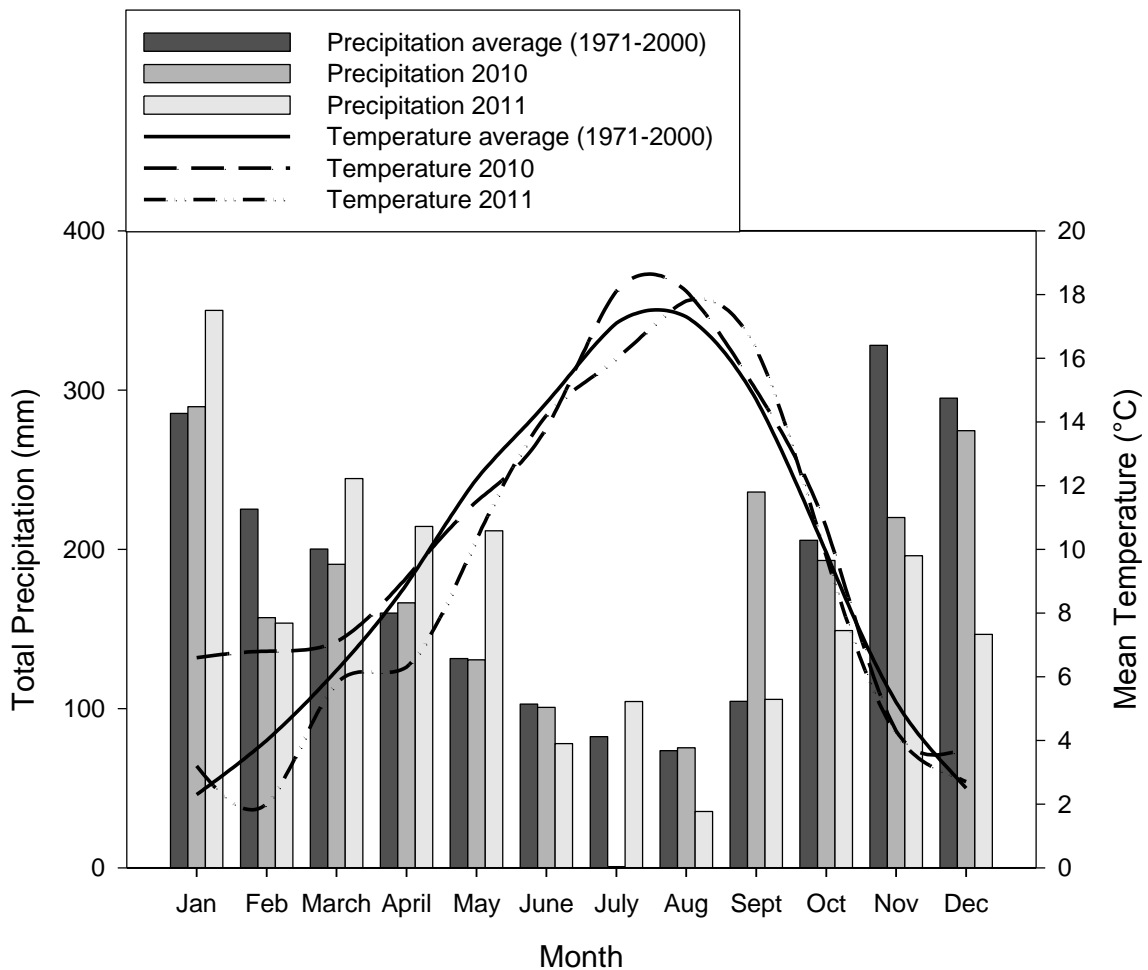


Figure 1.4: Monthly average precipitation (mm) and temperature (°C) at Haney, BC. Data from Environment Canada, 2012.

2. Stemflow amount and timing in a mature forest in coastal BC

2.1. Introduction

Stemflow is the portion of precipitation that falls on the forest canopy and flows down tree branches and stems to the forest soil at the base of trees (Johnson and Lehmann, 2006). Previous studies have shown the importance of stemflow for nutrient cycling, groundwater recharge, and plant water uptake (Chang and Matzner, 2000; Liang et al., 2007; and Li et al., 2008). Stemflow ranges from less than 1% to 20% of gross incident precipitation (GIP) for forests (Levia and Frost, 2003; Johnson and Lehmann, 2006), and can be up to 45% of GIP for some desert shrubs (Levia and Frost, 2003). Stemflow in tropical forests is mainly funnelled by palms and small trees (5 – 10 cm DBH) and often underestimated (Germer et al., 2010). Few studies on stemflow have been conducted in mature temperate coniferous forests on the west coast of the USA and Canada. Those that have been conducted show that only a small amount of stemflow is transmitted by those trees (Chin, 2009).

Although stemflow is usually only a small fraction of the total amount of precipitation reaching the forest floor, it can influence soil moisture and nutrient dynamics around the base of a tree and contribute to a disproportionately large amount of groundwater recharge (Taniguchi et al., 1996; Chang and Matzner, 2000; Liang et al., 2007). Stemflow can increase soil moisture at the base of a tree and macropores around roots can allow stemflow water to infiltrate deep into the soil (Liang et al., 2011). This can result in a saturated zone around the tree that is not present further away from the tree,

where water infiltrates from the surface of the soil (Liang et al., 2007; 2009b; 2011). For Japanese red pine (*Pinus densiflora*), stemflow was only 0.5 – 1.2% of net precipitation, whereas the ratio of recharge from stemflow to total recharge was 10.9 – 19.1% (Taniguchi et al., 1996). Li et al. (2008) suggest that this deeper infiltrated stemflow water also provides a soil moisture resource that is available for plant water uptake when other moisture is not available. Understanding the amount and timing of stemflow is thus important for understanding soil moisture dynamics and water availability in forests (Liang et al., 2007; Li et al., 2008).

Associated with the concentrated point source of stemflow water is a micro-site of higher concentrations of nutrients and a localized pocket of acidic soils because stemflow water has a different chemical composition and pH than precipitation due to contact and exchange with the bark and leaf surfaces (Gersper and Holowaychuk, 1971; Mahendrappa, 1974; Chang and Matzner, 2000). Nutrients and ions accumulate on tree surfaces by dry deposition and are carried with the stemflow water to the soil surface (Johnson and Lehmann, 2006). As distance from the tree increases, the effects of the point source of nutrients and hydrogen ions become weaker and soil chemistry is more similar to that influenced by direct precipitation and throughfall (Gersper and Holowaychuk, 1971; Chang and Matzner, 2000; Levia and Frost, 2003). Nikodem et al. (2010) showed in their simulation models that when a large volume of stemflow water is delivered to the soil, toxic elements can be transported deep into the soil and to groundwater. For example, aluminium can react with other chemicals in the soil and become toxic.

The amount of precipitation that reaches the soil as stemflow varies greatly, depending on factors such as plant morphology, precipitation intensity and duration, and wind direction (Levia and Frost, 2003; Johnson and Lehmann, 2006). Plant morphology,

especially, is an important factor because it determines the initial capture of precipitation. Before stemflow can travel down the stem, it must wet the surface of the leaves, branches, and stem and exceed their surface water-holding capacity (Cape et al., 1991; Aboal et al., 1999; Crockford and Richardson, 2000; Germer et al., 2010). Leaf and branch morphology, branch angle, and bark texture determine how much water remains on the surfaces of branches and stems before stemflow occurs and how much drips off (Levia and Frost, 2003; Johnson and Lehmann, 2006; Li et al., 2008). Aboal et al. (1999) showed for a laurel forest in Tenerife, Canary Islands that trees required on average 2 mm of precipitation to wet the tree surfaces before stemflow was transmitted to the soil. Germer et al. (2010) showed for a tropical forest that initial precipitation intensity and the duration of the dry period prior to an event affect how much precipitation is required before the onset of stemflow.

Stemflow varies between and within species (Levia and Frost, 2003). Variations in stemflow have been attributed to differences in canopy structure, bark water capacity, precipitation amount and intensity (Li et al., 2008), diameter at breast height (DBH), crown projection area, epiphyte cover, and tree species (Oyarzun et al., 2010). Voigt (1960) and Levia et al. (2010) showed that species variation in stemflow was largely due to bark texture and the resulting bark water storage capacity, where more stemflow is lost from rougher bark trees due to a higher bark water storage capacity. Conversely, Germer et al. (2010) showed that tree size caused variation between species. Stemflow depths were especially high in aborescent palms (*Orbignya phalerata*) and small trees and if these size classes were ignored, stemflow as a percent of GIP would have been underestimated by 6% (2% GIP instead of 8% GIP; Germer et al., 2010). Levia et al. (2010) also showed that within species variation was largely due to tree size and differences in bark water storage capacity. For American beech (*Fagus grandifolia*),

larger trees funnelled more stemflow than smaller trees. For yellow poplar (*Liriodendron tulipifera*), the trend depended on storm size; for small events the larger poplar trees were able to funnel more stemflow than smaller poplar trees (Levia et al., 2010). Thus, it is important to study multiple trees of each tree species within a forest to gain an accurate representation of the variation in stemflow and to be able to scale up the measurements to the watershed (Li et al., 2008).

Some studies suggest that stemflow varies between seasons (leaf-on and leaf-off periods) (Neal et al., 1993; Levia and Frost, 2003). Stemflow is thought to be less in summer than in winter because of increased evaporation and because less of the tree bark is wetted directly by precipitation due to the denser canopy (Neal et al., 1993). However, results from Cape et al. (1991) suggested that stemflow from some tree species (e.g. coniferous trees) does not vary seasonally due to a lack of significant changes in canopy characteristics but, instead, was related to seasonal variation in precipitation intensity.

Precipitation amount and intensity determine the amount of stemflow that occurs. After initial wetting, stemflow generally increases linearly with increasing precipitation (Manfroi et al., 2004; Li et al., 2008). Xiao et al. (2000) showed that when precipitation was less than 1 mm per event, there was no stemflow from a pear tree (*Pyrus calleryana*) unless the tree was already wet from earlier storms. Aboal et al. (1999) showed that the amount of precipitation required to wet tree surfaces in laurel forests on the Canary Islands was different for each species. Higher precipitation intensities resulted in larger amounts of stemflow (Van Elewijck, 1989; Aboal et al., 1999). Li et al. (2008) showed for three semiarid shrubs, that stemflow increased with precipitation intensity up to an intensity of 2 mm/hr, after which stemflow decreased with increased precipitation intensity. This was supported by Levia et al. (2010) who showed that

stemflow funneling ratios decreased as the 5-minute precipitation intensity increased. Levia et al. (2010) suggested that this is due to the conversion of stemflow to drip and throughfall when stemflow pathways are exceeded.

Although stemflow has been shown to vary with DBH, canopy crown projection area, and other factors (Ford and Deans, 1978; Oyarzun et al., 2010), wind may affect this relation when precipitation does not fall directly on the forest canopy (Van Stan II et al., 2011). Precipitation can be intercepted by the tree stem or neighbouring trees, causing increased or decreased interception per crown area (Van Stan II et al., 2011). Wind-blown precipitation can be caught or blown onto the side of tree stems, which would decrease the distance stemflow needs to travel and bypass potential dripping nodes, thus increasing stemflow (Crockford and Richardson, 2000). Wind speed also influences stemflow because it reduces the water-holding capacity of the canopy due to leaf fluttering, which increases canopy drip and decreases the amount of stemflow (Herwitz and Slye, 1995; Xiao et al., 2000).

2.2. Objectives

The objective of this study was to expand our knowledge on stemflow amount and timing in a mature coastal British Columbia forest. In order to do this, stemflow volumes and intensities were measured and compared to precipitation volumes and intensities.

2.2.1. Research questions

- 1) How much stemflow occurs along various tree species in a mature forest in coastal British Columbia?
- 2) How does stemflow amount vary between species?

- 3) How does stemflow vary with tree size for the same species?
- 4) How does total precipitation (event size) affect stemflow volume?
- 5) How does stemflow intensity vary with precipitation intensity?
- 6) What is the lag time between the start of precipitation and the start of stemflow?

2.2.2. Hypotheses

Given the outcomes of previous studies, I hypothesized that Western hemlock, Western red cedar, and Douglas fir trees would likely not transmit large amounts of stemflow or have large funneling ratios due to the large branch angles and their needle morphology, whereas birch trees would transmit more stemflow and have larger funneling ratios due to more inclined branches and larger leaf area. Tree species with smoother bark would transmit more stemflow because less water would be lost to bark storage, which would also result in a faster onset of stemflow. Within species, larger trees would transmit more stemflow than smaller trees because they have a larger collecting area. Stemflow would increase with precipitation amount. I also hypothesized that stemflow intensity would increase with precipitation intensity. Precipitation intensities that occur in coastal BC are generally low and would not cause flowpaths to become overwhelmed, so that stemflow intensity or amount would not decrease with increasing precipitation intensity.

2.3. Methods

Stemflow was collected from 5 Western hemlock (*Tsuga heterophylla*), 7 Western red cedar (*Thuja plicata*), 4 Douglas fir (*Pseudotsuga menziesii*), and 2 Birch (*Betulaceae*) trees (Table 2.1 and Figure 2.1) in the study site in the MKRF (see Chapter

1.1 for the site description). Stemflow from maple trees was not measured because their small complex branches make stemflow measurements difficult and because there are few maple trees within the study site (only 3% of all trees). Soft plastic tubing (2 cm inside diameter, with one third cut out to create a trough) was nailed to the trees in a spiral orientation to direct stemflow down the tree stems into containers (Figure 2.2). Silicone sealant and putty was used to fill holes between the tubing and the bark to minimize stemflow losses during the measurement period.

Either water-collecting containers (e.g. Cape et al., 1991; Martinez-Meza and Whitford, 1996; Herwitz and Levia, 1997), or tipping buckets (e.g. Liang et al., 2007, 2009a/b, 2011; Germer et al., 2010; Levia et al., 2010) can be used for stemflow measurements. Water-collecting containers give a volumetric measurement of total stemflow during a specific time period. In order to get detailed information, measurements have to be taken after each event. Conversely, tipping buckets measure precipitation, or stemflow, intensities by recording the time of each tip. However, most manufactured tipping buckets are built to tip at small volumes (e.g. 5 ml). The Onset rain gauge and the Vaisala precipitation sensors, for example, have maximum precipitation rates of 127 mm/hr and 120 mm/hr, respectively. This corresponds to approximately 10 tips per minute or 50 ml per minute (Onset, 2005; Vaisala, n.d.). Because trees in this study site can yield large volumes of stemflow (e.g. >3 l/hr), this can lead to significant errors during high intensity stemflow events when maximum tipping rates are exceeded (Duchon and Biddle, 2010). A potential solution to this problem is to increase the volume of the bucket. However, this increases measurement errors for small low-intensity events because of the decrease in tipping frequency so that the beginning and end of events will not be measured as accurately as with smaller tipping buckets (Habib et al., 2001).

Other measurement errors may occur in response to wind, wetting, evaporation, splashing, and instrument error (Niemczynowicz, 1986; Habib et al., 2001).

In this study, stemflow was measured with both methods: 19 l plastic water-collecting containers with a lid, and tipping bucket rain gauges. Stemflow was measured using water-collecting containers for 10 trees from February 2010-June 2010 and 16 trees from June 2010-November 2010 (Table 2.1). The volume of water in the containers was measured with a 1000 ml graduated cylinder after each precipitation event. An Onset tipping bucket rain gauge, with a 5 ml tipping volume, was used to measure stemflow from a cedar tree (tree 301) that had a consistently small volume of stemflow per event from April 2010 to March 2011. A larger tipping bucket with a 25 ml tipping volume was built to measure stemflow from a hemlock tree (tree 601) from June 2010 to May 2011. To obtain a more complete data set and better understand variation in stemflow intensities for all species, 6 other tipping buckets were installed in November 2010 (Table 2.1). Three home-built tipping buckets, with tipping volumes of 25 ml, measured stemflow until May 2011. Three Onset tipping buckets measured stemflow until March 2011; however, freezing temperatures and snow resulted in only a few useful events during this period.

Precipitation was measured using an Onset tipping bucket rain gauge (0.2 mm/tip) in a clearcut located just north of the study site. Precipitation measured in the clearcut is assumed to represent precipitation falling on the canopy. Precipitation data is missing from mid November 2010 to February 2011 due to freezing temperatures, snow, and battery malfunction.


Table 2.1: Trees monitored for stemflow. Freezing temperatures and snow resulted in only a few useful events between mid November 2010 and February 2011 for all tipping buckets. For the location of the trees see Figure 2.1.

| Tree Number | Species | DBH (cm) | Collecting Bucket Measurement Period | Tipping Bucket Measurement Period |
|--------------------|----------------|-----------------|---|--|
| 191 | Cedar | 16 | 25 Jun 10 – 5 Nov 10 | – |
| 495 | Cedar | 23 | 25 Jun 10 – 15 Nov 10 | – |
| 301 | Cedar | 30 | 12 Feb 10 – 26 Mar 10 | 17 Apr 10 – 7 Mar 11 |
| 403 | Cedar | 31 | 12 Feb 10 – 5 Nov 10 | 5 Nov 10 – 4 May 11 |
| 274 | Cedar | 32 | 27 May 10 – 15 Nov 10 | – |
| 141 | Cedar | 37 | 12 Feb 10 – 15 Nov 10 | – |
| 300 | Cedar | 57 | 12 Feb 10 – 5 Nov 10 | – |
| 601 | Hemlock | 29 | – | 25 Jun 10 – 4 May 11 |
| 433 | Hemlock | 30 | 12 Feb 10 – 15 Nov 10 | 2 Dec 10 – 7 Mar 11 |
| 72 | Hemlock | 31 | 12 Feb 10 – 15 Nov 10 | 2 Dec 10 – 7 Mar 11 |
| 102 | Hemlock | 41 | 28 Jun 10 – 15 Nov 10 | – |
| 306 | Hemlock | 50 | 12 Feb 10 – 15 Nov 10 | – |
| 199 | Douglas fir | 26 | 25 Jun 10 – 15 Nov 10 | – |
| 338 | Douglas fir | 31 | 12 Feb 10 – 15 Nov 10 | – |
| 233 | Douglas fir | 34 | 27 May 10 – 5 Nov 10 | 5 Nov 10 – 4 May 11 |
| 116 | Douglas fir | 43 | 12 Feb 10 – 15 Nov 10 | 2 Dec 10 – 7 Mar 11 |
| 600 | Birch | 16 | 27 May 10 – 5 Nov 10 | 5 Nov 10 – 4 May 11 |
| 505 | Birch | 27 | 12 Feb 10 – 15 Nov 10 | – |


Legend


Tree Species and DBH (cm2)

Birch

 16 - 30


Hemlock

 16 - 30

 31 - 45

 46 - 60


Cedar

 16 - 30

 31 - 45

 46 - 60


Douglas Fir

 16 - 30

 31 - 45

 Stream

Contour interval = 2 m

0 5 10 20 30 40
 Meters

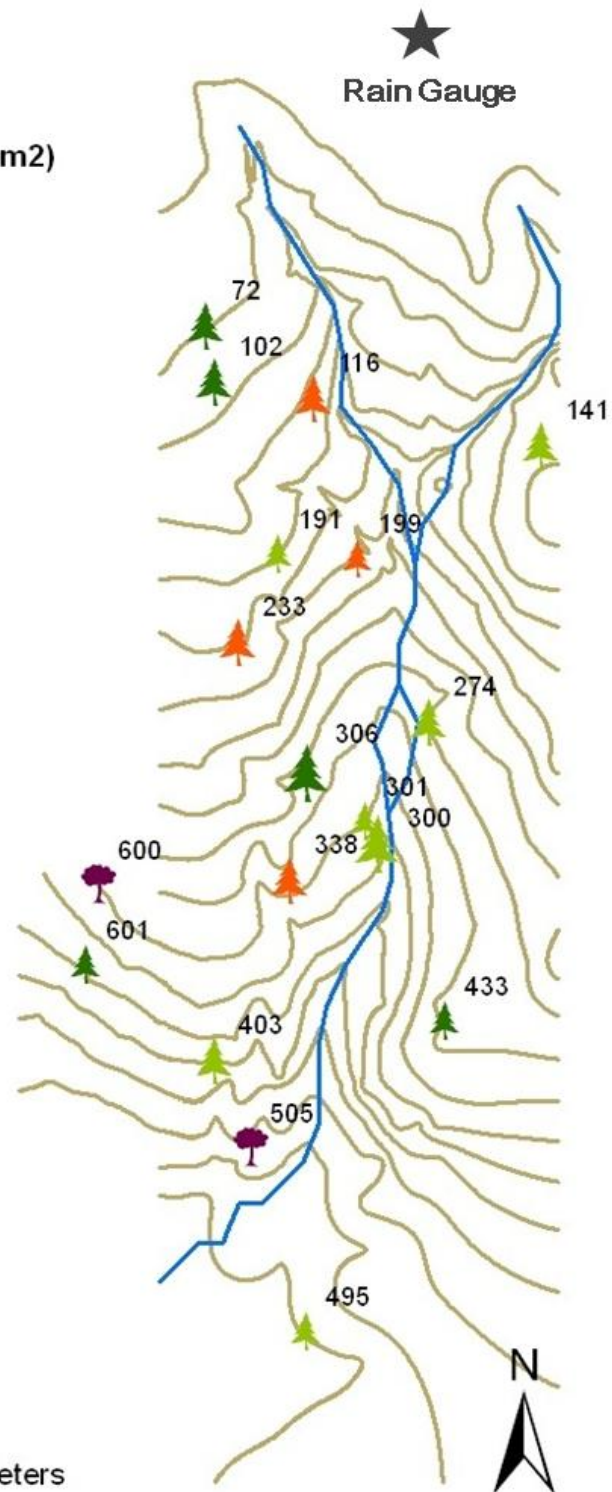


Figure 2.1: Location of trees for which stemflow was measured. Symbol size represents DBH. See Table 2.1 for the details of the measurement period.



Figure 2.2: Stemflow setup with the 19 litre container (Tree 306).

2.4. Data analysis

2.4.1. Stemflow

Stemflow data were converted to a representative depth by dividing the measured stemflow volume by the basal area of the tree. Stemflow as a percent of gross incident precipitation describes how much of the precipitation that falls on the forest canopy reaches the soil as stemflow (Johnson and Lehmann, 2006):

$$SF\% = SF/PPT \times 100\%$$

where SF is the amount of stemflow on a per unit area basis, and PPT is the rainfall depth. Funneling ratios, which describe how much precipitation is concentrated as stemflow, were calculated using the following equation (Herwitz, 1986):

$$F = V/(B \cdot G)$$

where V is the measured stemflow volume (ml), B is the basal area of the tree (cm^2), and G is the depth of gross incident precipitation (cm).

2.4.2. Division of data into events

Tipping bucket data were converted from tips into hourly and 15 minute stemflow amounts by adding all tips that occurred in these intervals. Stemflow and precipitation intensity data were then divided into events using a Matlab code (*'Storm script'*; Appendix A). Events were defined as periods of precipitation that were separated by at least 12 hours of no precipitation and had a total precipitation larger than 2.5 mm.

Stemflow data was divided into events based on the assumption that stemflow can only begin once precipitation had begun. Because stemflow often continued after precipitation ended, the end of a stemflow event was defined either as the start of the next precipitation event or the start of a 12 hour period with no stemflow. For each event, the total volume, peak intensity, and average intensity of both stemflow and precipitation were calculated using hourly data because the 15 minute data contained many periods without any tips for the stemflow measurements.

2.4.3. Lag times

To better understand stemflow timing, the start time, the centroid (the time when half of the event total precipitation or stemflow occurred), and the coefficient of variation of stemflow and precipitation were determined for each event. The amount of precipitation before stemflow started was calculated as well. The lag time between the start of precipitation and the start of stemflow and the lag time between the stemflow and precipitation centroids were calculated using 15 minute data because of the higher resolution required to determine the start and centroid time of each event.

2.4.4. Cross correlation

For 9 events, for which data was available for most trees, the cross correlation between precipitation and stemflow intensity time series was calculated using another Matlab script (*'Cross-correlation script'*; Appendix A). The maximum forward lag was set at 24 time steps (6 hours) and the maximum negative lag was set at 12 time steps (3 hours). The code identified the lag (or time shift) that is associated with the highest Spearman rank correlation between the precipitation and stemflow time series.

2.5. Results and discussion

2.5.1. Stemflow amount

2.5.1.1. Stemflow as a function of precipitation

Stemflow increased linearly with precipitation once wetting had occurred (mean $r^2=0.85$; Figure 2.3), which agrees with previous studies (e.g. Manfroi et al., 2004; Li et al., 2008; Liang et al., 2009). Variation in stemflow depth could not entirely be explained by differences between the species. In fact, for trees of the same size, there was little variation between species. Smaller trees tended to have more stemflow per basal area than larger trees (e.g. trees 600 and 191; Figure 2.3). This can be misinterpreted as a species specific difference in stemflow because birch trees are generally smaller than the Douglas fir or cedar trees. Voigt (1960) and Levia and Herwitz (2005), showed that trees with smooth bark texture were able to funnel more stemflow than trees with rougher bark because it takes more precipitation to wet highly texturized bark. The results of this study may suggest that hemlock trees transmit less stemflow than the other trees, which may be due to its rough, flaky bark creating more drip points. As stemflow flows over the bark, these nodes or bark flakes create points where stemflow is able to drip off the surface to the ground. Smooth barked trees have fewer nodes where

stemflow can drip off the stem. Similarly, Voigt (1960) showed that beech trees (*Fagus grandifolia*) transmitted more stemflow than hemlock (*Tsuga canadensis*) and pine (*Pinus resinosa*) trees due to thin, smooth bark. However, the smallest hemlock measured in this study has a DBH of 29 cm, which is larger than the smallest tree of the other species (Table 2.1) and may skew the measurements for the hemlock trees. Furthermore, some medium sized Douglas fir and cedar trees (trees 403 and 233), were able to transmit large amounts of stemflow, despite their rough or spongy bark. Levia and Herwitz (2005) suggested that trees with rough bark with deep linear furrows are able to transmit more stemflow than rough bark without linear furrows. This may be why Douglas fir trees were able to transmit large amounts of stemflow despite their rough bark, compared to hemlock trees that do not have these large furrows.

In general, funneling ratios increased with event size until a threshold or maximum and remained constant thereafter (Figure 2.4). This plateau occurred on average at approximately 50 mm of precipitation. Liang et al. (2009) suggested that this threshold is the amount of precipitation required to satisfy bark water storage, however, the threshold occurred at approximately 5 mm of precipitation for the Stewartia (*Stewartia monadelpha*) trees in their study. These trees have smoother bark than the hemlock, Douglas fir, and cedar trees in this study, which may explain why they required significantly less precipitation for the plateau to occur. However, it is more likely that the 50 mm threshold is not the amount of precipitation that it takes to initially wet the tree's surfaces because stemflow occurred for events smaller than 50 mm. Instead, 50 mm is the precipitation depth that is required before trees can transmit stemflow at their maximum efficiency. Stemflow will occur in events smaller than 50 mm because some flow pathways will be activated but not all surfaces are wet (Figure 2.5). During larger

events, more surfaces are wet and flowpaths are able to connect, which creates the conditions for maximum stemflow efficiency (Carlyle-Moses and Price, 2006).

For some trees, funneling ratios decreased for events larger than 100 mm (e.g. trees 403 and 233 in Figure 2.4). As suggested by Carlyle-Moses and Price (2006) and Li et al. (2008), a tree has a maximum funneling ability and drip losses increase for larger and higher intensity events. However, it is difficult to determine if this trend occurs for all trees because data for events larger than 100 mm is missing for some trees due to the limited size of the containers. The decrease in funneling ratios after 100 mm may also be due to the longer duration of large events. Most events larger than 100 mm occurred over longer periods and precipitation stopped periodically during the event (for periods shorter than 12 hours and thus not long enough to be characterized as a new event), or had a low precipitation intensity for several hours. When precipitation began again, some surfaces may need to be re-wetted again, which would decrease the total amount of stemflow for the event.

2.5.1.2. Stemflow funneling ratios as a function of tree size

Differences in stemflow amount could partly be explained by the differences in tree size. In general, smaller trees tended to transmit more stemflow than larger trees (Figure 2.4). Looking specifically at how funneling ratios varied with DBH for all tree species combined, it is evident that smaller trees, regardless of tree species, were able to funnel more stemflow than the larger trees (Figure 2.6). Event size had a much larger effect on the funneling ratios of small trees than the funneling ratios of larger trees (see the larger range of data points for the smaller trees in Figure 2.6). Smaller trees tend to have a smaller precipitation threshold compared to larger trees (Manfroi et al., 2004), which could cause a larger variation in funneling ratios for smaller events.

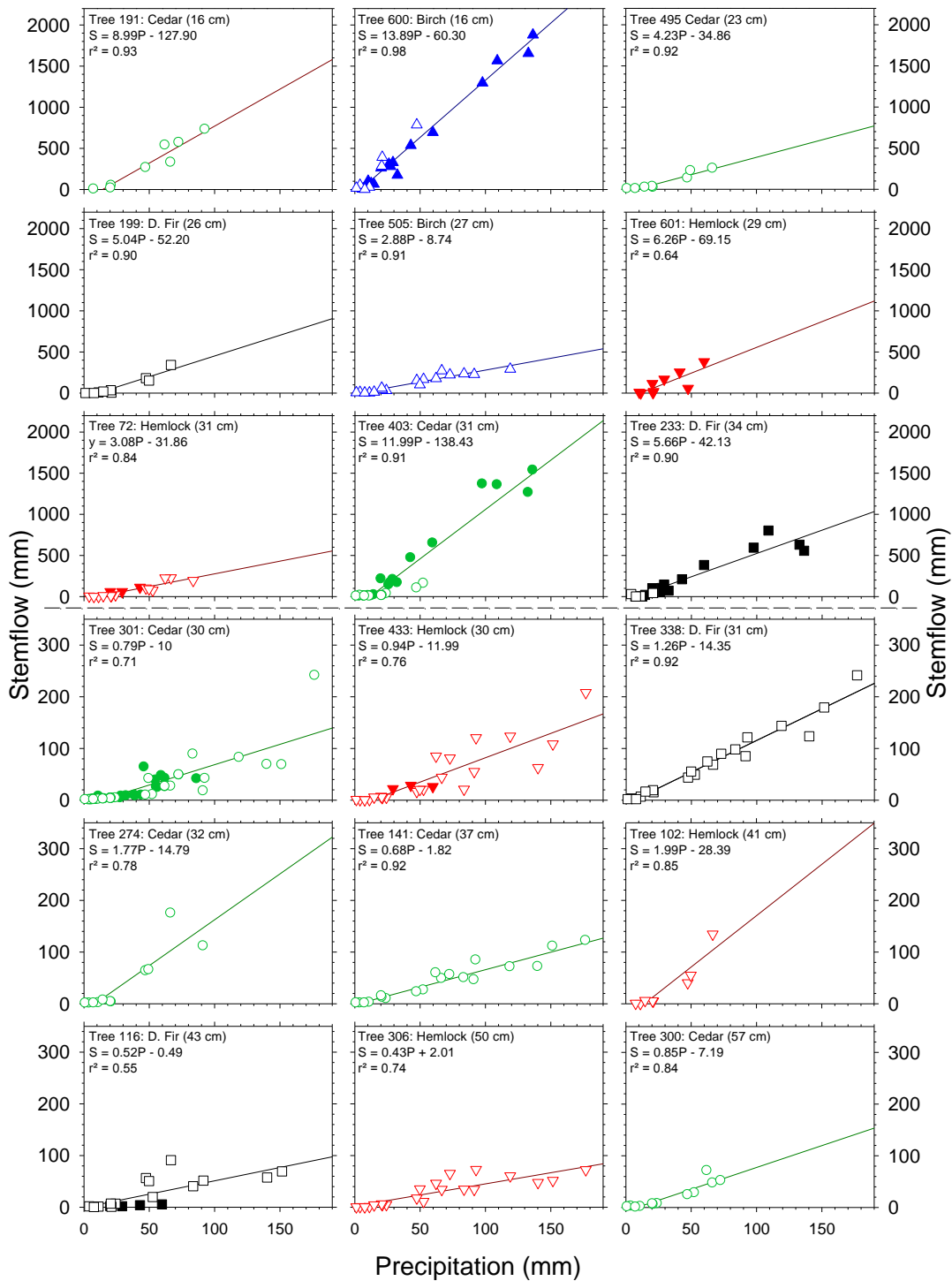


Figure 2.3: Stemflow as a function of precipitation for all trees that were studied. Stemflow volumes were standardized by dividing them by the basal area of the tree. Open symbol = water-collecting container data, closed symbol = tipping bucket data. All regression lines are statistically significant ($p < 0.05$). S = Stemflow (mm), P = Precipitation (mm). The black dashed line depicts change in stemflow axis, in which each group is organized due to tree size from top left to bottom right. For the location of the trees, see Figure 2.1.

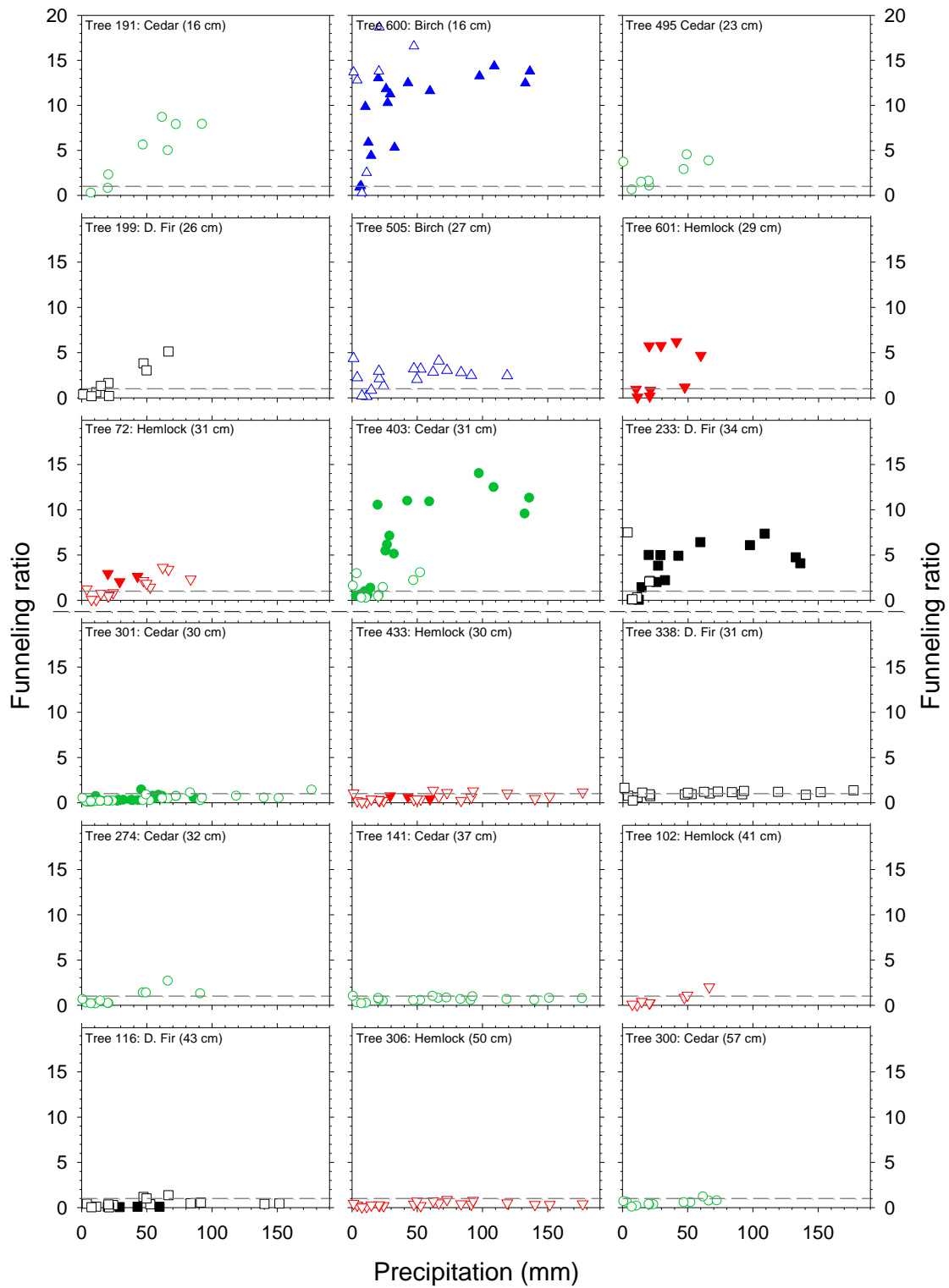


Figure 2.4: Funneling ratios (unitless) as a function of event size for all monitored trees. Open symbol = water-collecting container data, closed symbol = tipping bucket data. The grey dashed line represents a funneling ratio of 1 (i.e. stemflow per unit basal area = precipitation). Trees are organized in the same order as Figure 2.3.



Figure 2.5: Hemlock tree showing stemflow has reached the base of the tree but the stem surface is not entirely wet. Additional precipitation can be used to further fill bark water storage.

The larger trees almost exclusively had funneling ratios smaller than 1, regardless of event size, and were thus diverting precipitation away from the stem rather than concentrating it at the base of the stem. Older trees generally have rougher bark and more branch nodes, thereby making them less efficient in transporting water along the branches and stem and more likely to lose stemflow on the way to the ground (Carlyle-Moses and Price, 2006). Older branches also have larger branch angles (>90 degrees) compared to younger branches (<90 degrees) (Ford and Deans, 1978), which would cause precipitation to flow away from the tree stem rather than towards the stem, resulting in more canopy drip from older trees (Hutchinson and Roberts, 1981; Crockford and Richardson, 2000). The boundary between “funnelers” ($F > 1$) and “diverters” ($F < 1$) occurred at a DBH of approximately 35 cm (Figure 2.6). 65% of all trees in the study site

had a DBH less than 35 cm, representing 24% of the total basal area of the study site. As a result, stemflow should be measured for small trees to determine total stemflow in a forest (c.f. Germer et al., 2010).

The “funnelers” are located throughout the study site and do not appear to be clustered in specific regions; however, small birch trees are primarily located around the stream (Figure 1.2). The generally random distribution of small trees throughout the study site may lead to uneven soil moisture dynamics and impact water available for plant water uptake (Li et al., 2008 and Germer et al., 2010). This could be important during dry summer months because smaller trees are able to funnel (relatively) more precipitation to their roots than larger trees, which could give them access to water when they may not be able to use much deeper soil water that larger trees with more expansive roots can access (Germer et al., 2010).

Even though tree size determines whether a tree is a “funneler” or “diverter” (Figure 2.6), for the medium sized trees with a DBH between 23 and 31 cm, there is some variation in funneling ratios that cannot be explained by tree size alone. This variation in funneling ratios could be caused by variations in tree height, canopy interaction, or tree location. Taller trees with canopies located above surrounding trees collect more precipitation and therefore have the largest potential to transmit stemflow. However, trees in the lower canopy may transmit more stemflow if they have deep tree crowns, rather than broad tree crowns (Manfroi et al., 2004). Although the smallest trees in this study (i.e. trees 600 and 191) are lower in the canopy, and therefore should receive throughfall (instead of precipitation), resulting in less stemflow (Manfroi et al., 2004), they transmit large quantities of stemflow. This may be due to gaps in the canopy above the small trees, in which case, they would still receive direct precipitation despite being lower in the canopy. Unfortunately, it is not possible to observe the canopy

conditions above the trees because the canopy in this site is too high and the understory trees make direct observations difficult. Therefore, it is difficult to separate location and size effects because most small trees are lower in the canopy.

Canopy interaction between adjacent trees may further explain some of the variation in funneling ratios. Herwitz and Slye (1995) showed that rain shadows produced by neighbouring trees may cause trees with the same crown area to intercept different amounts of precipitation, leading to more variation in the amount of stemflow between trees. Furthermore, Crockford and Richardson (2000) indicate that gaps in the canopy allow precipitation to directly reach the tree trunk, thus increasing stemflow as only one side of the tree needs to be wetted before stemflow can begin. For instance, tree 403 shares much of its canopy with tree 402, a hemlock tree located within 1 metre of tree 403. Without direct observations of the tree canopy, it is difficult to determine whether either of these trees is producing a rain shadow for the other tree. However, we can assume that tree 402, which is much larger (DBH 45 cm vs. 31 cm) and thus likely taller, collects more precipitation. This may produce a rain shadow for tree 403, depending on the wind direction. However, tree 403 is one of the larger “funnelers”. It is therefore more likely that tree 402 contributes some of the collected precipitation to tree 403, diverting stemflow away from itself rather than causing a rain shadow for tree 403. Unfortunately, stemflow was not recorded for tree 402 because stemflow trees were distributed randomly throughout the forest rather than directly adjacent to one another. It is therefore unknown if and how much stemflow flowed along tree 402 or was transmitted to tree 403.

Tree 233 also transmitted large amounts of stemflow despite being a medium sized Douglas fir tree. The crown of tree 233 does not come into contact with the surrounding canopy; however, a few smaller cedar trees lower in the canopy touch the

trunk of tree 233. Precipitation may drip off the ends of the cedar branches, as described by Hutchinson and Roberts (1981), which would add to the amount of stemflow being transmitted along tree 233. Although the top portion of the canopy likely contributes the majority of the stemflow, due to near-vertical angles of the young branches (Hutchinson and Roberts, 1981), the neighbouring cedar trees that interact with the trunk may add additional stemflow to tree 233.

Observations of the trees that transmitted less stemflow than expected in the medium DBH size class show that the majority of these trees have very little or no interaction with the surrounding canopy. Trees 601, 433, 301, and 388 all have large open areas around their canopy. These trees are located in various parts of the study site (Figure 2.1) and are different species (Table 2.1), eliminating tree location and species as major confounding effects. This contradicts the suggestion that trees in canopy gaps can funnel more wind driven precipitation (Xiao et al., 2000; Van Stan II et al., 2011) and that rain shadows decrease stemflow (Herwitz and Slye, 1995). Wind direction and wind speed were not measured, therefore it is difficult to determine if there is any direct evidence of this; however, it is clear that stemflow dynamics are not fully described by simple species and size based classifications. The tree canopy needs to be studied in much more detail in order to understand the variability in stemflow and how much stemflow is transmitted by individual trees in a mixed species forest during a precipitation event.

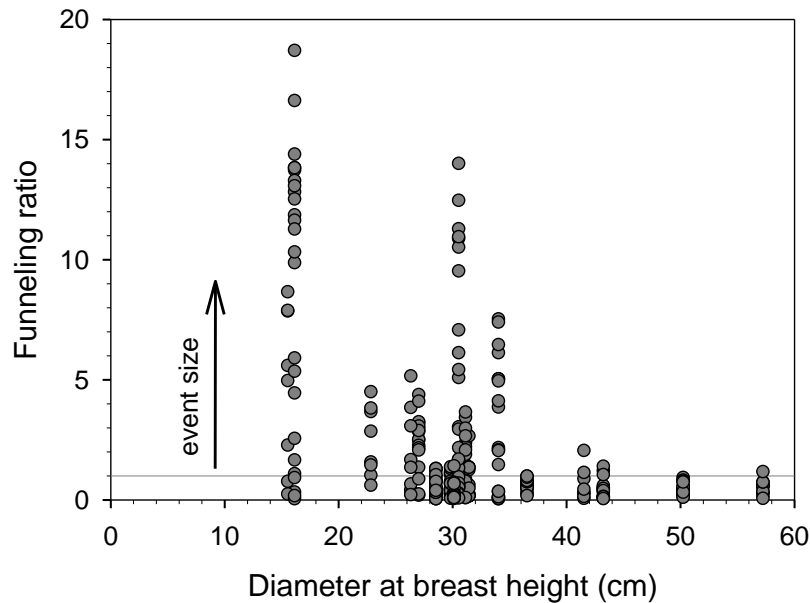


Figure 2.6: Funneling ratio (unitless) as a function of DBH (cm) for all species and events. The grey line represents a funneling ratio of 1. Funneling ratios increase with event size for each tree (black arrow indicates this general trend).

2.5.1.3. Total stemflow

Total stemflow from all trees in the watershed was calculated using the regression equations for the relations between stemflow and precipitation ($S = aP - b$; Figure 2.3). The slopes of these lines (a) were related to DBH (Figure 2.7). The minimum amount of precipitation required before stemflow occurred was set at 8 mm for all trees as this was the mean of the maximum precipitation for which no stemflow was measured (i.e. the mean of b/a was 8). This offset represents the amount of precipitation required to wet the tree surfaces before stemflow reaches the base of the tree. Using individual regressions for the five species or separating the data into size classes (c.f. Germer et al., 2010) did not improve the regression and thus a single equation ($S = a(P - 8)$) was used to estimate the amount of stemflow for all 550 trees in the watershed for all events larger than 8 mm for which total precipitation was measured during the spring to winter 2010 period (21 events; total precipitation = 1311 mm; median event size = 52.6 mm). Total stemflow during this 10 month period was 13.2 mm or 1.0% of GIP.

Trees with a DBH smaller than 35 cm contributed 72% of the total stemflow in the watershed. Thus, despite representing only a small fraction of the total basal area (24%), smaller trees funnelled the majority of stemflow.

This 1.0% of GIP is at the lower end of the range for temperate forests (0.94 – 20.0% GIP) reported by Levia and Frost (2003). However, of the studies reported in Levia and Frost (2003) none were conducted in cedar-hemlock mixed forests or along the west coast of North America and few were conducted in mature forests. Many factors contribute to the percentage of stemflow (i.e. canopy structure, bark texture, and precipitation intensity and duration; Levia and Frost, 2003), which makes it difficult to determine the importance of stemflow or the factors that cause differences in stemflow between different forests. Basal area is only 0.5% of the total study area, suggesting an overall average funneling ratio of 2.

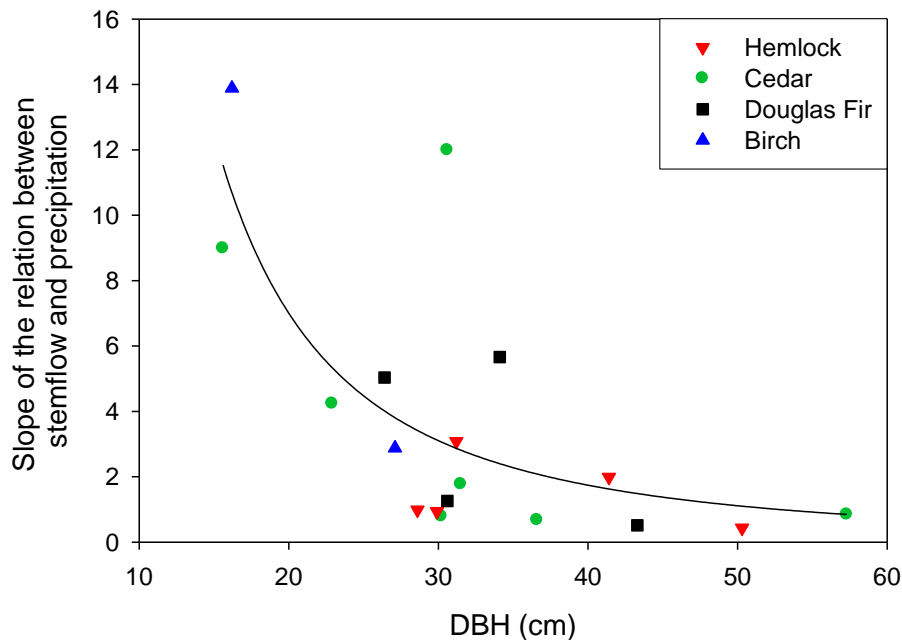


Figure 2.7: Slopes of the relation between stemflow and precipitation (a in the equation $S=aP-b$; see Figure 2.3) as a function of DBH (cm). The equation of the best fit line is: $a=(6700*DBH)^{-2.35}$, $r^2 = 0.51$, $p = 0.0008$.

2.5.2. Stemflow timing and intensity

2.5.2.1. Time series

Very few studies have compared stemflow timing and intensity with precipitation timing and intensity (Germer et al., 2010; Levia et al., 2010; Van Stan II et al., 2011). However, it is important to understand stemflow timing and intensity to better understand the effects of stemflow on soil moisture (Liang et al., 2011), recharge (Taniguchi et al., 1996), and overland flow generation (Germer et al., 2010). Time series were plotted for events for which tipping bucket data was available for three studied trees (see Figure 2.8 – Figure 2.10). The time series indicate a lag between the start of precipitation and the start of stemflow. This represents the time it takes to wet the surface of the tree before stemflow is initiated (Liang et al., 2009a). Stemflow intensity also appears to be less variable (in time) compared to precipitation intensity (Figure 2.8 - Figure 2.10).

For some events, stemflow peak intensities increased in a stepwise manner, regardless of the peak precipitation intensity (e.g. the event that occurred on 13/04/11-16/04/11 for trees 233 and 403, and the event that occurred on 06/06/10-07/06/11 for tree 301; Figure 2.8 - Figure 2.10). This indicates that the tree reached its storage capacity and became more efficient in transporting stemflow during the event (Carlyle-Moses and Price, 2006; Liang et al., 2009a). However, when there were several hours between precipitation bursts, there was often a decrease in stemflow intensity during the next peak, indicating that the storage had to be partly refilled (e.g. 19/09/10-21/09/10 and 26/08/10-28/08/10 for tree 301; Figure 2.8 - Figure 2.10). As a result, the maximum stemflow intensity did not always occur at the same time as the maximum precipitation intensity. Furthermore, when there were two smaller precipitation bursts, stemflow often peaked during the second precipitation burst (c.f. Germer et al., 2010). When looking at the data in more detail, peak stemflow and peak precipitation intensity within the same

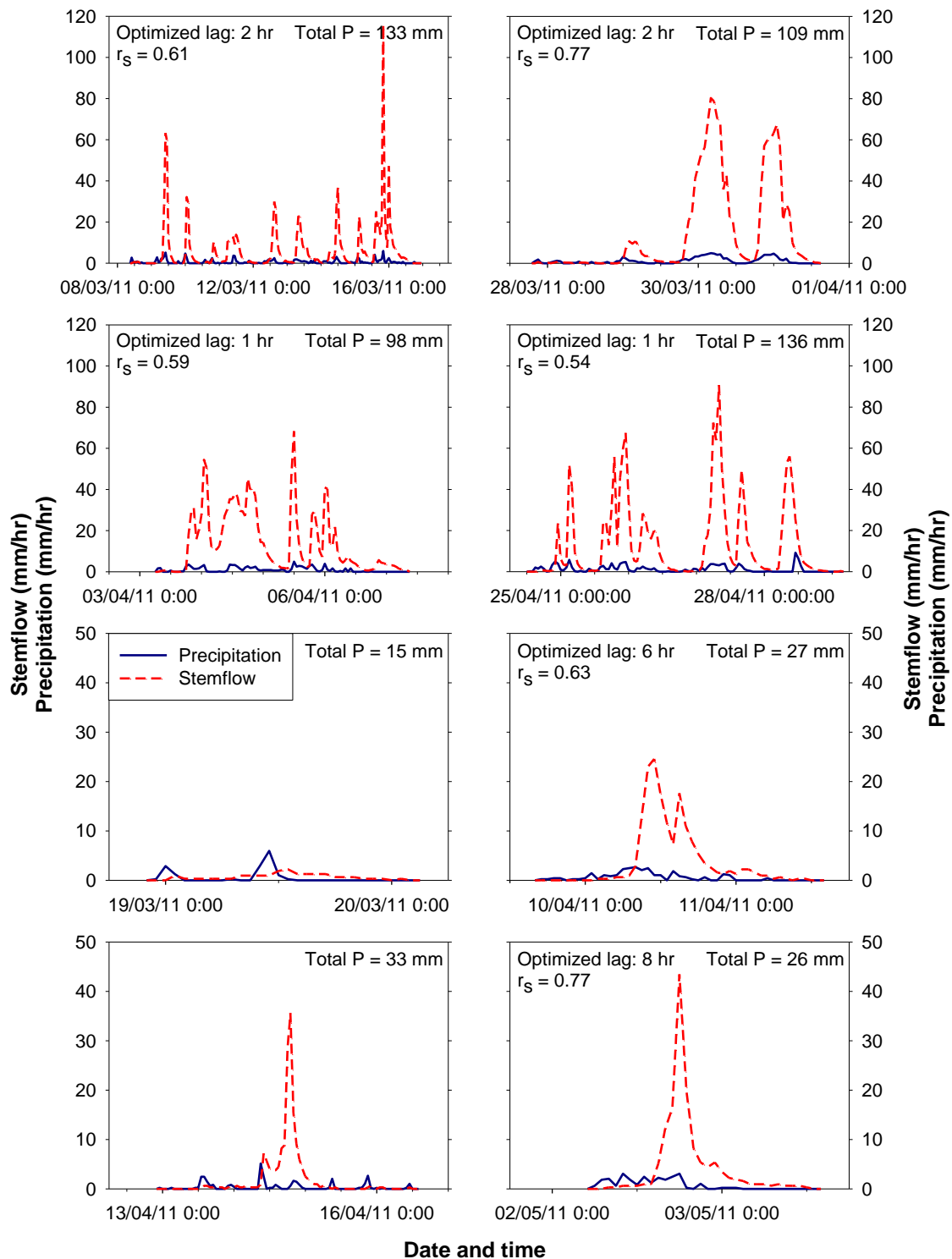


Figure 2.8: Stemflow (dashed line) and precipitation intensity (solid line) time series for 8 events for tree 403 (cedar; DBH = 31 cm). Optimized lag time is given in the top left corner for events for which the lag-optimized spearman rank correlation coefficient (r_s) was greater than 0.5. Total event precipitation is reported in top right corner.

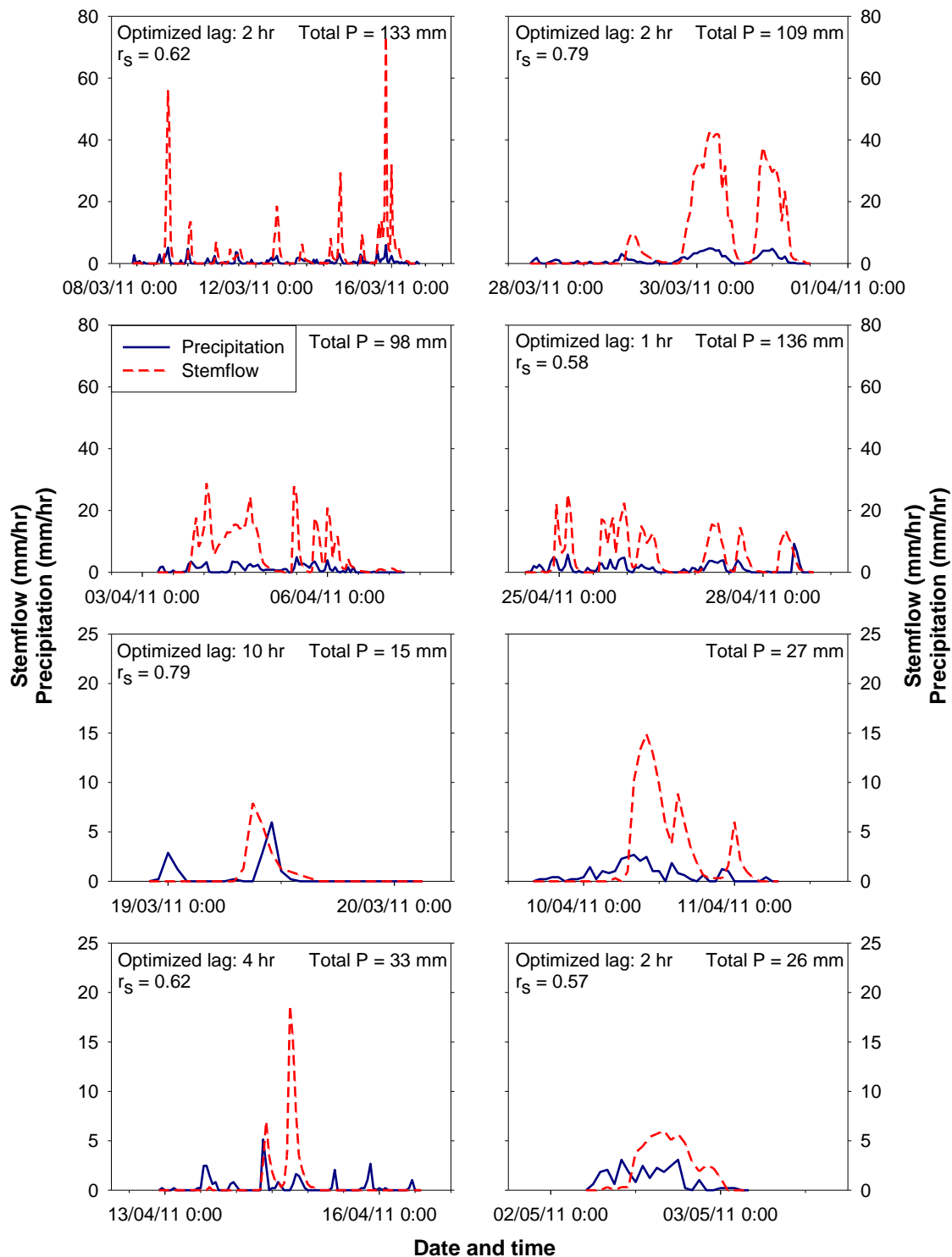


Figure 2.9: Stemflow (dashed line) and precipitation intensity (solid line) time series for 8 events for tree 233 (Douglas fir; DBH = 34 cm). Optimized lag time is given in the top left corner for events for which the lag-optimized spearman rank correlation coefficient (r_s) was greater than 0.5. Total event precipitation is reported in top right corner.

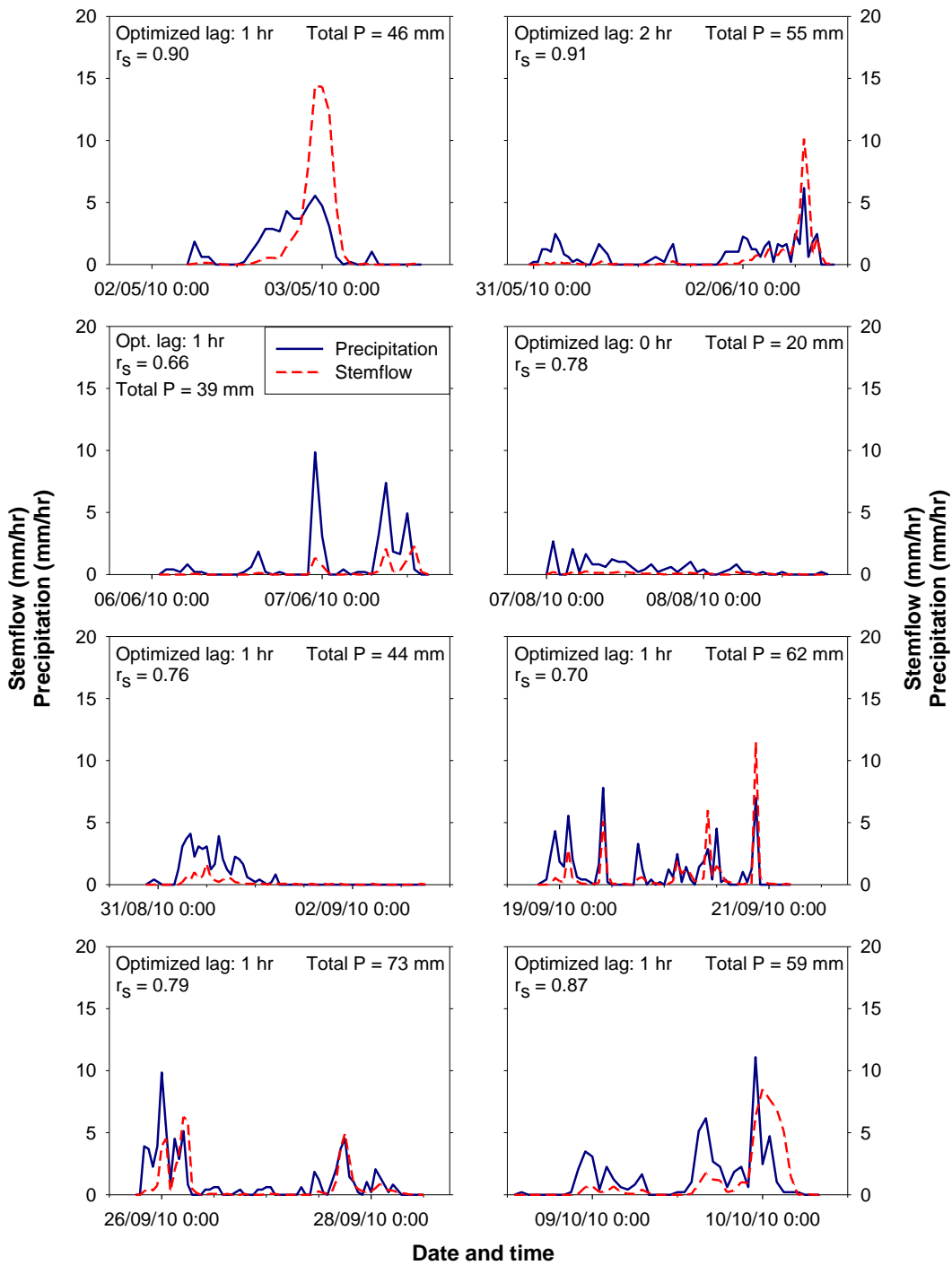


Figure 2.10: Stemflow (dashed line) and precipitation intensity (solid line) time series for 8 events for tree 301 (Cedar; DBH = 30 cm). Optimized lag time is given in the top left corner for events for which the lag-optimized spearman rank correlation coefficient (r_s) was greater than 0.5. Total event precipitation is reported in top right corner. Note that this figure shows different events than Figure 2.8 and Figure 2.9. The tipping bucket for tree 301 malfunctioned during the period that measurements were taken at trees 233 and 403. However intensity data was collected for a longer period for this tree so that data is available for more events for this tree.

precipitation burst occurred within 15 – 30 minutes of each other. These results correspond with those of Germer et al. (2010), who compared stemflow timing to precipitation timing for one aborescent babassu palm (*Orbignya phalerata*). They found that there were time lags for the start of stemflow and peak stemflow intensity for all events, except for one event (Germer et al., 2010).

In general, the mean optimized lag time was approximately 4 hours (Figure 2.11), except for trees 433 and 301, which had a mean optimized lag times of 13.5 hours and 1 hour respectively. Both trees can be categorized as “diverters” (Figure 2.4) and yet are at the extremes of the optimized lag time range. Although trees 403, 233 and 600 are classified as “funnelers” and trees 301 and 116 are classified as “diverters”, mean optimum lag time was approximately the same for these trees.

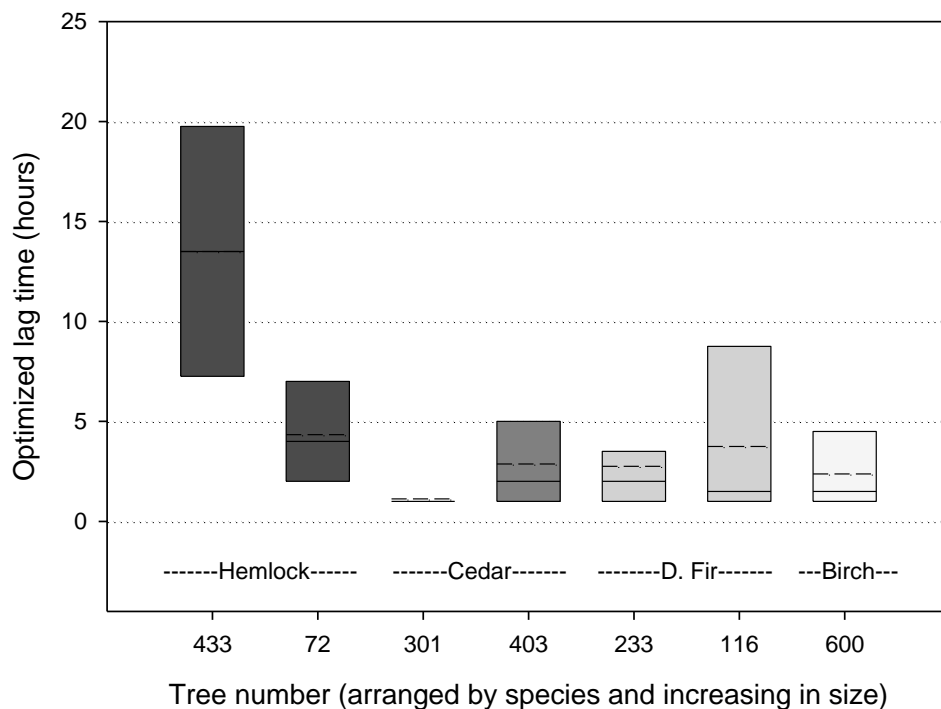


Figure 2.11: Optimized lag time (hours) for all trees monitored with tipping buckets. Upper box boundary = 75th percentile, black line in box = median, dashed black line in box = mean, lower box boundary = 25th percentile.

2.5.2.2. Start lag time and precipitation lag

On average, there was a 4 hour delay in the start of stemflow (Figure 2.12a), corresponding to approximately 3 mm of precipitation (Figure 2.12b), with little variation in the start lag time between species. However, trees 233 and 600 had longer start lag times (11 hrs and 7 hrs, respectively) and higher precipitation lags (7 mm and 5 mm, respectively) than the other trees. These start lag times are much longer than the lag times reported by Levia et al. (2010) and similar to the lag times reported by Germer et al. (2010). A range of precipitation lags (less than 1 mm – 8 mm) have been reported in several studies (Aboal et al., 1999; Manfroi et al., 2004; Liang et al., 2009a; Germer et al., 2010). The precipitation lags for this site are similar to the lower range of values reported (Aboal et al., 1999; Manfroi et al., 2004); however trees 233 and 600 are similar to the higher range of values (Liang et al., 2009a; Germer et al., 2010). Tree species (bark water storage capacity), tree size (Levia et al., 2010), canopy structure (rain shadows from neighbouring trees when wind driven precipitation is the main contributor; Van Stan II et al., 2011), and antecedent wetness conditions (Germer et al., 2010) all influence the start of stemflow. Smaller trees are expected to respond faster after the onset of precipitation; rougher bark is expected to cause a delay in stemflow generation (Levia et al., 2010). However, this was not observed in this study. Tree 116, for example, is a large Douglas fir tree, which should have a large bark water storage capacity but does not have a longer start lag time than the other trees. This may be because this tree has a dense canopy that is in contact with the surrounding trees and only has a few gaps in the surrounding canopy. Tree 233, which is smaller than tree 116, has a fairly open canopy; however, it is in contact with a number of cedar trees. Larger start lag time and precipitation lag may be caused by the neighbouring trees intercepting or diverting stemflow before they contribute to stemflow of tree 233, or alternatively this is the precipitation amount that is required for flow to occur over the bark.

Tree 600 is particularly interesting in that it is the only deciduous tree studied for stemflow timing and has very thin bark, which should theoretically result in a much smaller bark water storage capacity (Levia and Herwitz, 2005). However, this birch tree does not grow straight. It curves significantly uphill and has a number of notches along its surface. This would produce more drip off the trunk (Carlyle-Moses and Price, 2006), and delays the onset of stemflow. Despite clear effects of bark water storage capacity on stemflow lag times (Levia and Herwitz, 2005), it is clear that other factors control the onset of stemflow for tree 600. Although tree 600 is lower in the canopy, it transmits the same amount of stemflow as the other trees. This may also explain the delay in the onset of stemflow because it receives less direct precipitation and more throughfall (Manfroi et al., 2004). Once stemflow has begun, tree 600 is able to transmit stemflow at a high peak intensity (Section 2.5.2.4).

The outliers for start lag time and precipitation lag did not correspond to the same events. In general, outliers that had smaller start lag times corresponded with shorter periods without precipitation prior to the event. Outliers that had longer start lag times or precipitation lag times had long periods of no precipitation prior to the event, although there were also some exceptions. Most exceptions for long start lag times with wet antecedent conditions corresponded to small events with low precipitation intensities. Most exceptions for short start lag times with dry antecedent conditions corresponded to events with high initial precipitation intensities. These results are similar to those of Germer et al. (2010), who showed that shorter dry periods resulted in shorter start lags because the bark is already wet and does not require the bark water storage to be filled before stemflow began. They also showed that high initial precipitation intensity could cause stemflow to occur after only 15 minutes.

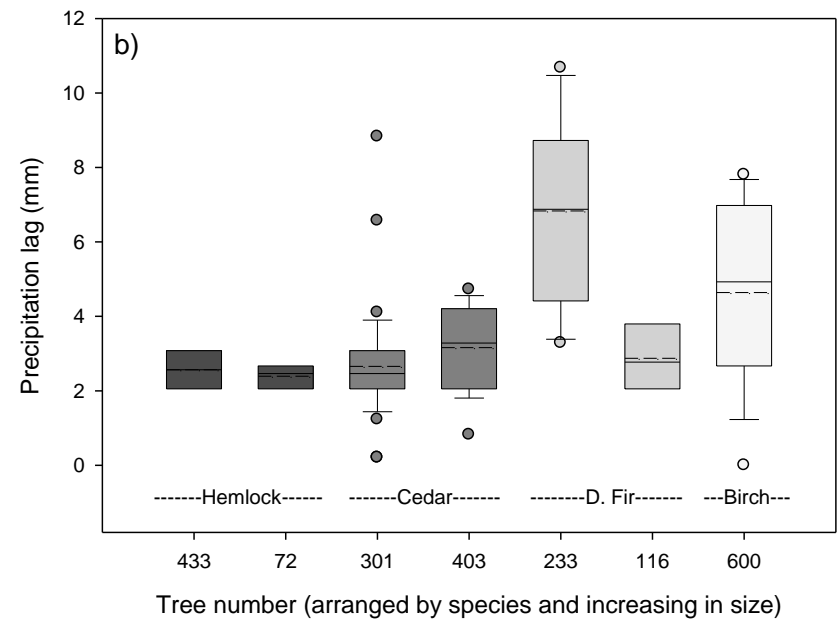
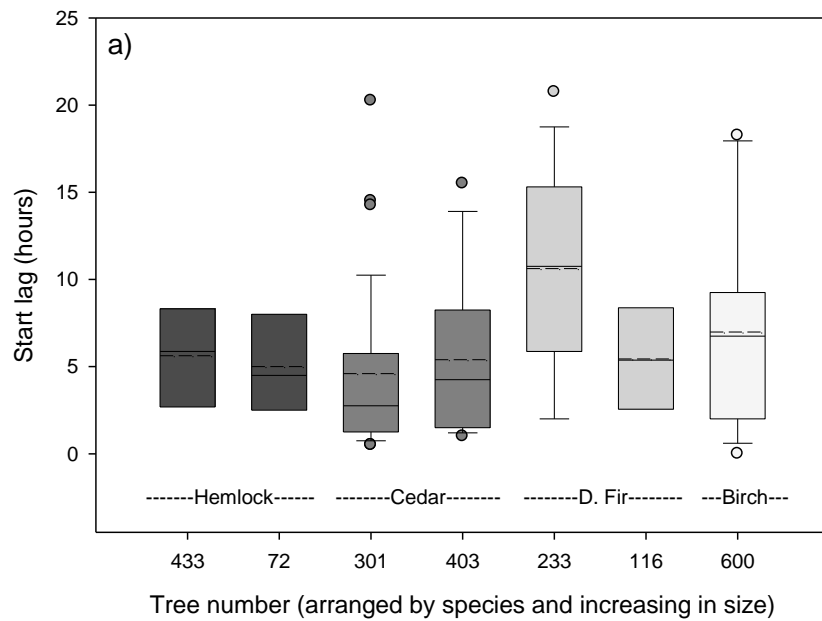


Figure 2.12: a) Start lag time for all trees monitored with tipping buckets. b) Precipitation amount required before stemflow begins. Circles outside boxes = outliers, upper whisker = 95th percentile, upper box boundary = 75th percentile, black line in box = median, dashed black line in box = mean, lower box boundary = 25th percentile, and lower whisker = 5th percentile.

2.5.2.3. Centroid lag times

The centroid lag time is the difference between the time it takes for half of the event total precipitation to occur and half of the event total stemflow to occur. On average the centroid lag was 4 hours for all trees, regardless of species or size, which is similar to the start lag time. This suggests that the factor that most influences stemflow timing is the time it takes for stemflow to start. This corresponds to results of Levia et al. (2010), who showed for American beech (*Fagus grandifolia*) and yellow poplar (*Liriodendron tulipifera*) that once stemflow had started, responses to precipitation were the same for both trees.

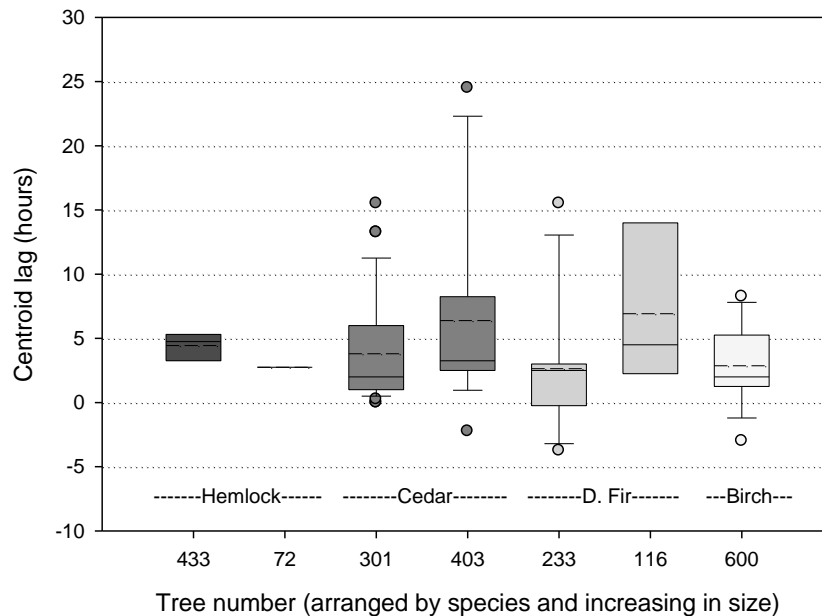


Figure 2.13: Centroid lag time for all trees monitored with tipping buckets. Circles outside boxes = outliers, upper whisker = 95th percentile, upper box boundary = 75th percentile, black line in box = median, dashed black line in box = mean, lower box boundary = 25th percentile, and lower whisker = 5th percentile.

2.5.2.4. Peak stemflow and precipitation intensities

Peak stemflow intensity increased with peak precipitation intensity (Figure 2.8 – Figure 2.10 and Figure 2.14). There may be a threshold at 2 mm/hr, above which peak stemflow intensity increased faster than peak precipitation intensity. However, details for this trend cannot be analyzed due to the limited number of events and trees for which

stemflow intensity data are available. For some trees peak stemflow intensities were much higher than peak precipitation intensities (trees 600, 403, and 233) but for other trees peak stemflow intensities were generally lower than peak precipitation intensities (trees 433 and 301). However, even for these trees peak stemflow intensity was sometimes higher than the peak precipitation intensity.

Whether peak stemflow intensity was higher or lower than peak precipitation intensity did not depend on tree size or species. For example, trees 301 and 403 are cedar trees of roughly the same size, yet tree 403 had much higher peak stemflow intensities than tree 301 (Figure 2.14). As discussed in section 2.5.1.2, this may be due to canopy interaction. The canopy of tree 403 interacts with the canopy of tree 402, whereas tree 301 has a large open area to the north and east of the canopy and little interaction with surrounding trees.

Carlyle-Moses and Price (2006) suggested that stemflow intensity would increase with precipitation intensity until it reaches a maximum funneling and transport capacity. At this intensity, stemflow exceeds flowpaths along branches and causing more drip and less stemflow (Carlyle-Moses and Price, 2006); rougher bark associated with Douglas fir and hemlock trees would also cause more drip during high intensity events. This was not observed in this study (except perhaps for the 10 mm/hr event for trees 600 and 403; Figure 2.14), as high peak stemflow intensities were not limited to one particular species, nor did it occur consistently for a particular species.

A higher peak stemflow intensity than peak precipitation intensity could allow for quicker recharge of groundwater (e.g. Liang et al., 2011) and may contribute to the rapid delivery of stemflow water to streamflow as suggested by Germer et al. (2010). Stemflow intensity may also become greater than the hydraulic conductivity of the soil surrounding the tree, resulting in overland flow (e.g. Herwitz, 1986; Germer et al., 2010). Germer et

al. (2010) showed that stemflow intensities were lower than the hydraulic conductivity of surface soils but that the hydraulic conductivity at depth was lower than peak stemflow intensities for their site in Brazil. This could lead to lateral subsurface flow and contribute to the rapid delivery of precipitation to streamflow, rather than groundwater recharge (Herwitz, 1986; Germer et al., 2010). The maximum measured stemflow intensity in this study (~120 mm/hr ; Figure 2.14) is still 3 times smaller than the hydraulic conductivity of the soil (Haught and van Meerveld, 2011), and thus it is unlikely that stemflow results in overland flow.

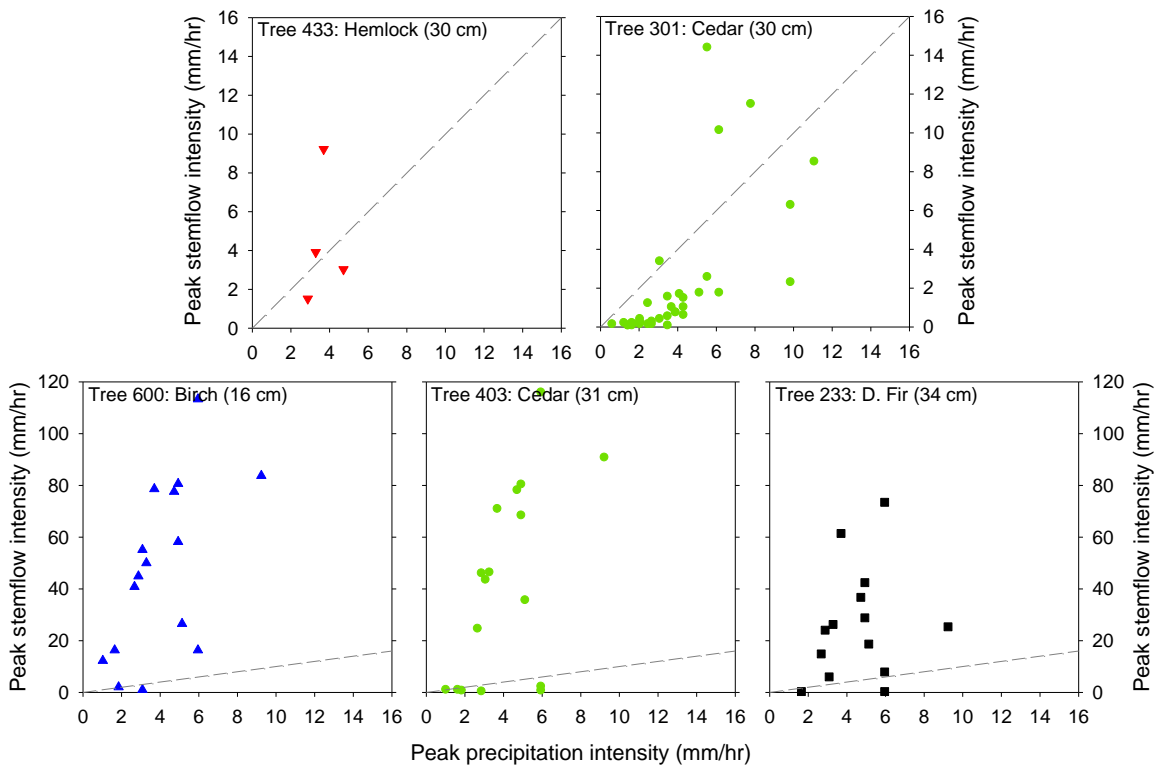


Figure 2.14: Peak stemflow intensity (mm/hr) as a function of peak precipitation intensity (mm/hr). The dashed line represents the 1:1 line. DBH is given in parentheses.

2.6. Conclusion

Stemflow in the MKRF study site was approximately 1% of GIP. Funneling ratios for individual trees ranged from less than 1 to nearly 20. There was less variation

between species than within species because the amount of stemflow was largely a function of tree size; smaller trees funnelled more stemflow. The threshold between “funnelers” ($F > 1$) and “diverters” ($F < 1$) occurred at a DBH of approximately 35 cm. 65% of all trees in the study site have a DBH smaller than 35 cm. They represent 24% of the total basal area and contributed 72% of the total stemflow. The distribution of small trees throughout the study site may lead to uneven soil moisture dynamics and impact water available for plant uptake, particularly during dry summer months.

Funneling ratios increased with event size up to 50 mm. After 50 mm, funneling ratios plateaued until approximately 100 mm, after which they tended to decrease. Stemflow started on average 4 hours after the start of precipitation. Approximately 3 mm of precipitation was required for stemflow to begin. The centroid lag time was also 4 hours, suggesting that the time it takes to wet the leaf and bark surfaces and transmit initial stemflow is the primary influence on stemflow timing. Peak stemflow intensity was much larger than peak precipitation intensity for some trees and did not always occur at the same time as peak precipitation intensity; however, peak stemflow intensity occurred approximately 15 minutes after the corresponding peak precipitation intensity. Peak stemflow intensity was not related to tree species or tree size. Higher peak stemflow intensities than peak precipitation intensities could contribute to faster groundwater recharge.

The large variation in stemflow responses (timing, amount, peak intensity) and the influence of tree size on stemflow amount suggest that it is important to study all tree species in a mixed forest stand and trees of all sizes in order to fully understand stemflow and its importance for ecohydrological processes.

3. Tracing stemflow flowpaths in the soil

3.1. Introduction

Water and solutes in forest soils can move through the soil matrix and macropores (fast direct routes) (Weiler and Fluhler, 2004; Phillips, 2010). Macropores consist of animal burrows, earthworm holes, live and decayed roots, soil fissures, and cracks (Bogner et al., 2010). They offer a much faster pathway for water to flow through than the matrix, especially if they are open at the soil surface (Gaiser, 1952; De Vries and Chow, 1978). However, soils are not simply a soil matrix with long interconnected macropores located throughout it. Gaiser (1952) found that forest soils in Ohio contained many decayed root channels due to previous clearcutting. Similarly, Chamberlin (1972) and De Vries and Chow (1978) found that forest soils in coastal British Columbia are highly complex and contain a large number of voids or air pockets due to past disturbances, such as logging and forest fires. As forests regenerate and soils build up, not only do decayed roots create large preferential flow paths, but fallen trees and rocky soils create voids beneath the soil surface that add to the complexity of soils and the hydrological pathways in them (Chamberlin, 1972; De Vries and Chow, 1978).

Preferential flowpaths also change seasonally due to changing soil moisture conditions (Onodera and Kobayashi, 1995; Sidle et al., 2000). Short macropores can become connected through nodes, such as mesopores and pockets of organic matter, and start to transmit water when soil moisture is high (Sidle et al., 2000). This increases the connectivity of flow pathways and increases the distance that water can travel

through the soil (Sidle et al., 2000). In dry seasons, nodes can switch off, shortening the distance water can travel through preferential flowpaths. This effect can be amplified (or occur more regularly) in shallow soils, where saturation occurs more often than in deeper soils (Sidle et al., 2000).

Few studies have been conducted to determine preferential flow of stemflow (Martinez-Meza and Whitford, 1996; Li et al., 2009; Liang et al., 2011). Studying rooting patterns and flow through preferential pathways is not an easy task. Most studies have used dye to determine subsurface flow and preferential flowpaths (Weiler and Fluhler, 2004; Anderson et al., 2009; Bogner et al., 2010). Dye is sprinkled on the surface or poured along a transect and the soil is excavated to determine the location of primary flow pathways in the soil (e.g. Weiler and Fluhler, 2004; Anderson et al., 2009), leaving behind a disturbed soil structure, unlike what it once was (Anderson et al., 2009). This technique is time consuming, yet cost effective and simple (Allaire et al., 2009). It enables researchers to observe and document details such as macropore lining that may be missed with other approaches (Allaire et al., 2009). Unfortunately, the excavation process is destructive and can cause small macropores to be missed. The excavation also prevents the experiment from being repeated and as a result, it only represents a single snapshot in time (Anderson et al., 2009; Allaire et al., 2009).

Martinez-Meza and Whitford (1996) studied flow pathways associated with stemflow and direct precipitation on three desert shrubs in New Mexico using simulated precipitation. They sprinkled Rhodamine-B dye powder at the base of the shrubs and found that stemflow infiltrated preferentially along roots and that the depth that stemflow was able to infiltrate was related to the size of the shrub (Martinez-Meza and Whitford, 1996). For creosotebush (*Larrea tridentata*) and tarbush (*Flourensia cernua*), maximum stemflow infiltration depth (35 cm and 20 cm, resp.) occurred under the smallest bush,

whereas for mesquite (*Prosopis glandulosa*), maximum stemflow infiltration depth (37 cm) occurred under the bush with the largest canopy (Martinez-Meza and Whitford, 1996). Li et al. (2009) studied two semi-arid shrubs in northern China, also using Rhodamine-B dye powder, and compared stemflow to infiltration of direct precipitation in nearby bare soils for a range of natural precipitation events. They found that direct precipitation resulted in uniform flow through the upper layers of the soil (Li et al., 2009), whereas stemflow infiltrated preferentially along roots and infiltrated into deeper soil layers (18 – 20 cm and 20 – 26 cm for *Hedysarum scoparium* and *Salix psammophila*, resp. vs. 8 – 14 cm for direct precipitation). Smaller events and higher precipitation intensities resulted in more distinct preferential flow, whereas larger events resulted in deeper preferential flow (Li et al., 2009). Liang et al. (2011) is the only known study to date to mimic stemflow and throughfall in a forested stand. They used two dye tracers on a hillslope in central Japan; blue dye on a tall Stewartia tree (*Stewartia monadelphica*; 17.47 m tall; DBH = 22.3 cm) and red dye on the soil underneath the tree to differentiate between stemflow pathways and throughfall pathways (Liang et al., 2011). They found that stemflow and throughfall were transported through different flowpaths and that stemflow water infiltrated deeper into the soil than throughfall (60 cm and 50 cm for stemflow and throughfall, respectively) (Liang et al., 2011). Throughfall was able to infiltrate through preferential flow into deep soil layers as well (Liang et al., 2011).

Preferential flow from stemflow influences soil moisture dynamics in forest soils (Liang et al., 2007; 2009b; 2011) as it concentrates the input of precipitation at the base of trees and increases soil moisture around the tree. Stemflow that bypasses the surface soil layers can cause a larger increase in soil moisture at depth than at the surface (Liang et al., 2011). Li et al. (2009) suggested that the increase in soil moisture below semiarid shrubs from stemflow could concentrate water deep in the soil for use during

drought conditions. Using chloride concentrations of stemflow, throughfall, and deep soil water (150 cm), Taniguchi et al. (1996) found for a Japanese red pine (*Pinus densiflora*) forest that even though stemflow was only 0.5 – 1.2% of net precipitation, the ratio of recharge from stemflow to total recharge was 10.9 – 19.1%. This contribution of stemflow to groundwater recharge is thus considerably larger than the volume of precipitation it represents (Taniguchi et al., 1996).

3.2. Objectives

The objective of this study is to understand the flow pathways of stemflow that infiltrates at the base of Western hemlock (*Tsuga heterophylla*) trees in a mature forest in coastal British Columbia, and compare it to throughfall infiltration. To do this, I mimicked stemflow using a blue dye tracer and excavated the soil around two hemlock trees once the stemflow had infiltrated into the soil. Throughfall infiltration was also mimicked using blue dye and results were compared to the stemflow infiltration experiments.

3.2.1. Research questions

- 1) How is water from stemflow distributed vertically and laterally around a Western hemlock tree in a humid mature forest?
- 2) How do preferential flow of stemflow and throughfall differ in maximum depth and interaction with the soil matrix in a mature forest in coastal British Columbia?

3.2.2. Hypotheses

Given the outcomes of previous studies, I hypothesized that stemflow would infiltrate deep into the soil along preferential flow pathways around roots. Root pathways

would also allow stemflow to flow far from the tree due to large macropores located throughout the soil profile. I also hypothesized that stemflow would infiltrate deeper into the soil than throughfall and that throughfall would flow primarily through the soil matrix.

3.3. Methods and analysis

Two stemflow and one throughfall blue dye experiments (Figure 3.1) were conducted in the Malcolm Knapp Research Forest (see Chapter 1.1 for the site description). Soil moisture was measured at 27 locations throughout the study site using a 20 cm HydroSense probe (Campbell Scientific) prior to all experiments to ensure that the antecedent moisture conditions were relatively similar for all experiments. Average soil moisture was 14.2 % and 13.5 % for stemflow experiment 1 in September 2010 and the throughfall experiment in August 2011, respectively. Stemflow experiment 2 began 10 days after the throughfall experiment. It is likely that average soil moisture was slightly lower than 13.5 % for stemflow infiltration experiment 2 because there was no precipitation during the period between the throughfall experiment and stemflow experiment 2. However, it was assumed that this small decrease in soil moisture would not significantly alter results at these percentages.

The first stemflow infiltration experiment (SIE 1) was conducted in September 2010. Eighteen litres of diluted Brilliant Blue dye (5 g/l) were sprayed evenly onto a Western hemlock stem (tree 601; DBH = 29 cm) over a 3 hour period using a backpack sprayer. This amount of stemflow was previously measured for this tree during a 50 mm rainfall event (Chapter 2). Brilliant Blue dye was used because of its low sorption and high mobility, allowing the dye to travel further through preferential flow pathways than other dye tracers, and because it has less interaction with the soil matrix, which results in a highly defined edge of the pathways (Anderson et al., 2009). The soil surrounding

the tree was excavated two days after the application and analyzed for the presence of blue dye (c.f. Weiler and Naef, 2003; Anderson et al., 2009) in order to determine the location and type of preferential flowpaths, as well as the interaction between the preferential flowpaths and the surrounding soil matrix. The excavation began 2 meters away from the base of the tree because Wang et al. (2002) suggested that Western hemlock tree roots in coastal BC can expand far from the parent tree. The width of the excavation was approximately 3 meters (Figure 3.1). Careful excavation occurred in slices 30 cm apart but increased to 10 cm apart as the excavation moved closer to the tree. For each profile, detailed notes and digital photographs were taken and scaled diagrams were drawn to document the location and patterns of the preferential flowpaths and the location and distribution of roots. Tarps were hung above the excavation plot and around the tree to avoid precipitation from diluting the dye during the 5-week excavation. However, subsurface stormflow at the soil-bedrock interface may have influenced the dye in the lowest 5 – 10 cm of the profile.

In August 2011, a second stemflow infiltration experiment (SIE 2) was conducted on another Western hemlock tree (tree 411; DBH = 52 cm). Six litres of diluted Brilliant Blue dye (5 g/l) were sprayed on the tree over a 2.5 hour period. This represents the amount of stemflow that was measured during a 50 mm event for a similar sized hemlock tree (tree 306; DBH = 50 cm; Chapter 2). The excavation began only 1 meter from the tree because in SIE 1 blue dye was only found near the tree. The excavation occurred in slices 20 cm apart, increasing to 10 cm apart as the excavation moved closer to the tree and was completed in 1 week.

A throughfall infiltration experiment (TIE) was completed in August 2011. 40 litres of diluted Brilliant Blue dye were sprayed evenly on a 0.81 m² soil patch free of large shrubs and trees over a 3 hour period using a backpack sprayer, also representing a 50

mm event. The excavation began 10 cm into the sprayed plot to avoid edge effects; excavation slices were 10 – 20 cm apart and was completed in 5 weeks.

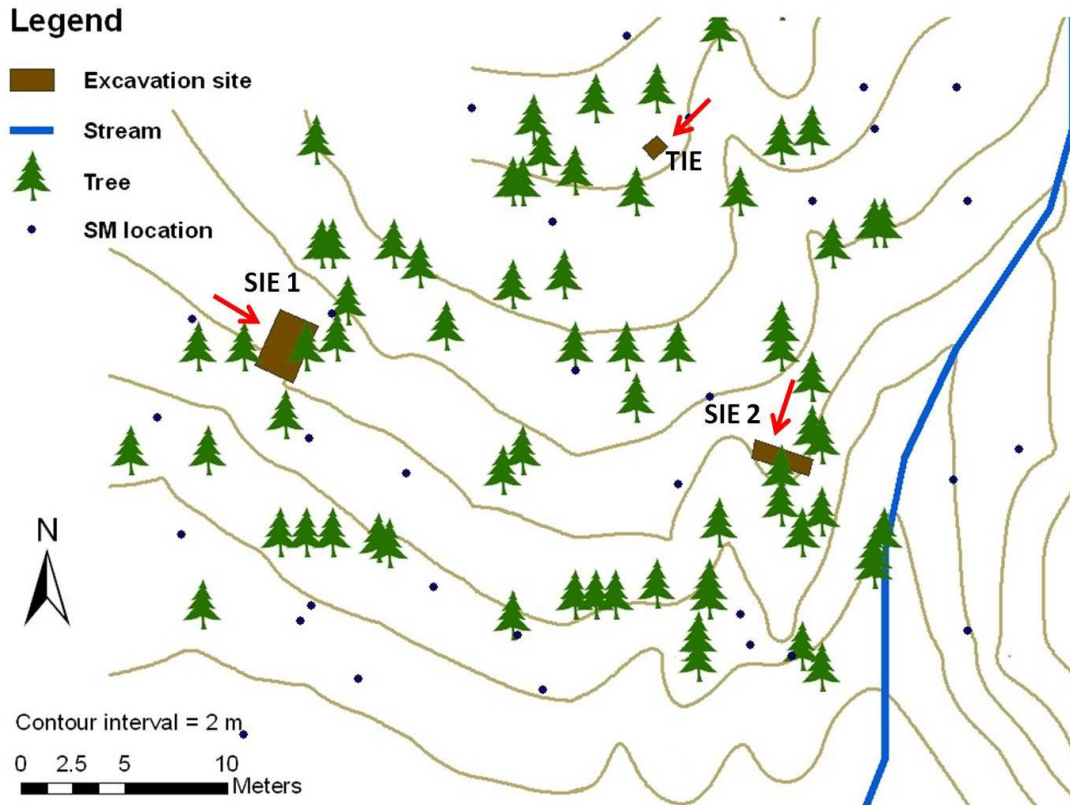


Figure 3.1: Locations of blue dye experiments. Red arrows show the direction in which the excavation occurred in. Stemflow excavation 2 (SIE 2) is oriented in the upslope/ downslope direction in relation to the stream, whereas stemflow excavation 1 (SIE 1) and throughfall excavation (TIE) are oriented perpendicular to the overall watershed slope. SM location = soil moisture measurement location.

The detailed field notes and scaled drawings were analyzed to analyze the blue dye patterns. Each square in the scaled drawings represented a 10 cm by 10 cm area in the soil profile. For every 10 cm of depth (starting from the surface), blue squares were counted and divided by total number of squares that represented the width of that subsection of the soil profile to determine the fraction of soil that the blue dye occupied. The widths of the profiles up to tree ($x = 0$ m) were 160 cm for SIE 1, 200 cm for SIE 2, and 90 cm for TIE. However, the widths decreased beyond the tree for SIE 1 and SIE 2 because these profiles only represented the downslope half of the excavation. Direct

analysis of the photos using Matlab or other software, as done in other studies (e.g. Weiler and Fluhler, 2004; Bachmair et al., 2009; Bogner et al., 2010), was not possible. Large roots (up to 40 cm in diameter) and large boulders (> 1 m in diameter) caused significant shadows in the photographs and restricted the view, resulting in poor quality photographs and difficulty in processing the images (Figure 3.2). Instead, the detailed notes, drawings, and photos were used to digitize the location of all blue dye patches and rocks >2 cm in diameter in Google Sketchup ®.

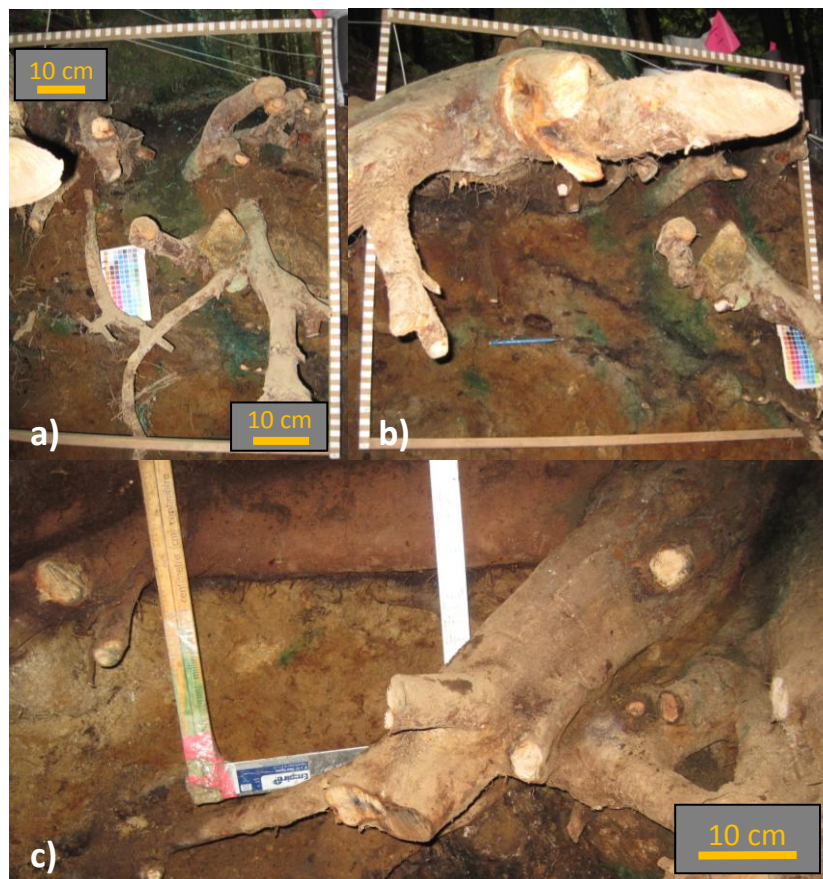


Figure 3.2: Large roots obstructed the view and limited the ability to automatically detect the locations of blue pixels. a) and b) are from SIE 1. b) Scale of wooden frame = 1m x 1m. c) is from SIE 2.

3.4. Results

3.4.1. Stemflow infiltration experiment 1

In stemflow infiltration experiment 1 (SIE 1; tree 601), blue dye was observed on live and dead roots, inside dead roots, around rocks, and in the soil matrix. Maximum observed depth of blue dye was 122 cm, approximately 9 cm above the bedrock (Figure 3.3 and Figure 3.5). Subsurface flow was observed along the bedrock during the excavation and may have leached the blue dye from the soil above or on the bedrock.

Lateral flow of stemflow was confined within 50 cm of the tree, with the exception of one location at 55 – 65 cm depth (~100 cm from the tree). Stemflow water preferentially flowed to the downslope side of the tree (Figure 3.3). Stemflow flowed through the organic layer in the top 10 cm of the soil profile directly around the tree before being funnelled between roots or along roots deeper into the soil (Figure 3.4). There was a strong bimodal distribution of blue dye with depth, with a higher occurrence of blue dye at approximately 20 cm and 70 cm below the soil surface, and a higher prominence at 70 cm than at 20 cm (Figure 3.5). A dense clay layer was observed below these depths. As the excavation moved 30 cm beyond the tree, blue dye bypassed the top 30 cm of soil, became very prominent at 50 - 90 cm depth, and no longer followed the bimodal distribution seen on the other side of the tree (Figure 3.3d, Figure 3.4b, and Figure 3.5).

3.4.2. Stemflow infiltration experiment 2

In stemflow infiltration experiment 2 (SIE 2; tree 411), lateral flow of stemflow was confined within 60 cm of the tree (Figure 3.6). Upslope and downslope differences were minimal compared to those in SIE 1 (Figure 3.6c and d vs. Figure 3.3). Blue dye was found frequently at 40 cm and 70 cm below the soil surface, above dense clay layers. However, blue dye was also prevalent at the soil surface (Figure 3.6; Figure 3.7).

Stemflow infiltrated through the top 10 cm of the organic layer and then travelled along roots (and on occasion rocks) to deeper soil layers, causing stemflow to bypass much of the matrix (Figure 3.8). Maximum infiltration depth was 77 cm below the soil surface, approximately 14 cm above the bedrock (Figure 3.6e). Blue dye in experiment 2 was observed on live and dead roots, inside dead roots (Figure 3.8; Figure 3.9), around rocks, and in the soil matrix (Figure 3.10). More dye appeared to flow along roots than through the soil matrix (Figure 3.8).

3.4.3. Throughfall infiltration excavation

In the throughfall infiltration experiment (TIE), infiltration was dominated by matrix flow but some funneling was also observed, resulting in a steady decline in blue dye occurrence with depth (Figure 3.11 – Figure 3.12). Some lateral flow above a dense clay layer was observed for slices 4 and 6 at a depth of 40 cm, (Figure 3.13). Maximum infiltration depth was 85 cm below the soil surface, approximately 6 cm above the bedrock (Figure 3.12; Figure 3.14). Throughfall generally moved through the soil matrix, however, it also flowed around rocks and roots, and through dead roots (Figure 3.11; Figure 3.14). Stemflow in the blue dye patch circled in Figure 3.14a flowed through a dead root and spread into the soil matrix below (close up in Figure 3.14b).

Although blue dye was sprayed evenly across the soil surface during TIE application, there was variation in blue dye presence between profiles (Figure 3.12). The upslope profiles had less dye at depth than the downslope profiles. This could be due to channelling of throughfall in the litter layer (thatched roof effect) and surface layers. Blue dye also appeared to flow preferentially to the west side of the throughfall infiltration plot (Figure 3.11; Figure 3.13). There were remnants of a decaying fallen tree and large rocks in the upper layers of the soil, particularly on the east side of the plot, which could decrease the flow into deeper soil layers and divert flow around these obstacles (Figure

3.15). There was also a live tree root on the east side of the plot that appeared to divert throughfall away from deeper soil layers (Figure 3.13). The combination of these factors led to more blue dye on the west side of the plot.

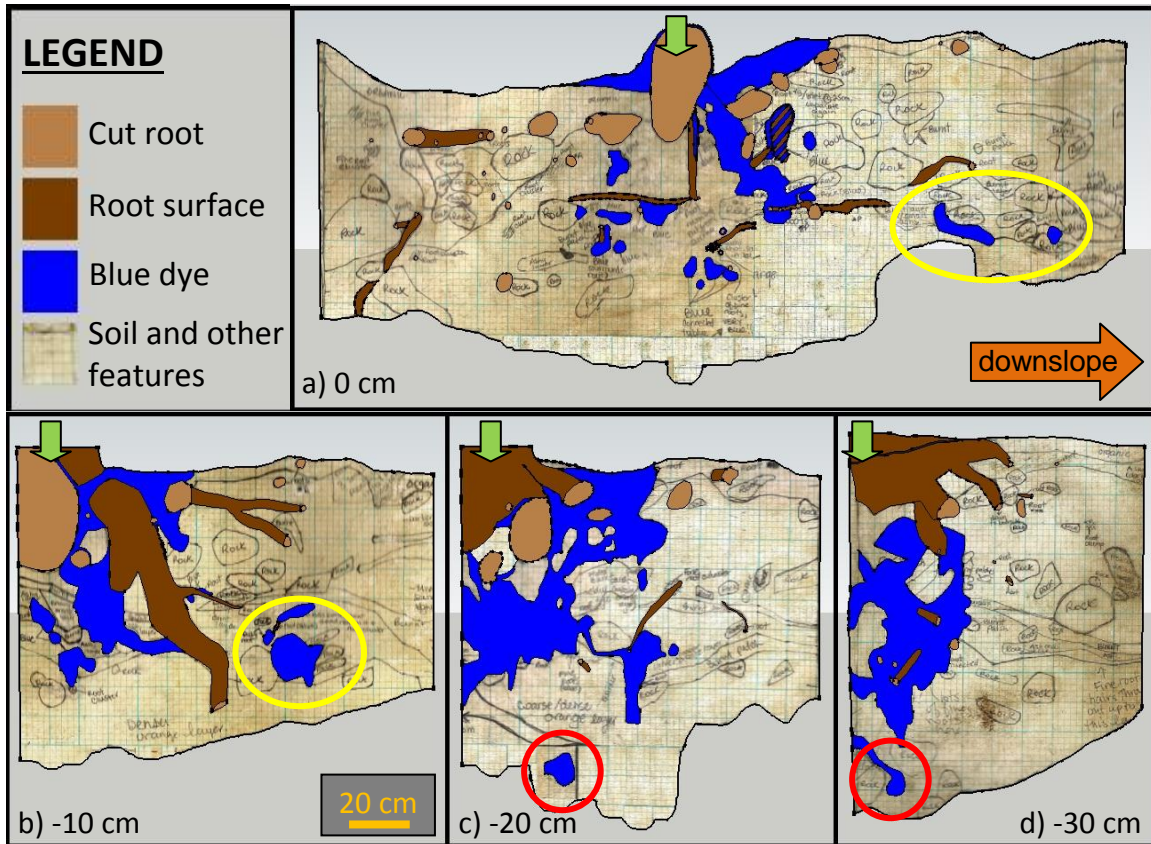


Figure 3.3: Diagrams drawn in Google Sketch-up for SIE 1. Yellow circles in a and b indicate where stemflow flowed laterally downslope beyond 50 cm from the tree. Red circles in c and d indicate maximum stemflow infiltration depth at 122 cm below the surface. Sites to the west of the tree are indicated by positive distances, while sites to the east of the tree are indicated by negative distances. The tree stem is located at $x=0$ cm, and indicated by the green arrow. See Appendix B Figure 5.1 for excavation layout.

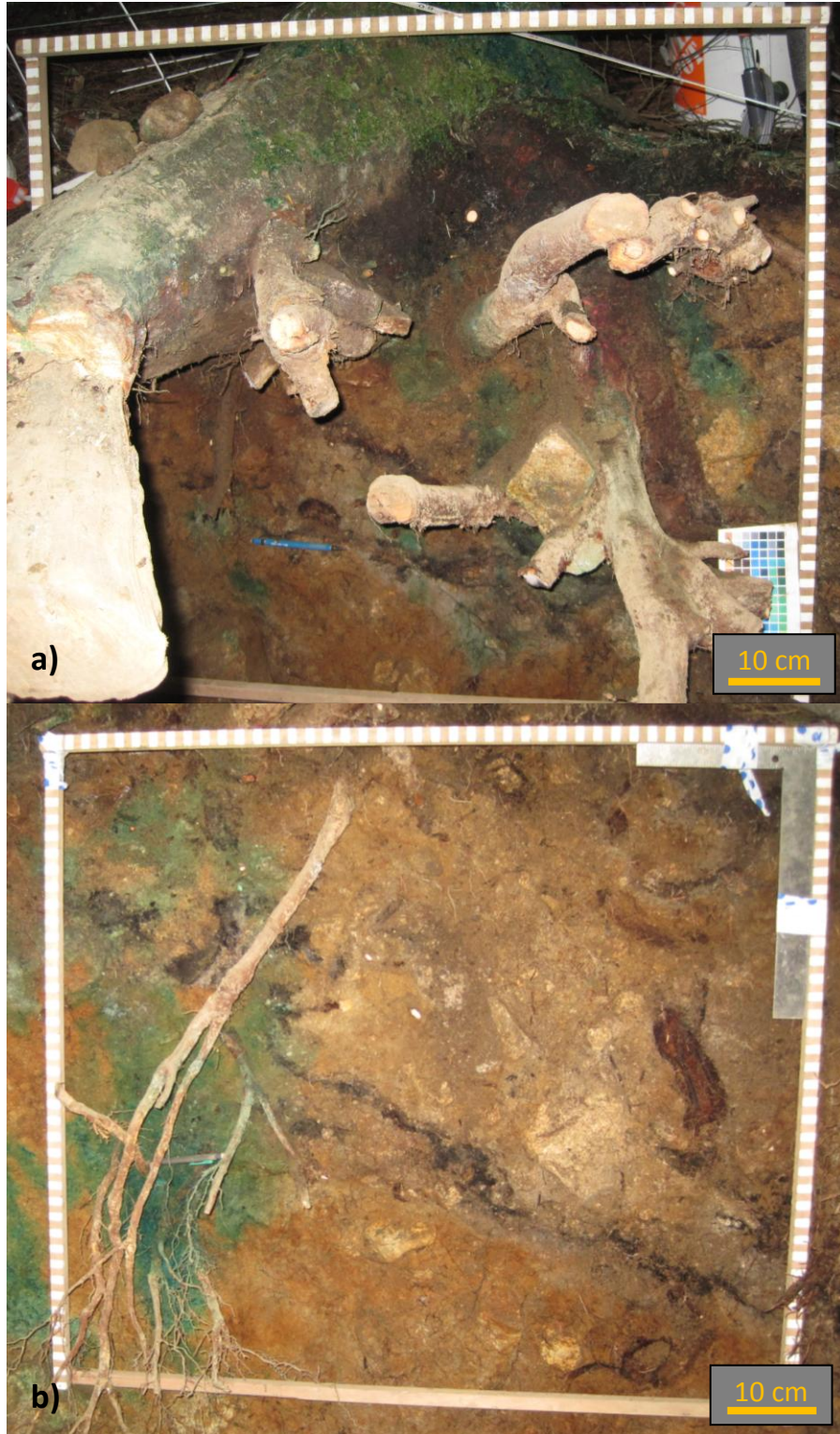


Figure 3.4: Stemflow water between roots and rocks, as well as along roots deeper into the soil at (a) -10 cm from the tree (scale skewed slightly due to camera angle) and (b) -30 cm from the tree for SIE 1; Frame is 1m x 1m.

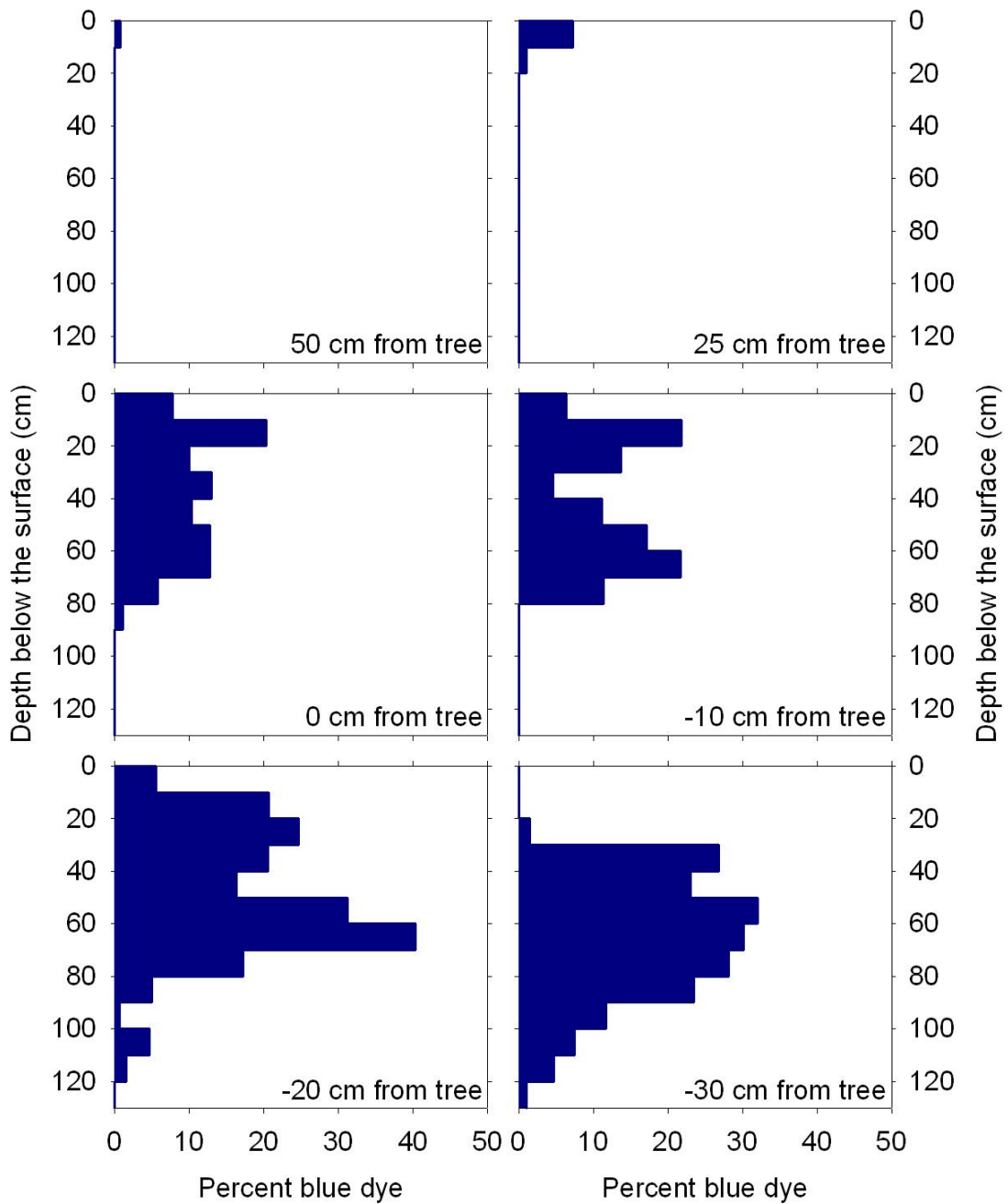


Figure 3.5: Percent blue dye as a function of depth and distance from the tree for SIE 1. Sites to the west of the tree are indicated by positive distances, while sites to the east of the tree are indicated by negative distances. The tree stem is located at $x=0$ m. The width of the excavation was 160 cm, except for excavations east of the tree (-10 cm, -20 cm, and -30 cm), for which the width was 140 cm, 120 cm, and 90 cm, respectively.

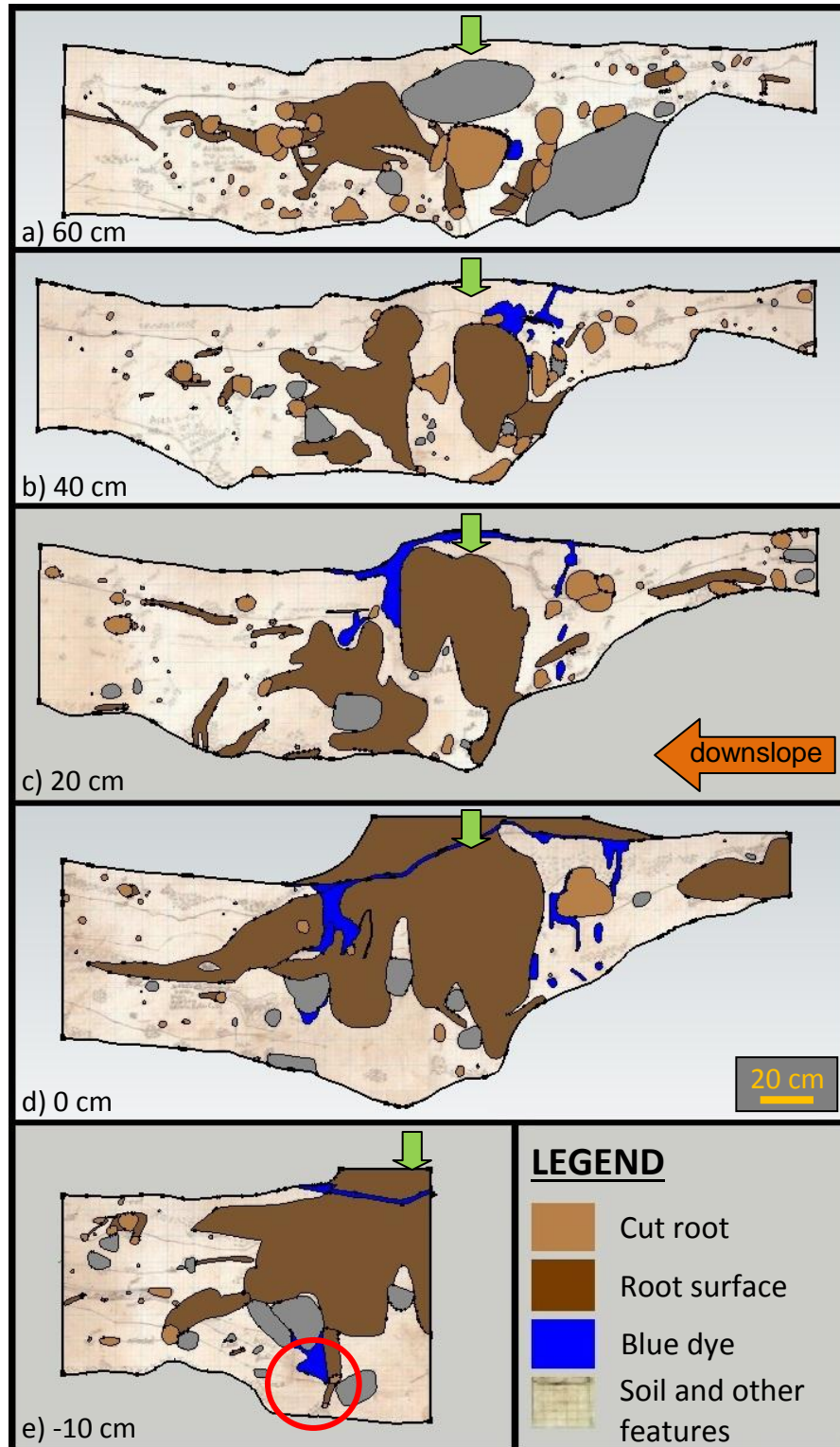


Figure 3.6: Diagrams drawn in Google Sketch-up for SIE 2. Green arrow indicates tree location. Stemflow was confined within 60 cm of the tree. Flow generally occurred around tree roots and rocks. The red circle in e indicates the maximum stemflow infiltration depth at 77 cm. A negative distance represents an excavation profile on the east side of the tree. See Appendix B Figure 5.2 for excavation layout.

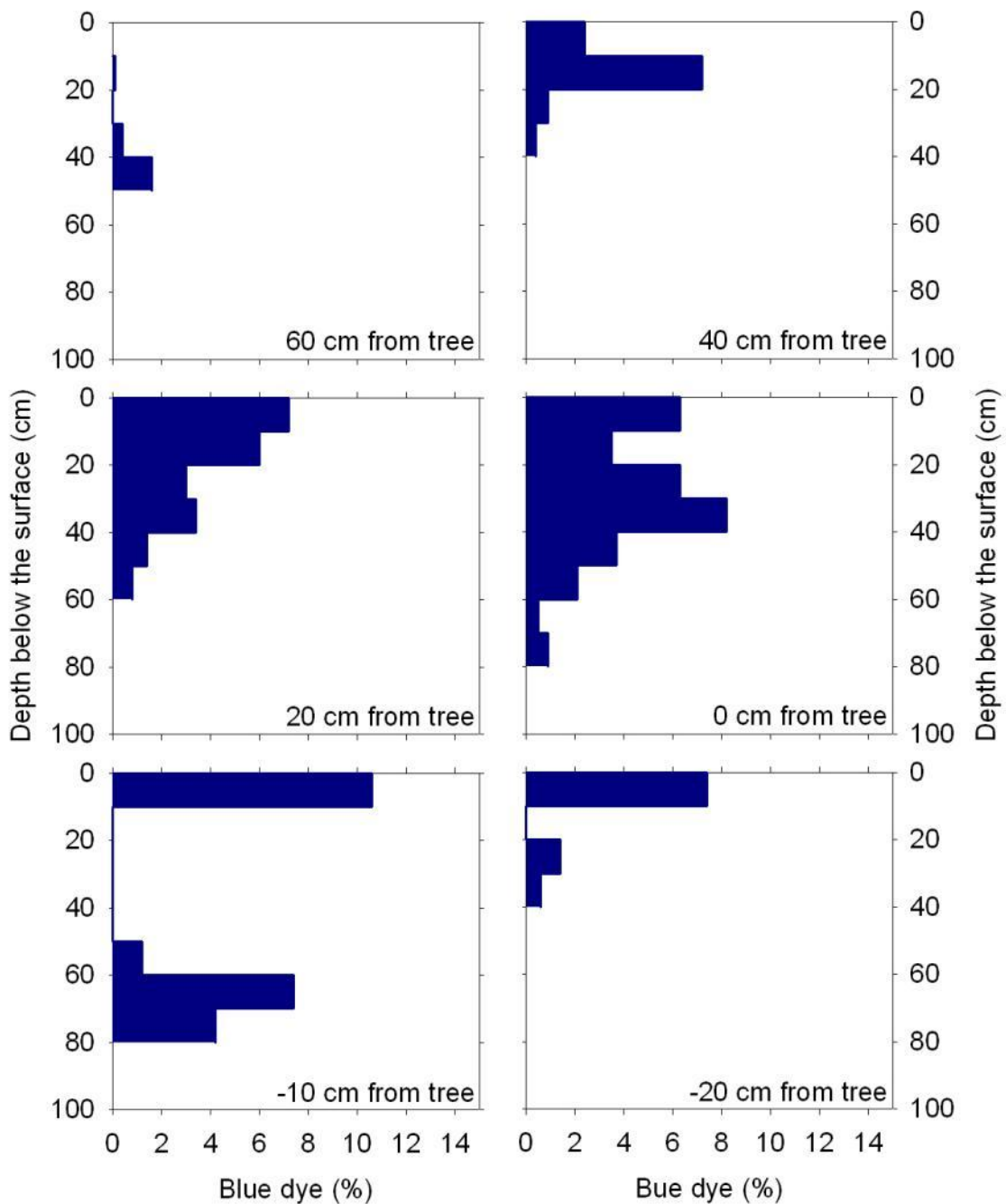


Figure 3.7: Percent blue dye as a function of depth and distance from the tree for SIE 2. Sites to the west of the tree are indicated by positive distances, while sites to the east of the tree are indicated by negative distances. The tree stem is located at $x=0$ m. The width of the excavation was 200 cm, except for excavations on the east side of the tree (negative distances), for which the width was 100 cm.



Figure 3.8: Stemflow infiltrated along roots for SIE 2. Dye present in organic surface layer and along roots to depth. Scale of frame is 1 m x 0.3 m.



Figure 3.9: Blue dye stains inside a decaying root (SIE 2). Stemflow water flowed laterally through the decaying root.

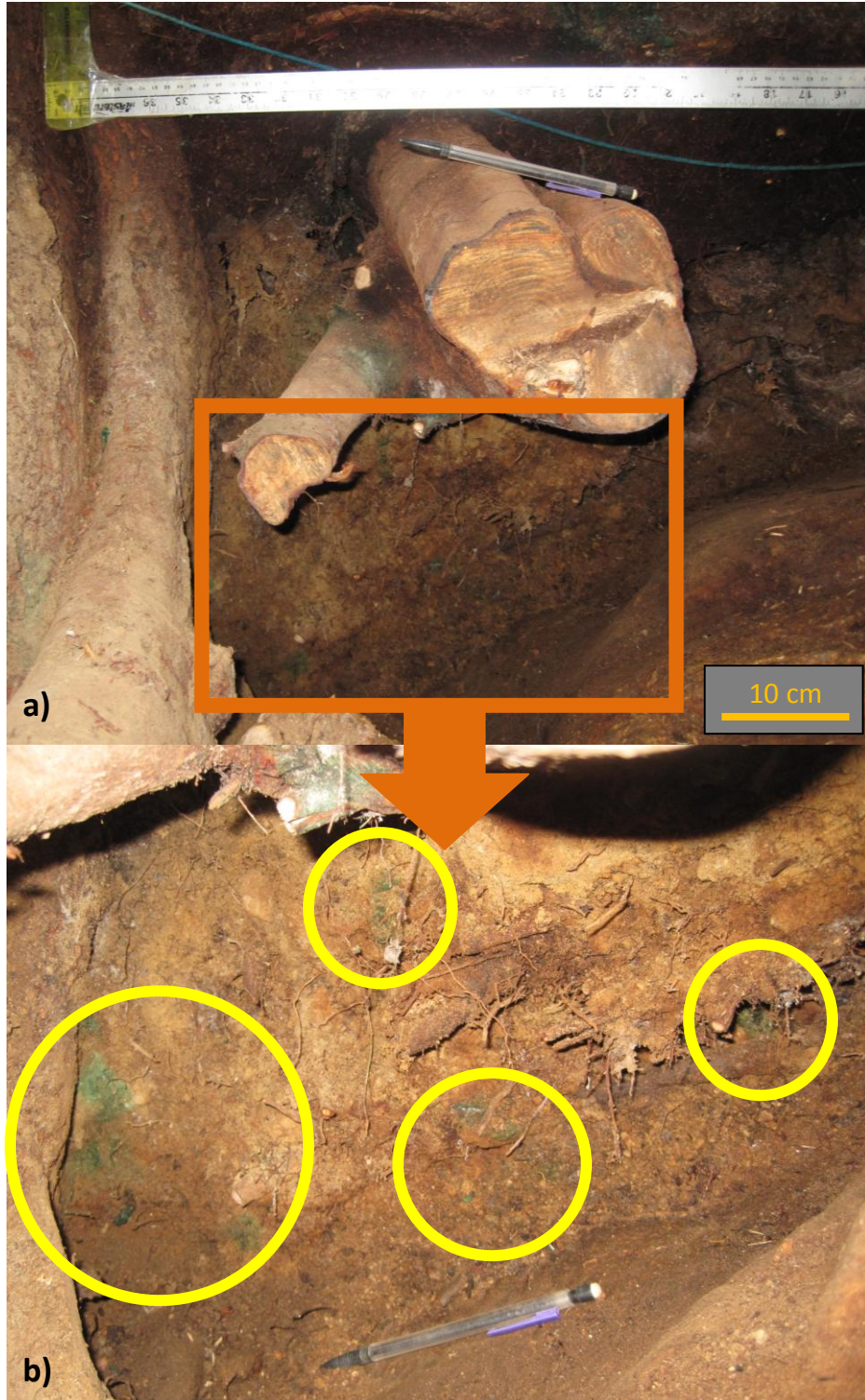


Figure 3.10: Stemflow water flows along roots and into the soil matrix along fine roots, or through the soil matrix in SIE 2. Orange box in (a) is zoomed in for (b). Yellow circles highlight light blue staining.

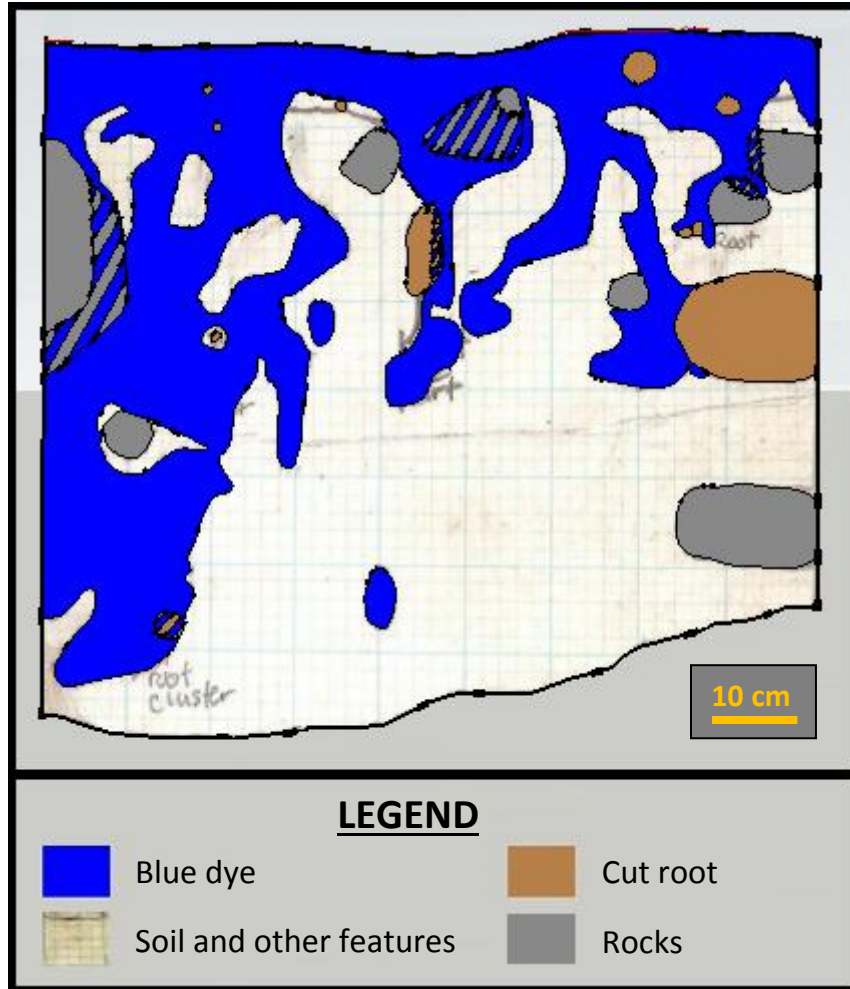


Figure 3.11: Throughfall infiltrated through the soil matrix and decreased steadily. See Appendix B Figure 5.3 for excavation layout.

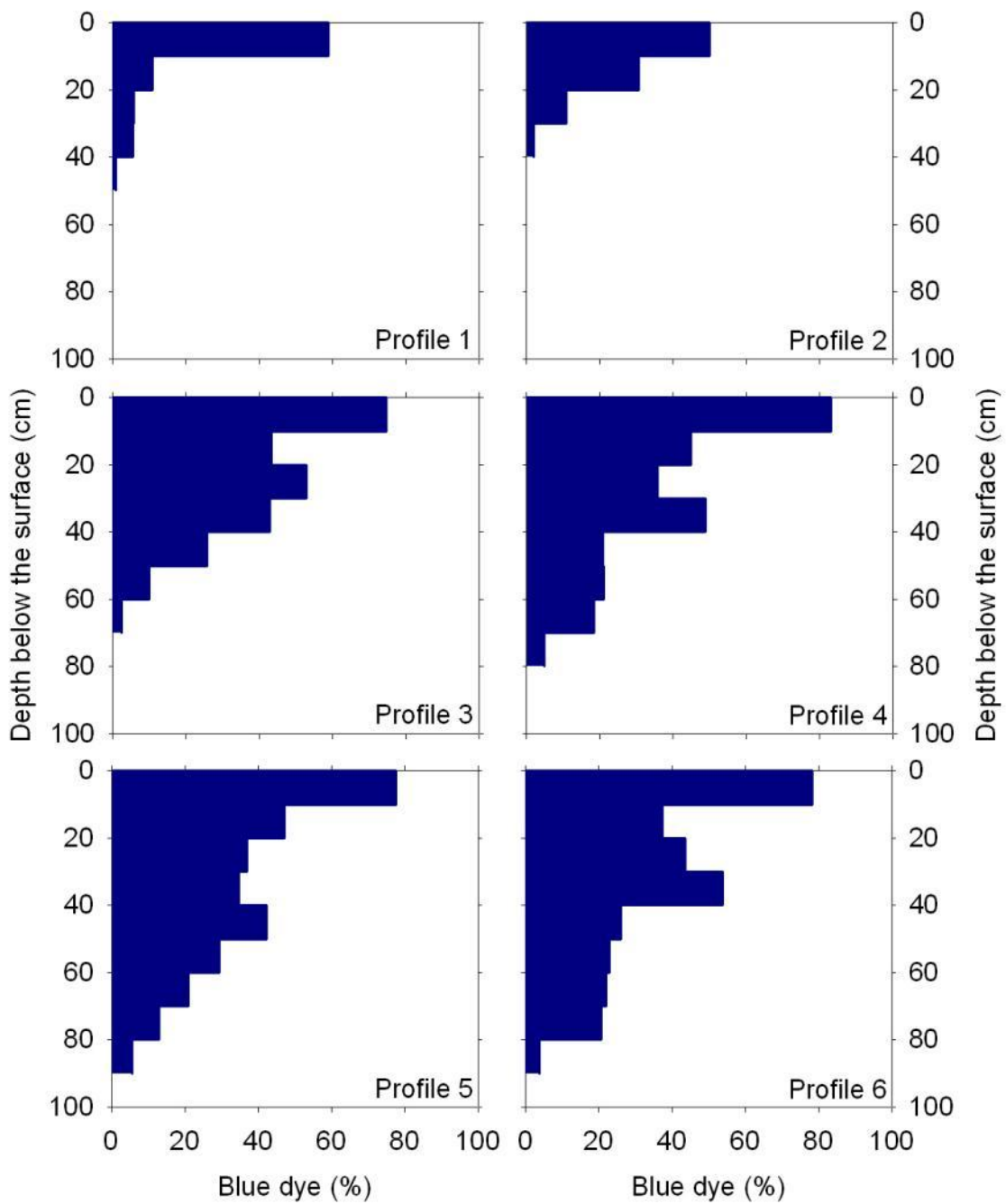


Figure 3.12: Percent blue dye as a function of depth for TIE. Profile 1 is located the furthest upslope, while profile 6 is located the furthest downslope. The width of the excavation was 90 cm.

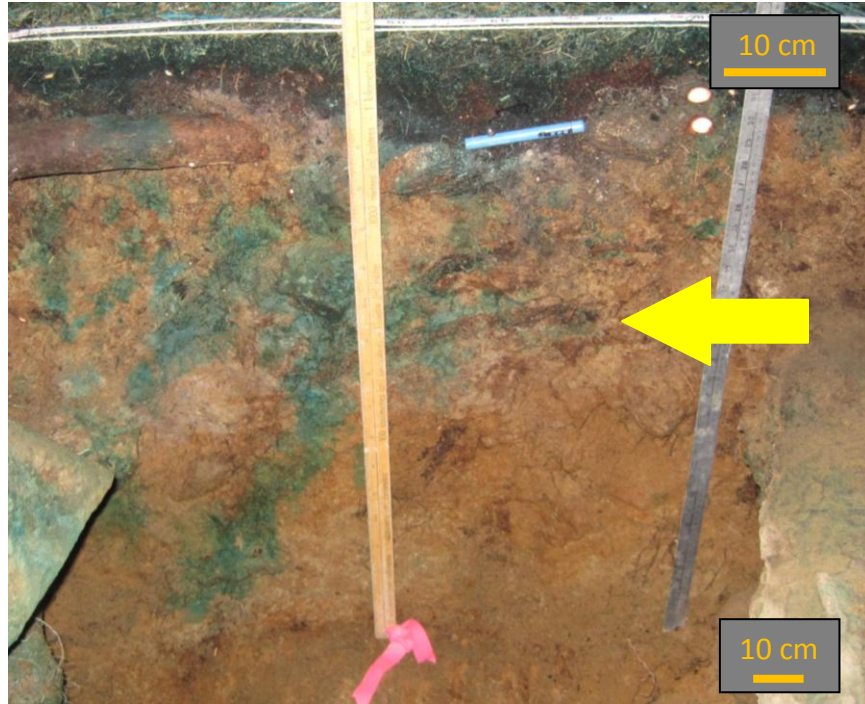


Figure 3.13: Lateral flow at 40 cm depth (at the yellow arrow) in TIE, profile 6. Scale distorted vertically.



Figure 3.14: a) Flow along a decayed root in profile 5 of the TIE, where the maximum infiltration occurred at 85 cm (outlined in orange). Scale distorted vertically. b) Close up of infiltration through decayed root and fine roots, into matrix below.



Figure 3.15: Decayed tree, active roots, and rocks directing vertical flow, TIE profile 2.

3.5. Discussion

3.5.1. Stemflow infiltration and flow pathways

The stemflow infiltration experiments generally showed a bimodal distribution in the location of blue dye with depth, with a higher prominence of dye deeper in the soil. This suggests that infiltration of stemflow increases soil moisture at depth more than at the surface. Stemflow bypassed surface soil layers via preferential flow pathways along roots, which is consistent with results from Liang et al. (2011). However, in this study, it appears that stemflow also moved through loose topsoil between roots next to the tree (Figure 3.4a; Appendix B Figure 5.4). Blue dye was visible along fine root hairs and medium roots as well as in the soil around the end of these roots (Figure 3.14). These results correspond with the results in Bogner et al. (2010) that showed for throughfall dye experiments that water flowed along macropores and into the surrounding matrix.

A dense clay layer at approximately 40 cm and 70 cm depths, which corresponded to the beginning of the next soil horizon, caused much of the stemflow to

remain above these depths and flow laterally along it, particularly in SIE 1 (Figure 3.3; Figure 3.13; Appendix B Figure 5.5). Few roots were able to grow through the clay layers, but where roots were able to grow through it, it was along these roots that stemflow was able to infiltrate deeper into the soil. Blue dye was also found in cracks in the upper clay layer without roots. In those locations, stemflow was able to infiltrate deep into the soil layers as well. Some lateral flow was visible at the confining clay layer at 40 cm in the TIE; however, the effects were not as pronounced as in the stemflow experiments.

Despite the strong bimodal distribution of blue dye, a small amount of blue dye was visible in the top 10 cm of the soil in both SIE 1 and SIE 2. Martinez-Meza and Whitford (1996) found similar results for creosotebush (*Larrea tridentata*) and mesquite (*Prosopis glandulosa*) shrubs in New Mexico, where dye would flow through the top 10 cm of soil but solely along roots thereafter. However, for tarbush (*Flourensia cernua*) more Rhodamine-B dye flowed into the soil matrix, likely because the soil contained more clay than soil around the other bushes (Martinez-Meza and Whitford, 1996). In SIE 1, there was more interaction between the soil matrix and the roots than in SIE 2, where stemflow primarily infiltrated along roots. Soils around trees 601 and 411 were similar, with identical clay layers at depth so it is unlikely that soil textural differences caused more interaction in SIE 1. Furthermore, where roots were present in the TIE, there were similar interactions between the soil matrix and root flowpaths as in SIE 1. Differences between flowpaths in SIE 1 and SIE 2 could be caused by physical differences. Tree 411 of SIE 2 (DBH = 52 cm) was much bigger than tree 601 in SIE 1 (DBH = 29 cm) and had bigger roots. Furthermore, there are other trees within 2 m of tree 411, whereas trees surrounding tree 601 were more than 3 meters away (Figure 3.1). Soil depth below tree 411 was also much shallower (between 20 cm to 90 cm) than below tree 601 (between

60 cm to 130 cm). The combination of these factors caused roots to be more confined within the soil beneath tree 411 than beneath tree 601 (Appendix B Figure 5.6 vs. Figure 3.4b). The confined nature of the roots of tree 411 likely caused stemflow to flow further through the surface layers than for tree 601. Blue dye was able to infiltrate in the top 10 cm but matrix flow was blocked by rocks and roots, causing blue dye to primarily flow along roots to depths of 40 and 80 cm, bypassing the matrix. For tree 601 (SIE 1), stemflow was not contained as much. It was able to infiltrate into the soil and flow through the matrix as well as along tree roots. As a result, there was more interaction between preferential flowpaths and the surrounding matrix for SIE 1 than for SIE 2. Because stemflow was not contained between roots and rocks, there was also a greater downslope occurrence of dye for SIE 1 than for SIE 2.

For SIE 1, blue dye was found up to a depth of 122cm. This dye appeared to flow along a tree root through the dense clay layer. This could be evidence of stemflow causing enhanced recharge (Liang et al., 2011). Blue dye was not visible on the bedrock but it is possible that the blue dye that reached this layer was washed away by subsurface flow during the excavation process or was too diluted to be detected. However, blue dye was found just above the bedrock for all experiments. As a result, it appears that stemflow does not actually allow water to infiltrate much deeper into the soil than throughfall for this study site.

Stemflow appeared to flow preferentially through the soil to the downslope side of the tree for SIE 1. This corresponds to the results from Liang et al. (2011) that showed that stemflow mainly flowed to the downslope side of the tree. As described in Chapter 2, stemflow flows primarily on the north side (generally upslope) of the trees in this forest stand, except during large, long duration storms. Blue dye was sprayed evenly around the tree trunk in order to mimic a high intensity, large event that wets the entire surface

of the tree. In the *Stewartia monadelphica* forests of Japan, Liang et al. (2009b) determined that significantly more stemflow flowed down the downslope side of the tree than the upslope side, which could have a larger impact on soil moisture downslope from the tree compared to this study. Dye patterns in SIE 1 do appear to be more prevalent on the downslope side of the tree despite stemflow being sprayed on the entire tree stem. Results may differ slightly if blue dye was sprayed only on the upslope side of the tree, to mimic a smaller precipitation event.

3.5.2. Comparison of throughfall and stemflow infiltration

The throughfall infiltration experiment generally showed a steady decrease in dye presence with depth. This is consistent with other studies that looked at infiltration in forest soils (Bachmair et al., 2009; Bogner et al., 2010). Throughfall was able to infiltrate deep into the soil along live and dead roots. This is similar to the results of Liang et al. (2011) who showed that throughfall was able to flow through the same preferential flow pathways as stemflow; however, it took longer and did not infiltrate as deep as stemflow in their study. Much of the blue dye that was able to infiltrate deep into the soil in the throughfall experiment in this study came from either preferential flow along small or dead roots or from enhanced flow in less compacted areas of the soil. Fine root hairs with blue dye were observed throughout the soil profiles and corresponded with locations where the soil matrix was also dyed (Appendix B Figure 5.7; Figure 3.4b; Figure 3.14). Thus, tree roots were often responsible for distributing stemflow water and throughfall water deep into the soil in a dense forest. These results do not correspond with the result from Martinez-Meza and Whitford (1996) who found that stemflow was able to infiltrate deeper into the soil than throughfall. Liang et al. (2011) also found that stemflow could infiltrate deeper than throughfall. Due to the varying soil depth in this study site and because throughfall was not sprayed at the same location as stemflow, it

is difficult to determine if stemflow can significantly increase the maximum infiltration depth. However, even if the maximum infiltration depth is similar for throughfall and stemflow, stemflow may still enhance the rate of groundwater recharge because stemflow intensity is often higher than precipitation intensity (Chapter 2). Liang et al. (2011) found that stemflow infiltrated to depth faster than throughfall.

The preferential flowpaths were studied in the dry summer months to ensure that blue dye would be visible in the dark soils. The connectivity of preferential flow pathways decreases in dry seasons (Sidle et al., 2000), decreasing the distance water travels through preferential flowpaths. Therefore, stemflow may have travelled further from the tree due to the larger connectivity of flow pathways if these experiments had been conducted in the wet season. Therefore differences between TIE and SIE may have been more pronounced if the experiments had been conducted in the wet season.

3.6. Conclusion

Previous studies have shown that even though stemflow is only a small fraction of net precipitation (chapter 2), it can be important for groundwater recharge, soil moisture dynamics, and plant water uptake. However, few studies have attempted to visualize the flow pathways of stemflow once it infiltrates into the soil and how this differs from throughfall flow pathways. This study compared infiltration patterns of throughfall with infiltration patterns of stemflow in a mature forest in coastal British Columbia using blue dye to gain a better understanding of flow pathways in forest soils. In general, stemflow flowed through preferential flow pathways around roots, whereas throughfall flowed through the matrix and along (fine) roots. The preferential flow pathways allow stemflow water to bypass the soil matrix and cause a larger increase in soil moisture at depth than at the surface. Lateral flow of stemflow was observed above a dense clay

layer and along tree roots. However, stemflow was contained within 50 – 100 cm of the tree. Although stemflow appeared to infiltrate deeper into the soil (122 cm) than throughfall (85 cm), compared to the soil depth there was little difference. As a result, the maximum infiltration depth is not clearly affected by the source of water (stemflow vs. throughfall). However, groundwater recharge may be enhanced during bypass flow of stemflow due to higher stemflow intensities than precipitation intensities. The distribution of stemflow deep in the soil, around small and fine roots suggests that plants may be able to use this water during dry conditions, when evaporation limits the use of surface water.

4. Surface soil moisture around hemlock trees

4.1. Introduction

In the absence of vegetation, soil moisture dynamics are controlled by precipitation, evaporation, drainage, and lateral flow (Ziemer, 1968). Trees influence soil moisture dynamics by partitioning precipitation into interception, throughfall, and stemflow, and by water uptake (Ziemer, 1968). D'Odorico et al. (2007) suggested that plants also influence soil moisture by increasing soil infiltration capacity and canopy shading, which decreases evaporation. However, the effects of trees on soil physical parameters, such as bulk density, and the resultant water capacity depend on the species (Alameda et al, 2012).

Spatial variation in throughfall beneath a tree influences the soil moisture patterns around a tree (Alva et al., 1999). Precipitation wets branches and leaves before it begins to flow towards the tree stem; branch nodes and leaf fluttering can cause flowpaths to become overwhelmed and can cause drip to occur (Crockford and Richardson, 2000; Xiao et al., 2000). Despite being irregular in space, these throughfall patterns are relatively stable in time (Raaijmakers et al., 2002; Keim et al., 2005). Alva et al. (1999), for instance, showed that drip points are important throughfall contributors and can cause a concentration of precipitation, which increases soil moisture beneath these drip points. Voigt (1960) found an irregular distribution of precipitation beneath the forest canopy and related it to crown drip, interception, and stemflow, yet, he also showed a more even distribution of soil moisture due to the redistribution of precipitation by wind.

Coenders-Gerrits et al. (2012) used a hillslope hydrological model to show that throughfall hotspots influenced soil moisture patterns during and immediately after a precipitation event. However, bedrock topography had a stronger influence on soil moisture patterns after a storm than throughfall, especially on steeper slopes (Coenders-Gerrits et al., 2012). Other studies have shown that soil moisture patterns do not directly reflect throughfall patterns (Raat et al., 2002; Shachnovich et al., 2008). Shachnovich et al. (2008) found that throughfall was not related to soil moisture changes in the upper 15 cm of the soil, even when transpiration was taken into account. They suggested that the horizontal redistribution of throughfall in the soil matrix or above the surface might influence soil moisture patterns more than the spatial variation in throughfall (Shachnovich et al., 2008). Furthermore, Raat et al. (2002) showed for a Douglas fir (*Pseudotsuga menziesii*) stand in The Netherlands that forest floor thickness and drainage to the mineral soil, as well as throughfall, determined the soil moisture pattern. Due to the variation in results of these studies, soil moisture dynamics under trees needs to be further studied.

Several studies have shown that stemflow is an important factor that influences soil moisture dynamics around trees (Pressland, 1976; Li et al., 2009; Liang et al., 2011). The concentrated input of precipitation at the base of the tree where preferential flowpaths are located has significant impacts on soil moisture patterns around trees and shrubs (Specht, 1957; Pressland, 1976; Durocher, 1990; Li et al., 2009) and increases soil moisture downslope from the tree (Liang et al., 2007, 2009b, 2011). In fact, in forested sites stemflow inputs may be more important for soil water dynamics than soil physical parameters due to the high infiltration capacity of forest soils (Durocher, 1990). Li et al. (2009) compared soil moisture around shrubs with and without stemflow in a semi-arid region of China and found that stemflow increased soil water content by 10 –

60% and 10 – 140% for *Salix psammophila* and *Hedysarum scoparium*, respectively, compared to when stemflow was removed from the system (Li et al., 2009). Liang et al. (2011) similarly showed larger increases in soil moisture downslope from the tree when stemflow was allowed to enter the soil but similar soil moisture increases upslope and downslope from the tree when stemflow was removed from the system. However, a larger soil moisture response was still present at the point immediately downslope from the tree when stemflow was removed, which was attributed to the root structure and preferential flowpaths around the tree (Liang et al., 2011).

The increase in soil moisture due to stemflow decreases with distance from the tree (Specht, 1957; Pressland, 1976; Durocher, 1990). Specht (1957) determined that shrubs influenced soil moisture at the surface and below the ground due to rain-shadows and stemflow. Pockets of increased soil moisture were located directly below shrubs because of stemflow and reduced evaporation due to shading (Specht, 1957). Pressland (1976) sampled the soil at 0.5, 2 and 4 meters from the tree and found that stemflow only increased soil moisture within approximately 0.5 m of Mulga (*Acacia aneura*) trees in Australia. Results were more pronounced during drier periods because large precipitation events during wetter periods masked the stemflow effect (Pressland, 1976). Durocher (1990) showed that stemflow influenced the soil near and beneath sweet Chestnut (*Castanea sativa*) trees in England more than between trees as soil water pressure did not significantly change at 1.2 m or more from the tree. It is likely that stemflow primarily flowed vertically into the soil, thus only affecting soil moisture close to the tree (Durocher, 1990).

Stemflow can increase soil moisture at depth more than at the surface because stemflow tends to bypass the surface soil layers (Specht, 1957; Pressland, 1976; Gonzalez-Hidalgo and Bellot, 1997; Liang et al., 2011; Chapter 3). Liang et al. (2011)

found that soil moisture increased faster at depth beneath tall *Stewartia monadelphica* trees due to macropores delivering stemflow water to deeper soil layers more rapidly than throughfall. Gonzalez-Hidalgo and Bellot (1997) compared a cleared and uncleared plot of rosemary shrubs (*Rosmarinus officinalis*) in northwestern Spain and found that the shrubs were important for the redistribution and concentration of water below the soil surface. Events larger than 18 mm caused a similar response at 15 cm depth for cleared and vegetated plots; however, significant differences were seen at a depth of 30 cm. Larger soil moisture changes at 30 cm depth in the uncleared plot were attributed to stemflow (Gonzalez-Hidalgo and Bellot, 1997). Li et al. (2009) reported increases in soil water content at all depths below *Salix psammophila* and *Hedysarum scoparium* shrubs, although changes were largest at 60 cm depth.

Event size often determines how soil moisture is influenced by stemflow. Liang et al. (2007) showed that for small events, soil water content and pore water pressure at depth increased significantly only downslope of the tree. Preferential flowpaths were likely responsible for altering soil moisture dynamics deep in the soil (Liang et al., 2007). At all other points (downslope and upslope), changes in soil water content occurred near the soil surface due to the slow wetting front movement (Liang et al., 2007). For large events, soil moisture content changed similarly to small events, but pore water pressure increased both upslope and downslope of the tree, with downslope responses being larger and more rapid (Liang et al., 2007). The slope effect on soil moisture dynamics was likely caused by stemflow flowing predominantly on the downslope side of the tree (Liang et al., 2007), although this is not observed in all forests (Chapter 2).

Antecedent moisture conditions also determine how stemflow influences soil moisture. Pressland (1976) showed that when antecedent soil moisture was high, the effects of stemflow on surface soil moisture were masked; however, soil moisture at a

depth of 120 – 135 cm was higher near the tree. Ziemer (1968) also showed that during the wet season, soil moisture patterns were nearly uniform. However, this pattern was not persistent; during the dry season soil moisture increased with distance from the tree, which was attributed to water uptake (Zierner, 1968). Specht (1957) found pockets of higher soil moisture at varying depths directly beneath *Xanthorrhoea australis* and *Banksia ornata* trunks after precipitation, regardless of the antecedent conditions, although this was less obvious during wet conditions.

Although individual trees control soil moisture dynamics around a tree (Schume et al., 2003), forest composition (tree species) strongly influences the overall soil water balance (Schume et al., 2003; Jost et al., 2005). For instance, Jost et al. (2005) showed that spruce (*Picea abies*) trees start to transpire earlier in spring than beech (*Fagus sylvatica*) trees, which resulted in drier conditions surrounding the spruce trees. However, as the growing season progressed, beech trees started to transpire and spruce trees slowed their transpiration rates, which resulted in a more even soil moisture distribution (Jost et al., 2005). Schume et al. (2003) suggested that the even distribution of soil moisture during dry periods was also due to preferential growth of roots into wetter areas, thereby utilizing pockets of higher water content. In the wet season, tree architecture was the primary control on soil moisture patterns, although soil properties such as macropores also influenced soil moisture patterns (Schume et al., 2003).

4.2. Objectives

It is important to understand soil moisture dynamics around a tree, in order to understand plant water uptake (Schume et al., 2003), nutrient dynamics (Chang and Matzner, 2000), as well as ecohydrological responses to drought conditions (Li et al., 2009). Although stemflow and throughfall have been shown to influence soil moisture

patterns around a tree, the effects of stemflow on soil moisture patterns differ with soil depth, storm size, and antecedent moisture conditions. The objective of this study was to understand shallow soil moisture dynamics around hemlock trees in relation to stemflow and throughfall input. To do this, soil moisture was measured at 20 cm depth in multiple transects around three mature hemlock (*Tsuga heterophylla*) trees.

4.2.1. Research questions

- 1) How does stemflow influence surface (0 – 20 cm) soil moisture around hemlock trees in a mature forest in coastal British Columbia?
- 2) How is the spatial variation in throughfall around a tree related to the spatial variation in shallow soil moisture?

4.2.2. Hypotheses

I hypothesized that stemflow would concentrate water at the base of the tree and cause higher surface soil moisture near the tree than further from the tree. Surface soil moisture would also be higher downslope from the tree. I also hypothesized that the spatial variation in throughfall would be correlated with the spatial variation in surface soil moisture. Throughfall would be concentrated in some locations, which would correspond to the locations with higher soil moisture beneath the tree.

4.3. Methods

Soil moisture was measured approximately every 25 cm around 3 Western hemlock trees starting at the tree bole and radiating outward up to 3 m from the tree (Figure 4.1). Hemlock trees were chosen because they represent 40% of the trees in the study site (Chapter 1); the studied trees were chosen based on their location and structure. All trees were located in the lower section of the watershed and were not in

immediate proximity (within 1 m) of other trees to minimize the influence of other trees on surface soil moisture. The selected trees also had little or no epiphyte cover on their bark, relatively straight tree trunks, and no exposed roots at the base of the tree. For each tree, transects were oriented in the upslope and downslope directions (North and South), as well as in other directions (Figure 4.1). Seven transects were located around the stem of tree 411, while tree 409 had 4 transects (Figure 4.1). Trees 409 and 411 are located approximately 5 m from the stream, which resulted in two downslope directions: one downslope in the watershed direction and the other down the local slope. Both trees have a DBH greater than 35 cm (Tree 409: 46 cm; Tree 411: 52 cm), which means that they are classified as “diverters” (funneling ratios < 1, see Chapter 2). The average funneling ratios for a similar sized hemlock tree (Tree 306, DBH: 50 cm) was 0.34 (Chapter 2).

Four transects were located around tree 601 (DBH: 29 cm; Figure 4.1). This tree had an average funneling ratio of 3.51, which means it is classified as a “funneler”. This tree was one of the trees monitored for stemflow using a tipping bucket (Chapter 2), which redistributed stemflow (generally only on the upslope side of the tree) to a point downslope from the tree (i.e. the location of the tipping bucket). This tree was also the site of the first blue dye excavation (SIE 1; Chapter 3). These measurements influenced the period that soil moisture was measured around the tree without any artificial influences. However, it also presents an interesting comparison with the other trees, which were undisturbed and for which stemflow generally flowed down the upslope side of the tree.

Measurements were taken weekly from June 2010 to October 2010 with a 20 cm long time domain reflectometer (TDR) probe (Hydrosense, Campbell Scientific) for trees 409 and 411 and from June 2010 to September 2010 for tree 601. Soil moisture

measurements were also taken weekly at 126 points that were randomly distributed throughout the rest of the 0.9 ha study site from May 2010 to November 2010.

Throughfall was measured with 20 standard rainfall gauges next to the soil moisture transects around tree 409 at the same time as the soil moisture measurements (approximately weekly) to determine small scale variation in throughfall inputs.

Precipitation was measured in a clearing approximately 150 m north of the lower study site.

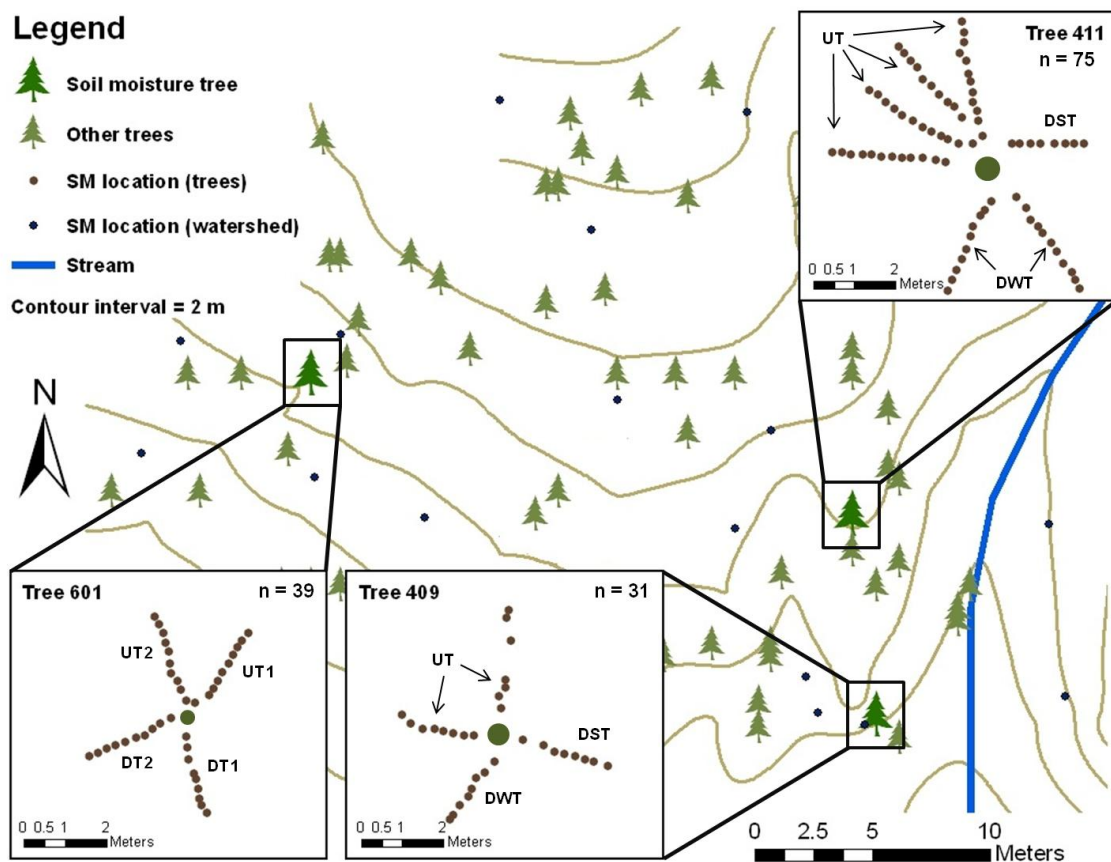


Figure 4.1: Soil moisture measurement locations. Tree trunks are indicated by green circles and are scaled by their DBH. UT = upslope transect; DWT = transect downslope in the watershed direction; DST = transect downslope towards the stream. Only the soil moisture measurements in the lower part of the watershed are shown (n = 16).

4.4. Analysis

4.4.1. Stemflow effects on soil moisture patterns

4.4.1.1. Proximity to tree

Soil moisture data were separated based on location: near tree locations (within 60 cm of the tree) and locations further from the tree (beyond 60 cm). This division was based on the stemflow infiltration observations that showed that blue dye at the surface was only visible within 60 cm of the tree (Chapter 3). Soil moisture values were averaged for each measurement day and time series were compared to determine differences in average soil moisture. Differences between near tree locations and locations further from the tree for each measurement day were tested for significance using a t-test ($\alpha = 0.05$). Differences between watershed average soil moisture and soil moisture near the studied trees were evaluated similarly.

4.4.1.2. Slope effects

Soil moisture data were also separated based on slope location: upslope vs. downslope of the tree. Soil moisture values were averaged for each measurement day and compared to determine if near surface soil moisture is influenced by slope position. Differences between upslope and downslope transects for each measurement day were also tested for significance using a t-test ($\alpha = 0.05$).

4.4.1.3. Mean difference

For all soil moisture locations, the difference from mean soil moisture on that measurement day was calculated. The mean of this difference (MD) was then calculated for each location and plotted by rank (see Figure 4.2 for tree 411). Locations with a mean difference minus one standard deviation above zero were classified as “consistently wet” and locations with a mean difference plus one standard deviation below zero were classified as “consistently dry” (Figure 4.2). Maps of mean difference

(MD) were created to determine if any persistent soil moisture patterns exist. MD was also calculated for all throughfall measurement sites around tree 409.

4.4.2. Throughfall effects on soil moisture patterns

Throughfall and the change in soil moisture between consecutive measurement days for tree 409 were compared to determine if the spatial pattern of the change in soil moisture was related to the throughfall pattern. The spearman rank correlation coefficient was calculated for the relation between throughfall and change in soil moisture for each measurement period and compared to mean and median throughfall and mean and median soil moisture at the start of the measurement period for which the change in soil moisture was determined.

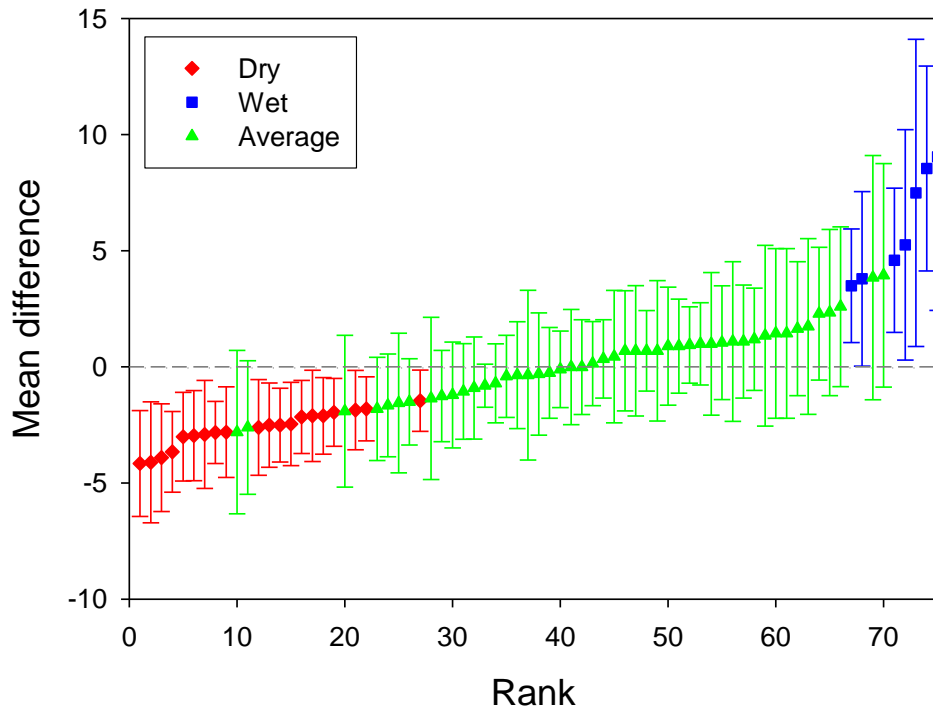


Figure 4.2: The mean difference for soil moisture (%) around tree 411 plotted as a function of rank. The error bar represents the standard deviation of the difference. Locations with a mean +/- one standard deviation above or below the mean were identified as “consistently wet” or “consistently dry”, respectively.

4.5. Results

4.5.1. Watershed average soil moisture

Mean soil moisture for the lower watershed ($n = 27$), where trees 601, 409, and 411 were located, was higher than mean soil moisture around the selected trees, except after August 2010 for tree 409 (Figure 4.3). Mean soil moisture for the entire watershed ($n = 126$) was also higher than mean soil moisture around the selected trees, except after August 2010 for tree 409 (data not shown because of data gaps).

The standard deviation of soil moisture over the measurement period was consistently lower below all trees than for the watershed (Figure 4.4). This means there was less spatial variation in soil moisture below the trees, regardless of mean soil moisture. The standard deviation of soil moisture below the trees during dry periods is on the order of the measurement precision (1-2 %), which means there is no measurable spatial variation in soil moisture.

4.5.2. Soil moisture patterns around individual trees

4.5.2.1. Tree 601

When the measurements started in June 2010, average soil moisture within 60 cm of the tree was higher than average soil moisture further from the tree (Figure 4.5b). After stemflow was removed from the tree and directed downslope, soil moisture near the tree was equal to or slightly less than average soil moisture further away from the tree. However, none of these visual differences in mean soil moisture were statistically significant. The measurements were stopped for the excavation in September 2010. Thus, it is unknown if average soil moisture within 60 cm of the tree would have become higher than average soil moisture further from the tree as soil moisture increased again in the fall or if this was strictly a change due to the redistribution of stemflow.

Before stemflow was redirected downslope, average soil moisture upslope and downslope from the tree were not significantly different, except for upslope transect 2 (UT2), which had a higher mean soil moisture than the other downslope transects (Figure 4.6b). This difference in soil moisture was statistically different for 1 of 2 measurement periods. When stemflow was redirected downslope, average soil moisture downslope from the tree was higher than average soil moisture upslope. These differences in soil moisture were statistically significant for 12 of the 14 measurement periods for upslope transect 1 (UT1) compared to downslope transect 1 (DT1) and for 9 of the 14 measurement periods for upslope transect 2 (UT2) compared to downslope transect 2 (DT2; Figure 4.6).

One location close to the tree and downslope from the tree consistently had higher soil moisture than average (Figure 4.7a). This is the location where stemflow input was redirected to the tipping bucket and concentrated. Locations that were drier than average were all located upslope from the tree.

4.5.2.2. Tree 411

Average soil moisture within 60 cm of tree 411 was consistently lower than average soil moisture further from the tree (Figure 4.5c). These differences in soil moisture were statistically significant for 11 of the 20 measurement periods (Figure 4.5). Average soil moisture for the transect downslope (to the stream; DST) was consistently lower than average soil moisture for the upslope transects (Figure 4.6c; UT), although they were significantly different for only 1 measurement period. Average soil moisture downslope from the tree in the overall watershed direction (DWT) was not significantly different from average soil moisture upslope from the tree (Figure 4.6c). Mean difference analysis also showed that locations close to the tree were drier than average (Figure

4.7b). The locations with above average soil moisture were all located more than 1 meter away from the tree (Figure 4.7b).

4.5.2.3. Tree 409

When the measurements started in June 2010, average soil moisture within 60 cm of the tree was lower than average soil moisture further from the tree (Figure 4.5d). However, as the soil dried out, this trend was reversed and average soil moisture near the tree became higher than further away from the tree. At the end of September, the trend reversed again and average soil moisture near the tree was once again lower (Figure 4.5d). However, none of these visual differences were statistically significant.

Average soil moisture downslope from the tree (DWT and DST) was generally lower than average soil moisture upslope from the tree (UT), as for tree 411 (Figure 4.6d). Differences in soil moisture were statistically significant for 12 of the 21 measurement periods in the watershed downslope direction (DWT) and for 4 of 21 measurement periods for the downslope direction to the stream (DST; Figure 4.6). Mean difference analysis also showed that the downslope transect (DWT) was consistently drier than average and that one location upslope from the tree that was consistently wetter than average (Figure 4.7c).

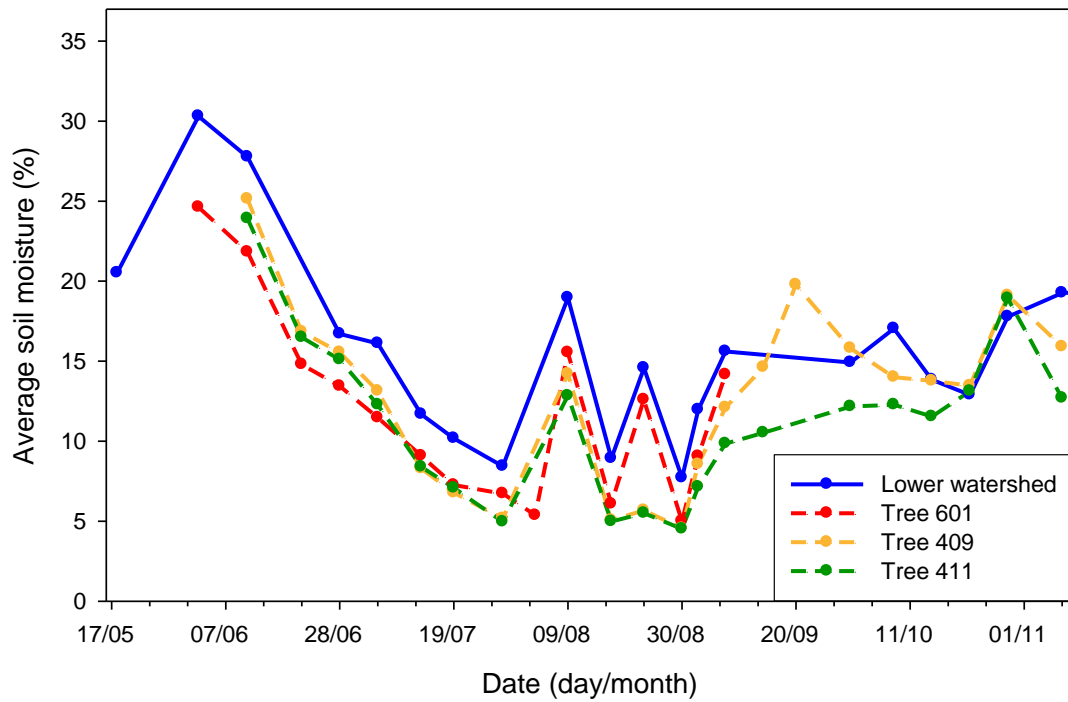


Figure 4.3: Average soil moisture below the trees compared to mean soil moisture in the lower watershed (n = 27).

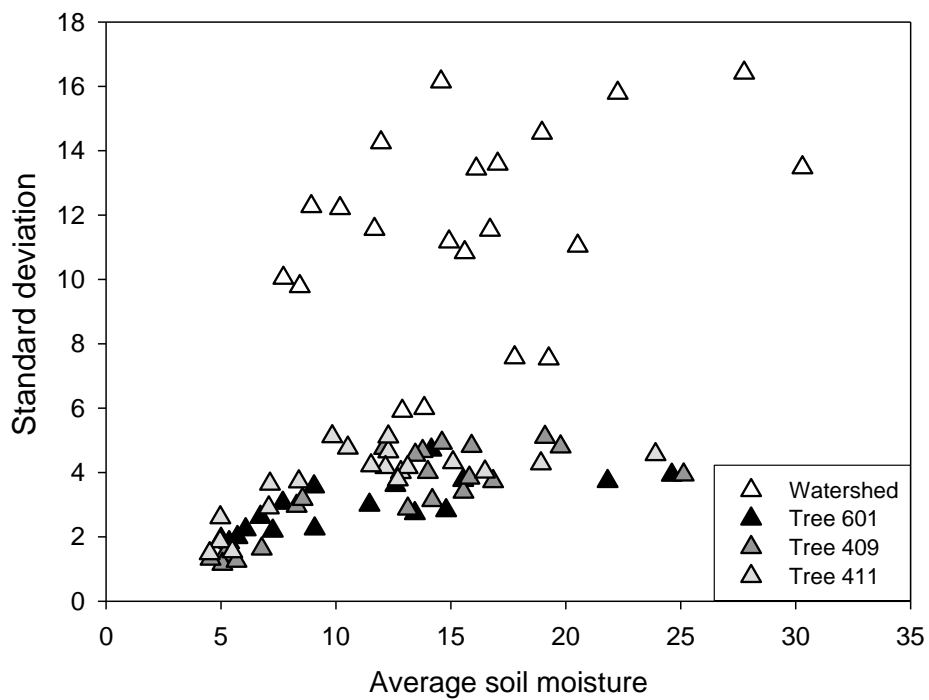


Figure 4.4: Standard deviation of soil moisture as a function of average soil moisture for all trees and the lower watershed (n = 27).

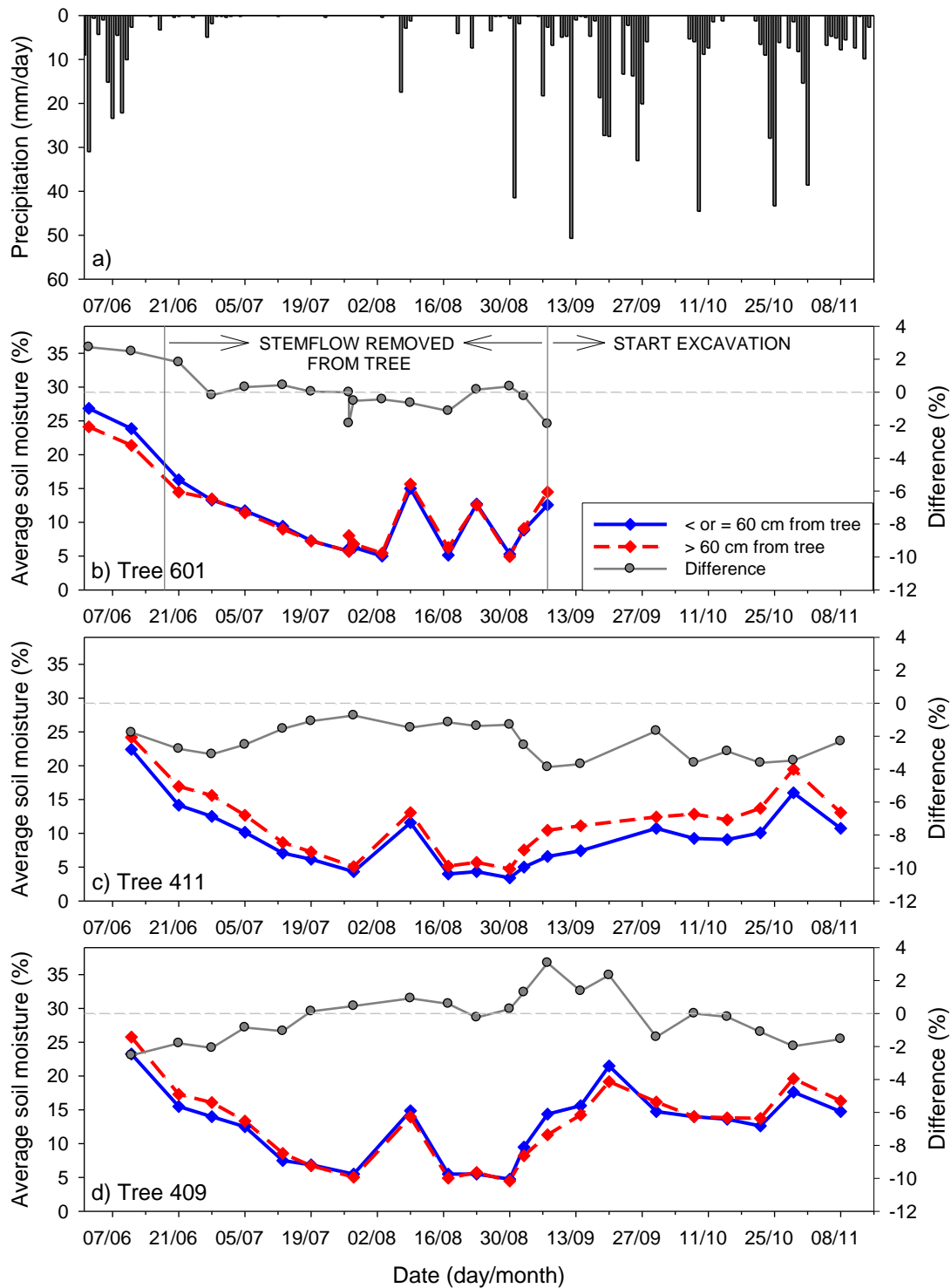


Figure 4.5: Average soil moisture near the tree and away from the tree for each tree as a function of time. Blue solid line = soil moisture points within 60 cm of the tree. Red dashed line = soil moisture points more than 60 cm from the tree. Grey line = the difference between average soil moisture near the tree and away from the tree. * = statistically significant differences.

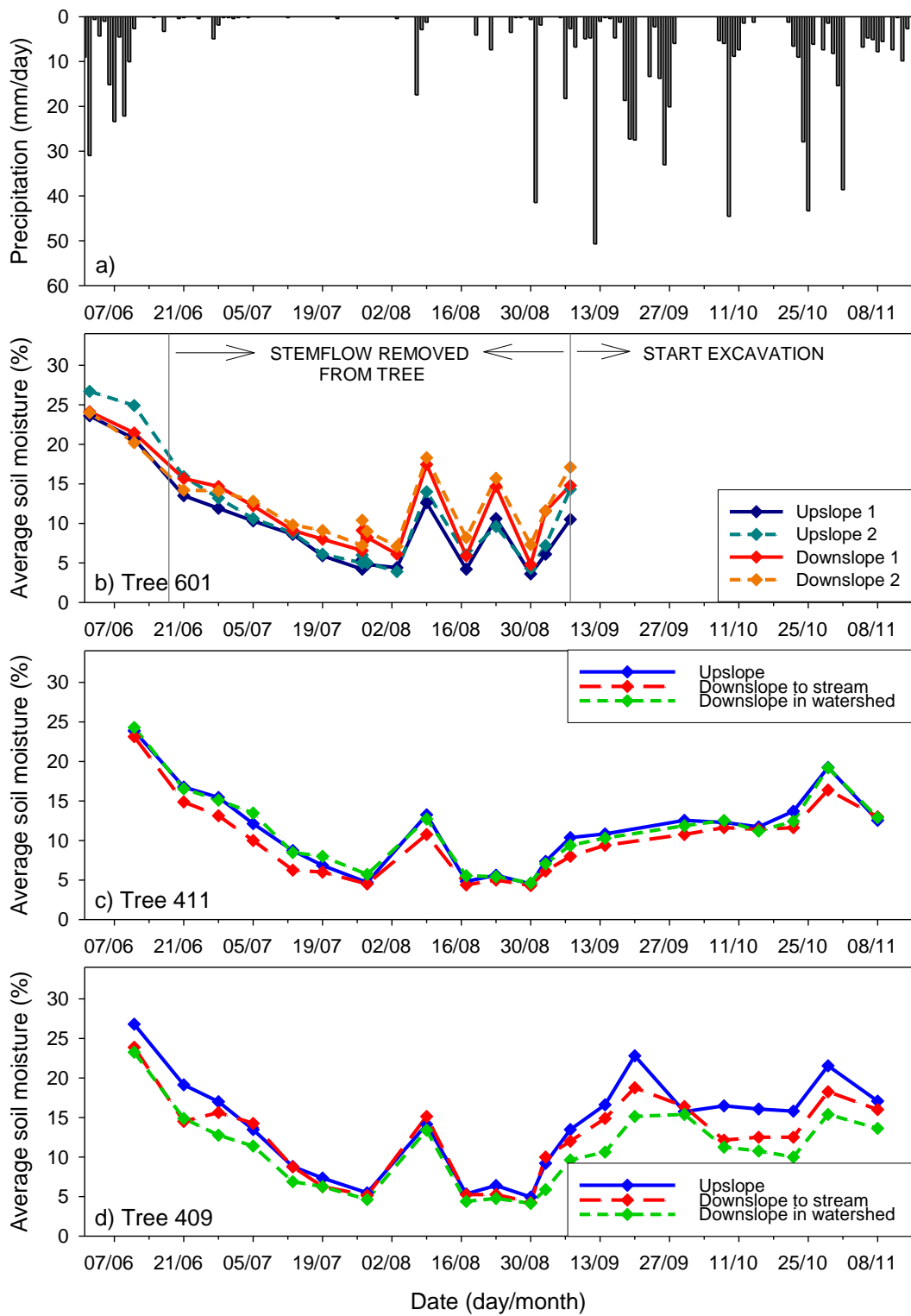


Figure 4.6: Time series of precipitation and average soil moisture for each tree by slope position. (Statistically significant differences: * = for DWT; x = for DST; ● = for UT1/DT1; ○ = for UT2 and DT2)

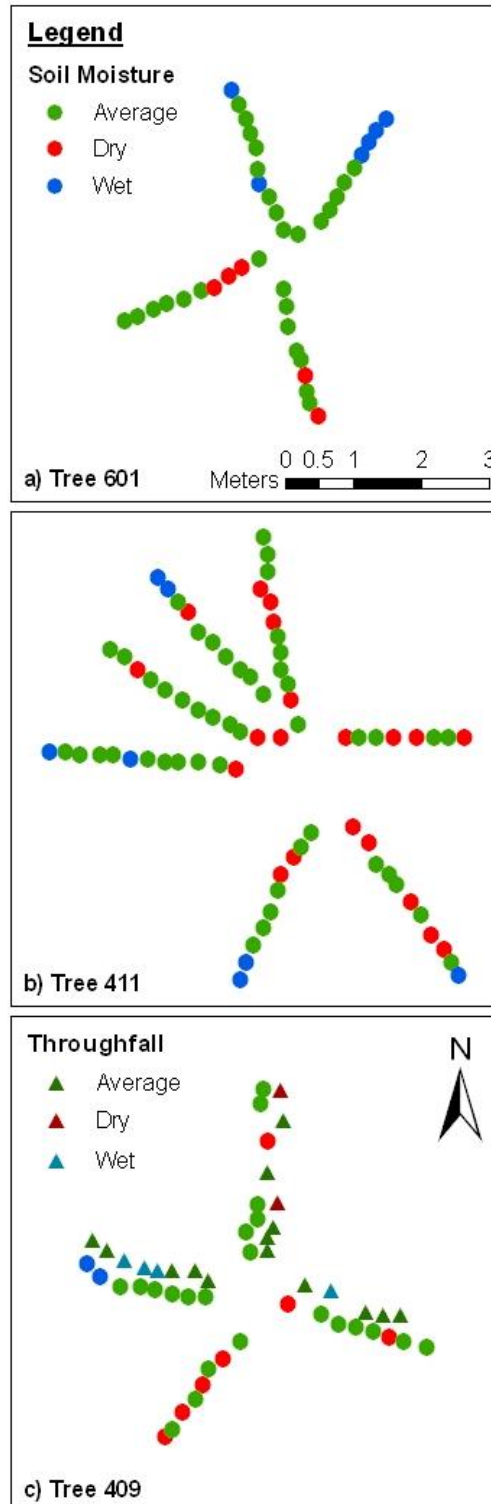


Figure 4.7: Spatial patterns in soil moisture (circles) and throughfall (triangles) patterns for the 3 trees. Red circles (triangles) are locations where the mean difference plus one standard deviation was below zero, and are thus considered dry locations. Blue circles (triangles) are locations where the mean difference minus one standard deviation was above zero, and are thus considered wet locations. Green circles (triangles) are locations with soil moisture/throughfall around the mean.

Table 4.1: Spearman rank correlation coefficient (r_s) for throughfall (TF) and soil moisture (Θ) change, and significance (p value) of the correlation for tree 409. None of the correlations were significant.

| Measurement Date | Measurement Period (Days) | Precip to Θ Measurement Lag (Days) | Total Precip (mm) | Median TF (mm) | Mean TF (mm) | Median Θ Before (%) | Median Θ After (%) | Δ Median Θ | Mean Θ Before (%) | Mean Θ After (%) | Δ Mean Θ | r_s | p |
|------------------|---------------------------|---|-------------------|----------------|--------------|----------------------------|---------------------------|--------------------------|--------------------------|-------------------------|------------------------|-------|------|
| 21/06/2010 | 10 | 0 | 4 | 2 | 2 | 25 | 16 | -9 | 25 | 17 | -8 | -0.08 | 0.74 |
| 28/06/2010 | 7 | 0 | 7 | 5 | 5 | 16 | 16 | 0 | 17 | 16 | -1 | 0.03 | 0.90 |
| 05/07/2010 | 7 | 1 | 1 | 1 | 1 | 16 | 12 | -4 | 16 | 13 | -3 | 0.38 | 0.10 |
| 09/08/2010 | 12 | 0 | 22 | 20 | 20 | 5 | 14 | 9 | 5 | 14 | 9 | -0.31 | 0.18 |
| 23/08/2010 | 6 | 1 | 12 | 9 | 9 | 5 | 5 | 0 | 5 | 6 | 1 | -0.20 | 0.40 |
| 02/09/2010 | 3 | 1 | 48 | 51 | 51 | 4 | 8 | 4 | 5 | 9 | 4 | 0.21 | 0.37 |
| 07/09/2010 | 5 | 0 | 21 | 21 | 21 | 8 | 11 | 3 | 9 | 12 | 3 | 0.32 | 0.17 |
| 14/09/2010 | 7 | 0 | 68 | 71 | 70 | 11 | 15 | 4 | 12 | 15 | 3 | -0.09 | 0.71 |
| 20/09/2010 | 6 | 0 | 70 | 64 | 65 | 15 | 20 | 5 | 15 | 20 | 5 | -0.38 | 0.10 |
| 30/09/2010 | 10 | 2 | 98 | 98 | 97 | 20 | 15 | -5 | 20 | 16 | -4 | 0.03 | 0.91 |
| 08/10/2010 | 8 | 0 | 6 | 7 | 7 | 15 | 13 | -2 | 16 | 14 | -2 | -0.23 | 0.34 |
| 15/10/2010 | 7 | 1 | 69 | 69 | 68 | 13 | 12 | -1 | 14 | 14 | 0 | 0.32 | 0.20 |
| 22/10/2010 | 7 | 1 | 8 | 5 | 5 | 12 | 12 | 0 | 14 | 13 | -1 | -0.25 | 0.30 |
| 29/10/2010 | 7 | 0 | 95 | 91 | 89 | 12 | 19 | 7 | 13 | 19 | 6 | 0.06 | 0.81 |
| 08/11/2010 | 10 | 0 | 83 | 75 | 74 | 19 | 14 | -5 | 19 | 16 | -3 | 0.03 | 0.90 |

4.5.3. Throughfall effects on soil moisture patterns

There was no relation between the spatial variation in throughfall input and the corresponding change in soil moisture. Locations where soil moisture changes were higher than average did not correspond with higher throughfall inputs, or vice versa (Figure 4.7). The Spearman rank correlation coefficient for the relation between throughfall and the change in moisture content varied between -0.38 and 0.38, but none of these relations were statistically significant (Table 4.1). To determine if evapotranspiration influenced the relation between throughfall input and change in soil moisture, the lag time (days) between the soil moisture measurements and the end of the event was determined. Measurement periods for which there was a negative relation between soil moisture change and throughfall input did not correspond to a longer time between soil moisture measurements and the end of the event. Other factors such as event size and antecedent moisture conditions also did not appear to be related to the r_s values (Table 4.1).

4.6. Discussion

4.6.1. Stemflow effects on surface soil moisture patterns

4.6.1.1. Proximity to the tree

A consistent soil moisture pattern was not observed in this study. Soil moisture near the tree was generally lower than soil moisture further from the tree for trees 409 and 411. This corresponds to Ziemer (1968), who showed that plant water uptake caused lower soil moisture near the tree. The low standard deviation of soil moisture under the trees also suggests that evapotranspiration had a homogenizing effect on soil moisture. However, measurements around tree 409 show that during drier summer months, soil moisture was higher near the tree than further from the tree. This could be

evidence that the influence of stemflow on soil moisture is larger during drier periods than wetter periods (c.f. Pressland, 1976) and corresponds with other studies that have shown that the influence of stemflow on soil moisture is clearer for small events and in drier periods (D'Odorico et al., 2007; Liang et al., 2007; Li et al., 2009). For tree 601, soil moisture was initially higher near the tree, whereas after stemflow was redirected downhill there was no significant change in soil moisture with distance from the tree. These results correspond to other studies (Specht, 1957; Pressland, 1976; Durocher, 1990). Specht (1957), for example, found that shrubs were able to increase soil moisture directly below the shrubs due to stemflow and reduced evaporation due to shading.

Trees 411 and 409 are classified as “diverters” because their DBH is greater than or equal to 35 cm (52 cm and 46 cm, respectively). This may create a rain-shadow around the base of the tree due to the denser canopy at the centre of the tree and because less precipitation reaches the soil as stemflow. Tree 601 is a “funneler” (DBH = 29 cm) so it will funnel more precipitation to the soil than trees 411 and 409. Therefore, more water is being delivered to the base of the tree, which can infiltrate into the soil immediately next to the tree (Chapter 3; Voigt, 1960; Li et al., 2009) and cause the visually higher (although not significantly different) soil moisture near tree 601, which was not observed for trees 411 and 409 in wetter months.

4.6.1.2. Slope effects

In general, soil moisture was higher on the upslope side of the tree than on the downslope side (Figure 4.6 and Figure 4.7). Soil moisture around tree 411 was either higher upslope or similar upslope and downslope from the tree. Soil moisture upslope from tree 409 was higher during wet periods; soil moisture was similar upslope and downslope from tree 409 in dry periods. After stemflow was redirected to the downslope side of tree 601, mean soil moisture for both downslope transects was significantly

higher than for the upslope transects. The results mimicked the results from Liang et al. (2011), where the downslope side of the tree received more stemflow than the upslope side of the tree. Although the observed soil moisture patterns were not consistent across all trees, these results suggest that the side of the tree along which most of the stemflow occurs influences the soil moisture dynamics around a tree. The tendency of stemflow to flow on the upslope side of the tree (Chapter 2) may explain why soil moisture was lower on the downslope transects than on the upslope transects.

Trees 409 and 411 are diverters as discussed above, which means there is not much water being delivered to the base of the tree and there is little water to be redistributed downslope. Furthermore, stemflow would infiltrate vertically into the soil (possibly as bypass flow; Chapter 3) and then flow laterally downslope at the soil bedrock interface or other confining layers (Chapter 3). This would limit the effect of stemflow on surface soil moisture but could increase soil moisture at depth, which was not measured in this study.

4.6.2. The effects of throughfall patterns on soil moisture

For 5 of the 15 measurement periods, mean throughfall under tree 409 was greater than or equal to precipitation (Table 4.1). This is likely due to the concentration of throughfall at drip points, which could increase soil moisture beneath the tree canopy rather than close to the stem. These results are similar to Shachnovich et al. (2008) who showed that some of their throughfall collectors collected more than 100% of the measured precipitation and Alva et al. (1999) who also showed that throughfall at the drip line was often more than 100% of gross precipitation. However, Chin (2009) showed that for 53 storms between September 2007 and May 2009 throughfall was on average 85% of gross precipitation for this study site.

Mean difference results showed that for trees 409 and 411 soil moisture was highest 1 – 2 m from the tree (Figure 4.7). This corresponds with the outer edge of the tree canopy and thus, a potential drip line. Because both trees are larger hemlock trees, their branches would droop more at the edges rather than bend towards the tree trunk. This would cause the water to drip at the edges rather than to flow down the trunk as stemflow and cause an increase in soil moisture at these locations (Alva et al., 1999). However, higher throughfall did not correspond to larger increases in soil moisture (Figure 4.7). In fact, there was no relation between the change in soil moisture and incoming throughfall for tree 409 (Table 4.1).

It is clear from Figure 4.7c that the points where soil moisture was consistently high do not correspond to the points where throughfall was consistently high. Shachnovich et al. (2008) compared average net water added to their study site (average throughfall over 7 points minus transpiration) to the average change in soil water content (average for the same locations) for 5 precipitation events and found a correlation coefficient of 0.99. However, when throughfall and soil moisture at each location were compared for the five precipitation events, there was no relation. They suggested that this was due to lateral movement of water in the soil matrix and into surface depressions (Shachnovich et al., 2008).

Soil moisture was measured once a week or the day after a precipitation event. During this time, trees may have taken up some of the water from the surface layers where most of the fine, active roots are located (Chapter 3) and drainage and soil evaporation may have decreased soil moisture (Bouten et al., 1992). Tree roots grow preferentially in areas of higher soil moisture, which may result in more water uptake from these areas (Schume et al., 2003). For instance, Alva et al. (1999) showed that there was a higher density of citrus tree (*Citrus sinensis*) roots along the drip line and at

shallow depths, which led to a faster depletion of the soil water. Durocher (1990) showed that an even distribution of soil moisture returned 13 hours after precipitation ended. The low standard deviation of soil moisture (comparable to the precision of the measurements) at low soil moisture suggests that evapotranspiration has a homogenizing effect on soil moisture. Although most changes in soil moisture were positive after precipitation events, changes in mean or median soil moisture were negative for some large events (e.g. 15/10/10 and 8/11/10; Table 4.1). For the event on 15/10/10, there was 1 day between the end of the event and the soil moisture measurements. This is likely enough time for soil water drainage and plant water uptake to occur, which affects soil moisture (Bouten et al., 1992; Schume et al., 2003). For the event on 8/11/10, most of the precipitation in this measurement period occurred in the first few days (62 mm), followed by 3 days with no precipitation and little (< 7 mm/day) precipitation thereafter. In these 3 days of no precipitation soil water drainage and plant water uptake could have occurred, thereby masking the effects of throughfall on soil moisture. The precision of the soil moisture probe (1-2%) could also limit the relation between soil moisture and throughfall when soil moisture changes are small.

4.7. Conclusion

Several studies have shown the influence of stemflow on soil moisture patterns around a tree (Pressland, 1976; Li et al., 2009; Liang et al., 2011). In general, stemflow increases surface soil moisture close to the tree (Durocher, 1990) and below the tree (Specht, 1957; Liang et al., 2011), with the largest increases on the downslope side of the tree (Liang et al., 2009b; 2011). However, results of this study do not show similar or consistent soil moisture patterns.

Stemflow did not influence soil moisture within 60 cm of tree 411, or downslope from the tree. Results from tree 409 showed that when soils were moist (mean $\Theta > 7\%$), stemflow did not influence soil moisture close to the tree, however, when soils were dry, stemflow may have increased soil moisture within 60 cm of the tree. Both trees are classified as “diverters”, which means that less water reaches the ground as stemflow than would have reached the ground as incident precipitation, thus creating a rain-shadow rather than concentrating precipitation. Conversely, tree 601 is a “funneler” and before stemflow was redirected downslope, soil moisture was higher upslope than downslope. After stemflow was redirected, there was no consistent or significant difference in soil moisture with distance from the tree; soil moisture downslope of the tree was higher than upslope. These results suggest that the side of the tree along which most stemflow occurs influences the soil moisture dynamics around a tree.

Patterns of changes in soil moisture and throughfall were not related. Furthermore, locations where throughfall was consistently higher (lower) than average did not correspond to locations where soil moisture was consistently higher (lower) than average. This suggests that throughfall is redistributed vertically and laterally in the soil and soil properties influence soil moisture patterns more than throughfall at this scale.

5. Conclusion

Double funneling is the process of precipitation being funnelled through the tree canopy to the stem, being transmitted along the stem to the forest floor as stemflow, and the movement of that water into the soil through macropores and along tree roots (Johnson and Lehmann, 2006). Stemflow can therefore infiltrate deeper and faster into the soil than throughfall and significantly influence soil water dynamics (Liang et al., 2011). The objective of this study was to examine double funneling in a mature hemlock (*Tsuga heterophylla*)-red cedar (*Thuja plicata*) forest in coastal British Columbia (BC). For this study, the double funneling process was separated into 3 parts: stemflow, preferential flow, and soil moisture dynamics. The aim of the study was to determine how much stemflow occurs in the study site and if it influences subsurface flow pathways and surface soil moisture dynamics around the tree.

In Chapter 2, we showed that stemflow accounted for only 1% of incoming precipitation. Stemflow increased with precipitation but the amount of stemflow and funneling ratios depended on tree size. Trees with a DBH larger than or equal to 35 cm were categorized as “diverters”, which means less water reached the ground as stemflow than would have reached the ground as precipitation in the absence of trees. Trees with a DBH smaller than 35 cm were categorized as “funnelers”, which means more water reached the ground as stemflow than would have reached the ground as precipitation. This may be a way for small trees, which likely have shallower roots and therefore less access to deep soil water than larger trees, to survive during dry conditions. For some trees, peak stemflow intensities were higher than peak

precipitation intensities. Peak stemflow intensities did not depend on tree species or tree size but appear to be influenced by interaction with the canopy of surrounding trees. These results show that it is important to study stemflow from trees of various sizes and species.

In Chapter 3, we showed that stemflow did not result in overland flow and that (subsurface) lateral flow of stemflow water was limited to one meter from the tree. Furthermore, stemflow water was more frequently found at depth than at the soil surface and often flowed through preferential flow pathways around roots. Conversely, throughfall water decreased steadily with depth and flowed through the soil matrix and along fine and dead roots. Although stemflow water was not observed on the bedrock surface and the maximum infiltration depth was similar to throughfall, higher stemflow intensities than precipitation intensities may still cause enhanced groundwater recharge.

Chapter 4 focused on shallow soil moisture patterns and throughfall patterns around individual trees. The results showed that soil moisture on the downslope side of the tree was not higher than soil moisture on the upslope side, which may be due to stemflow primarily flowing on the upslope side of the tree. Two of the three studied trees were classified as stemflow diverters, which may also have limited the influence of stemflow on shallow soil moisture dynamics. Results also showed that soil moisture patterns around a tree were not related to the throughfall patterns. It is likely that soil moisture patterns in this forest are influenced more by plant water uptake, spatial variation in soil physical parameters, and vertical and lateral redistribution of soil water than water inputs from throughfall and stemflow. Furthermore, the results from Chapter 3 suggest that stemflow controls soil moisture dynamics deeper in the soil more than at the surface. Future studies on the effects of stemflow on soil moisture and soil nutrients should therefore focus on soil moisture and soil chemistry at depth rather than only at

the surface because it appears that stemflow has a limited influence on surface soil water dynamics.

The combined results of this study help us to better understand stemflow, unobservable subsurface flow pathways, and the resultant soil moisture dynamics in a mixed-species forest in coastal BC. It appears that double funneling does occur for Western hemlock trees; however, it is important to also study the other tree species in this forest to determine if the infiltration patterns and soil moisture dynamics are similar to the studied hemlock trees. It is possible that the results are different for other tree species with different rooting patterns. Furthermore, because stemflow preferentially flows on one side of the tree, blue dye should be applied only to that side of the tree to determine if the infiltration patterns observed in this study would occur in those conditions as well. Future research should also focus on deeper soil moisture dynamics. However, the small scale of the blue dye patches (Chapter 2) suggests that it will be difficult to measure changes in soil moisture content due to deep infiltration of stemflow water. It is also important to determine if trees are actually using stemflow as a water source, particularly in the dry season. Stemflow water with a different isotopic composition than soil water could be applied to a tree, and branches from that tree could later be analyzed for isotopic composition. In a forest with trees in close proximity to each other, the surrounding trees could also be sampled to determine if they are able to use stemflow from other trees.

References

- Aboal JR, Morales D, Hernandez M, and Jimenez MS. 1999. The measurement and modelling of the variation of stemflow in a laurel forest in Tenerife, Canary Islands. *Journal of Hydrology* **221** : 161-175.
- Alameda D, Villar R, Iriondo JM. 2012. Spatial pattern of soil compaction: Trees' footprint on soil physical properties. *Forest Ecology and Management* **283** : 128-137. DOI: 10.1016/j.foreco.2012.07.018.
- Allaire SE, Roulier S, and Cessna AJ. 2009. Quantifying preferential flow in soils: A review of different techniques. *Journal of Hydrology* **378** : 179-204. DOI: 10.1016/j.jhydrol.2009.08.013.
- Alva AK, Prakash O, and Fares A. 1999. Distribution of rainfall and soil moisture content in the soil profile under citrus tree canopy and at the dripline. *Irrigation Science* **18** : 109-115.
- Anderson AE, Weiler M, Alila Y, and Hudson RO. 2009. Dye staining and excavation of a lateral preferential flow network. *Hydrology and Earth System Sciences* **13** : 935-944.
- Bachmair S, Weiler M, and Nutzmann G. 2009. Controls of land use and soil structure on water movement: Lessons for pollutant transfer through the unsaturated zone. *Journal of Hydrology* **369** : 241-252. DOI: 10.1016/j.jhydrol.2009.02.031.
- Bogner C, Gaul D, Kolb A, Schmiedinger I, and Huwe B. 2010. Investigating flow mechanisms in a forest soil by mixed-effects modelling. *European Journal of Soil Science* **61** : 1079-1090. DOI: 10.1111/j.1365-2389.2010.01300.x.
- Bouten W, Heimovaara TJ, Tiktak A. 1992. Spatial patterns of throughfall and soil water dynamics in a douglas fir stand. *Water Resources Research* **28**(12) : 3227-3233.
- Cape JN, Brown AHF, Robinson SMC, Howson G, and Paterson IS. 1991. Interspecies comparisons of throughfall and stemflow at three sites in northern Britain. *Forest Ecology and Management* **46** : 165-177.
- Carlyle-Moses DE, Price AG. 2006. Growing-season stemflow production within a deciduous forest of southern Ontario. *Hydrological Processes* **20** : 3651-3663. DOI: 10.1002/hyp.6380.
- Chamberlin TW. 1972. Interflow in the mountainous forest soils of coastal British Columbia. In: Slaymaker O, McPherson HJ (Editors). *Mountain Geomorphology: Geomorphological Processes in the Canadian Cordillera, B.C.*, Tantalus Research, Ltd., Vancouver, B.C. pp. 121-127.

- Chang S-C, Matzner E. 2000. The effect of beech stemflow on spatial patterns of soil solution chemistry and seepage fluxes in a mixed beech/oak stand. *Hydrological Processes* **14** : 135-144.
- Chin KS. 2009. The effects of vegetation on the spatial distribution of soil moisture at the hillslope and catchment scale. MSc thesis from Simon Fraser University.
- Coenders-Gerrits AMJ, Hopp L, Savenije HHG, and Pfister L. 2012. The effect of spatial throughfall patterns at the hillslope scale. *Hydrology and Earth System Sciences Discussions* **9** : 8625-8663. DOI: 10.5196/hessd-9-8625-2012.
- Crockford RH, Richardson DP. 2000. Partitioning of rainfall into throughfall, stemflow and interception: Effect of forest type, ground cover and climate. *Hydrological Processes* **14** : 2903-2920.
- DeVries J, and Chow TL. 1978. Hydrologic behavior of a forested mountain soil in coastal British Columbia. *Water Resources Research* **14**(5) : 935-942.
- D'Odorico P, Caylor K, Okin GS, Scanlon TM. 2007. On soil moisture-vegetation feedbacks and their possible effects on the dynamics of dryland ecosystems. *Journal of Geophysical Research* **112** : G04010. DOI: 10.1029/2006JG000379.
- Duchon CE, Biddle CJ. 2010. Undercatch of tipping-bucket gauges in high rain rate events. *Advances in Geoscience* **25** : 11-15.
- Durocher MG. 1990. Monitoring spatial variability of forest interception. *Hydrological Processes* **4** : 215-229.
- Environment Canada Data. 2012. Canadian Climate Normals 1971 - 2000: Haney UBC RF Admin, British Columbia. Retrieved from: http://www.climate.weatheroffice.gc.ca/climate_normals/results_e.html?stnID=776&lang=e&dCode=1&StationName=HANAY&SearchType=Contains&province=ALL&provBut=&month1=0&month2=12. Accessed: Dec. 2012.
- Ford ED, Deans JD. 1978. The effects of canopy structure on stemflow, throughfall and interception loss in a young sitka spruce plantation. *Journal of Applied Ecology* **15** (3) : 905-917.
- Gaiser RN. 1952. Root channels and roots in forest soils. *Soil Science Society Proceedings*. 62-65.
- Germer S, Werther L, Elsenbeer H. 2010. Have we underestimated stemflow? Lessons from an open tropical rainforest. *Journal of Hydrology* **395** : 169-179. DOI: 10.1016/j.jhydrol.2010.10.022.
- Gersper PL, Holowaychuk N. 1971. Some effects of stem flow from forest canopy trees on chemical properties of soils. *Ecology* **52** (4) : 697-702.
- Gonzalez-Hidalgo JC, and Bellot J. 1997. Soil moisture changes under shrub cover (*rosmarinus officinalis*) and cleared shrub as response to precipitation in a semiarid environment: Stemflow effects. *Arid Soil Research and Rehabilitation* **11**(2) : 187-199.
- Habib E, Krajewski WF, Kruger A. 2001. Sampling errors of tipping-bucket rain gauge measurements. *Journal of Hydrologic Engineering* **6** (2) : 159-166.

- Haught DRW, van Meerveld HJ. 2011. Spatial variation in transient water table responses: differences between an upper and lower hillslope zone. *Hydrological Processes*. DOI: 10.1002/hyp.8354.
- Herwitz SR. 1986. Infiltration-excess caused by stemflow in cyclone prone tropical rainforest. *Earth Surface Processes and Landforms* **11** : 401-412.
- Herwitz SR, Levia DF. 1997. Mid-winter stemflow drainage from Bigtooth Aspen (populus grandidentata michx) in central Massachusetts. *Hydrological Processes* **11** : 169-175.
- Herwitz SR, Slye RE. 1995. Three-dimensional modelling of canopy tree interception of wind-driven rainfall. *Journal of Hydrology* **168** : 205-226.
- Hutchinson I, Roberts MC. 1981. Vertical variation in stemflow generation. *Journal of Applied Ecology* **18** (2) : 521-527.
- Johnson MS, Lehmann J. 2006. Double-funneling of trees: Stemflow and root-induced preferential flow. *Ecoscience* **13** (3) : 324-333.
- Jost G, Heuvelink GBM, Papritz A. 2005. Analysing the space-time distribution of soil water storage of a forest ecosystem using spatio-temporal kriging. *Geoderma* **128** : 258-273. DOI: 10.1016/j.geoderma.2005.04.008.
- Keim RF, Skaugset AE, Weiler M. 2005. Temporal persistence of spatial patterns in throughfall. *Journal of Hydrology* **314** : 263-274. DOI: 10.1016/j.jhydrol.2005.03.021.
- Levia DF, Frost EE. 2003. A review and evaluation of stemflow literature in the hydrologic and biogeochemical cycles of forested and agricultural ecosystems. *Journal of Hydrology* **273** : 1-29.
- Levia DF, Herwitz SR. 2005. Interspecific variation of bark water storage capacity of three deciduous tree species in relation to stemflow yield and solute flux to forest soils. *Catena* **64** : 117-137. DOI: 10.1016/j.catena.2005.08.001.
- Levia DF, Van Stan JT, Mage SM, Kelley-Hauske PW. 2010. Temporal variability of stemflow volume in a beech-yellow poplar forest in relation to tree species and size. *Journal of Hydrology* **380** : 112-120. DOI: 10.1016/j.jhydrol.2009.10.028.
- Li X-Y, Liu L-Y, Gao S-Y, Ma Y-J, Yang Z-P. 2008. Stemflow in three shrubs and its effect on soil water enhancement in semiarid loess region of China. *Agricultural and Forest Meteorology* **148** : 1501-1507. DOI: 10.1016/j.agrformet.2008.05.003.
- Li X-Y, Yang Z-P, Li Y-T, and Lin H. 2009. Connecting ecohydrology and hydrogeology in desert shrubs: stemflow as a source of preferential flow in soils. *Hydrology and Earth Systems Science* **13** : 1133-1144. DOI: 10.5194/hess-13-1133-2009.
- Liang W-L, Kosugi K, Mizuyama T. 2007. Heterogeneous soil water dynamics around a tree growing on a steep hillslope. *Vadose Zone Journal* **6** : 879-889. DOI: 10.2136/vzj2007.0029.
- Liang W-L, Kosugi K, Mizuyama T. 2009a. Characteristics of stemflow for tall stewartia (stewartia monadelphica) growing on a hillslope. *Journal of Hydrology* **378** : 168-178. DOI: 10.1016/j.jhydrol.2009.09.027.

Liang W-L, Kosugi K, Mizuyama T. 2009b. A three-dimensional model of the effect of stemflow on soil water dynamics around a tree on a hillslope. *Journal of Hydrology* **366** : 62-75. DOI: 10.1016/j.jhydrol.2008.12.009.

Liang W-L, Kosugi K, Mizuyama T. 2011. Soil water dynamics around a tree on a hillslope with or without rainwater supplied by stemflow. *Water Resources Research* **47** : W02541. DOI: 10.1029/2010WR009856.

Mahendrappa M. 1974. Chemical composition of stemflow from some eastern Canadian tree species. *Canadian Journal of Forest Research* **4** : 1-7.

Manfroi OJ, Koichiro K, Nobuaki T, Masakazu S, Nakagawa M, Nakashizuka T, Chong L. 2004. The stemflow of trees in a Bornean lowland tropical forest. *Hydrological Processes* **18** : 2455-2474. DOI: 10.1002/hyp.1474.

Martinez-Meza E, Whitford WG. 1996. Stemflow, throughfall and channelization of stemflow by roots in three Chihuahuan desert shrubs. *Journal of Arid Environments* **32** : 271-287.

MKRF. 2010a. Malcolm Knapp Research Forest: Location and Ecology. Retrieved from: <http://www.mkrf.forestry.ubc.ca/about/location-and-ecology/>. Accessed: January, 2010.

MKRF. 2010b. Malcolm Knapp Research Forest: History. Retrieved from: <http://www.mkrf.forestry.ubc.ca/about/history/>. Accessed: January, 2010.

Neal C, Robson AJ, Bhardwaj CL, Conway T, Jeffery HA, Neal M, Ryland GP, Smith CJ, Walls J. 1993. Relationships between precipitation, stemflow, and throughfall for a lowland beech plantation, Black Wood, Hampshire, southern England: Findings on interception at a forest edge and the effects of storm damage. *Journal of Hydrology* **115** : 51-63.

Niemczynowicz J. 1986. The dynamic calibration of tipping-bucket rain gauges. *Nordic Hydrology* **17** : 203-214.

Nikodem A, Kodesova R, Drabek O, Bubenickova L, Boruvka L, Pavlu L, Tejnecky V. 2010. A numerical study of the impact of precipitation redistribution in a beech forest canopy on water and aluminium transport in a podzol. *Vadose Zone Journal* **9** : 238-251. DOI: 10.2136/vzj2009.0083.

Onodera S, and Kobayashi M. 1995. Evaluation of seasonal variation in bypass flow and matrix flow in a forest soil layer using bromide ion. *Tracer Technologies for Hydrological Systems*. IAHS Publ. **229** : 99-107.

Onset Computer Corporation. 2005. RG3 and RG3-M data logging rain gauge user's manual.

Oyarzún CE, Godoy R, Staelens J, Donoso PJ, Verhoest NEC. 2010. Seasonal and annual throughfall and stemflow in Andean temperate rainforests. *Hydrological Processes*. DOI: 10.1002/hyp.7850.

Phillips FM. 2010. Soil-water bypass. *Nature Geoscience* **3** : 77-78.

Pressland AJ. 1976. Soil moisture redistribution as affected by throughfall and stemflow in an arid zone shrub community. *Australian Journal of Botany* **24** : 641-649.

- Raat KJ, Draaijers GPJ, Schapp MG, Tietema A, and Verstraten JM. 2002. Spatial variability of throughfall water and chemistry and forest floor water content in a Douglas fir forest stand. *Hydrology and Earth System Sciences* **6**(3) : 363-374.
- Schume H, Jost G, and Katzensteiner K. 2003. Spatio-temporal analysis of the soil water content in a mixed Norway spruce (*Picea abies* (L.) Karst.)-European beech (*Fagus sylvatica* L.) stand. *Geoderma* **112** : 273-287.
- Shachnovich Y, Berliner PR, and Bar P. 2008. Rainfall interception and spatial distribution of throughfall in a pine forest planted in an arid zone. *Journal of Hydrology* **349** : 168-177. DOI: 10.1016/j.jhydrol.2007.10.051.
- Sidle RC, Tsuboyama Y, Noguchi S, Hosoda I, Fujieda M, and Shimizu T. 2000. Stormflow generation in steep forested headwaters: a linked hydrogeomorphic paradigm. *Hydrological Processes* **14** : 369-385.
- Specht RL. 1957. Dark Island Heath (Ninety-Mile Plain, South Australia) IV. Soil moisture patterns produced by rainfall interception and stemflow. *Australian Journal of Botany* **5**(2) : 137-150. DOI: 10.1071/BT9570137.
- Taniguchi M, Tsujimura M, Tanaka T. 1996. Significance of stemflow in groundwater recharge. 1: Evaluation of the stemflow contribution to recharge using a mass balance approach. *Hydrological Processes* **10** : 71-80.
- Vaisala. n.d. Vaisala sensors for Vaisala MAWS101/201 Automatic Weather Stations. Vaisala Oyj. P.O. Box 26. FIN-00421 Helsinki, Finland.
- Van Elewijck L. 1989. Stemflow on maize: A stemflow equation and the influence of rainfall intensity on stemflow amount. *Soil Technology* **2** : 41-48.
- Van Stan JT, Siegert CM, Levia DF, Scheick CE. 2011. Effects of wind-driven rainfall on stemflow generation between codominant tree species with differing crown characteristics. *Agricultural and Forest Meteorology* **151** : 1277-1286. DOI: 10.1016/j.agrformet.2011.05.008.
- Voigt GK. 1960. Distribution of rainfall under forest stands. *Forest Science* **6** (1) : 2-10.
- Wang XL, Klinka K, Chen HYH, de Montigny L. 2002. Root structure of western hemlock and western red cedar in single- and mixed-species stands. *Canadian Journal of Forest Research* **32** : 997-1004. DOI: 10.1139/X02-026.
- Weiler M and Fluhler H. 2004. Inferring flow types from dye patterns in macroporous soils. *Geoderma* **120** : 137-153. DOI: 10.1016/j.geoderma.2003.08.014.
- Weiler M, and Naef F. 2003. An experimental tracer study of the role of macropores in infiltration in grassland soils. *Hydrological Processes*. **17** : 477-493.
- Xiao Q, McPherson EG, Ustin SL, Grismer ME, Simpson JR. 2000. Winter rainfall interception by two mature open-grown trees in Davis, California. *Hydrological Processes* **14** : 763-784.
- Ziemer RR. 1968. Soil moisture depletion patterns around scattered trees. *U.S. Forest Service Research Note PSW-166*.

Zinke, P.J. 1962. The pattern of influence of individual forest trees on soil properties.
Ecology **43** (1) : 130-133.

Appendices

Appendix A.

Matlab scripts

'Storm script'

```
%-----  
% Rainfall event identification script based on 1hour rainfall data  
%  
% Finds all hour intervals with rain  
% Divides the data into rain events by determing which hours with rain  
are  
% separated by a large enough number of hours from previous hours with  
rain  
% Finds which rain events are considered storms by determining if they  
% produce more than a certain depth of rain in a 24 hour period  
% Finds the peak rain intensity, average rain intensity and total  
rainfall  
% depth during each storm  
%  
% I. vanMeerveld 2011, annotated by E. Baird  
% Changed by Sheena Spencer  
% Changed again on June 24, 2011 by I van Meerveld  
%-----  
clear all  
% Change the directory  
cd 'E:\thesis stuff\Thesis Data\Stemflow_tree Data\Stemflow  
Intensities'  
% Load the raw hourly precipitation data  
load stemflowforstormsjune.txt  
Data = stemflowforstormsjune;  
%-----  
% Set the input variables  
  
% Raw data  
Date = Data(:,1); % excel date and time in number  
format  
Counter = Data(:,2); % Gives the position of data in the  
original  
% data matrix  
timestep=1; % 1 for hourly data. 0.25 for 15 min  
data.  
Rain = Data(:,3); % precipitation intensity in  
mm/timestep  
  
Stemflow = Data(:,4); % stemflow data  
% Set tolerance levels  
noraintime=12; % Required time in hours with no rain to  
separate  
% rain events  
minstormsize=2.5; % Minimum amount of cumulative rain in  
mm for the
```

```

% first day following the start of an
event
% for it to count as a storm
    minimumendrain=12; %number of hours of no rain to determine
end of storm %minimumendrain must be smaller or equal
to noraintime
%-----
% Find all the timeperiods that it rains
% Find the number of datasteps
    numhours=numel(Rain);
    j=1;
    % Start with the first data point and go to the last data point
    for i=1:numhours
        % Find if there was rain recorded
        if Rain(i)>0
            % If there was rain, record location in the original data
matrix of % the timestamp in a new matrix called rainhours
                rainhours(j,1)=Counter(i);
                j=j+1;
            end
        end
    % Find the number of rainy periods in the data set
    numrainhours=length(rainhours);
%-----
% Find all rain events
% Rain events are defined as rainy hours with a long enough number of
rain
% free hours since the previous rainy hour
% The number of rain free hours required is given by noraintime
    j=1;
% Start with the first rainy period and go to the last rainy period
    for i=2:numrainhours
        % Find the number of timesteps between successive rainy hours
        timesincelastrain=rainhours(i)-rainhours(i-1);
        % If the number of hours is longer than noraintime record the
position % in the original data matrix of the rainy hour in a new
matrix called % startnewevent
        if timesincelastrain>noraintime/timestep
            startnewevent(j,1)=rainhours(i);
            j=j+1;
        end
    end
end
% Find the number of rain events
    numevents=length(startnewevent);
%-----
% Find all the storms

```



```

% Storms are defined as rain events which produce minstormsize mm of
rain
% in their first day
    j=1;
% Start with the first rain event and go to the last rain event
    for i=1:numevents
        % Find the position in the original data matrix of the start of
the event
            m=startnewevent(i);
            n=m-1+(24/timestep);    %number of timesteps in 1 day
        % If the start time of the event is more than 1 day before the
last
the
        % datapoint recorded in the data set, create a matrix containing
the
        % rainfall data from the start hour of the event and the next day
            if n<numhours
                rainonselectedday=Rain(m:n);
            % Find the total daily rainfall
                totalrain=sum(rainonselectedday);
            % If the daily rainfall is greater than minstormsize, mark the
position in the original data matrix in a new matrix called startstorm
                if totalrain >= minstormsize
                    startstorm(j,1)=startnewevent(i)-1;
                    j=j+1;
                end
            else
        % If the start time of an event is less than a day before the last
% datapoint recorded in the data set, create a matrix containing
the
        % rainfall data from the start of the event to the last data point
            rainonselectedday=Rain(m:numhours);
        % Find the total rainfall in mm from the start of the event to the
% datapoint
            totalrain=sum(rainonselectedday);
        % If the rainfall during the given period is greater than
% minstormsize, mark the position in the original data matrix
in the startstorm matrix
            if (totalrain >= minstormsize)
                startstorm(j,1)=startnewevent(i)-1;
            end
        end
    end
end

% Find the number of storms
    numstorms=length(startstorm);

%find the end of each storm
    for i=1:numstorms-1
        % Find the position in the original data matrix of the start of the
% event
            m=startstorm(i);
            n=startstorm(i+1)-1; %the start of the next storm
            K=0;
            M=0;
            for j=m:n-1

```

```

        if Rain(j)==0
            if (K>=minimumendrain/timestep) %there need to be a
minimum number of hours with no rain to call it the end of the event
                endstorm(i)=j-minimumendrain/timestep;
                break
            else
                M=M+1;
            end
            K=K+1;
        else
            endstorm(i)=n;
            K=0;
        end
    end
end
%repeat for last event
for i=numstorms
    % Find the position in the original data matrix of the start of the
event
    m=startstorm(i);
    n=numhours;
    K=0;
    M=0;
    for j=m:n
        if Rain(j)==0
            if (K>=minimumendrain/timestep)
                endstorm(i)=j-minimumendrain/timestep;
                break
            else
                M=M+1;
            end
            K=K+1;
        else
            endstorm(i)=n;
            K=0;
        end
    end
end
endstorm=endstorm';
stormlength=endstorm-startstorm;

%-----
% Find the total rainfall during a storm
% Find the maximum rainfall intensity during a storm
% Find the average rainfall intensity during a storm including rain
free hours
for a=1:numstorms
    j=startstorm(a); % Find the start time of the storm
    k=endstorm(a); % Find the end of the storm
    if k>0 && j>0 % only do it if there is a well defined
start and end of the storm

        % Find the total rainfall in the original data matrix recorded
        % between the start of the storm and the end of the
        % storm and record it in the matrix totalP

```

```

        totalP(a)= sum(Rain(j:k));

        % Find the maximum rainfall intensity in the original data
matrix    % recorded between the start of the storm and the end of the
        % storm, and the time of the peak intensity
        [C,I] = max(Rain(j:k));

        % Create a matrix giving the time of the peak rainfall and a
matrix    % giving the peak rainfall intensity
        timepeakrain(a)=I+j-1;
        peakrain(a)=C;

        % Find the average rainfall intensity in the original data
matrix    % for all intensities recorded between the start of the storm
and        % the end of the storm
        averagerain (a)= mean(Rain(j:k));
        else
            totalP(a)=NaN;
            timepeakrain(a)=NaN;
            peakrain(a)=NaN;
            averagerain(a)=NaN;
        end
    end
end

% find when half of the total storm precip occurs
% centroid of rainfall
    for a=1:numstorms
        jj=startstorm(a);
        kk=endstorm(a);
        for d=jj:kk
            tt=sum(Rain(jj:d));
            if (tt>totalP(a)/2)
                r50(a)=d;
                break
            end
        end
    end
end

% Transpose the row matrices into column matrices
totalP=totalP';
timepeakrain=timepeakrain';
peakrain=peakrain';
averagerain=averagerain';
r50=r50';

%plot data with end and storm times
Y = zeros(numstorms,1);
figure(1)
plot (Counter,Rain, '-b')
hold on
plot (startstorm,Y, '*r',endstorm,Y, 'og', r50, Y, 'ys')
hold on

```

```

    plot (timepeakrain,peakrain,'sb')
    xlabel('Counter')
    ylabel('Precipitation (mm/hr)')
    xlim([0 numhours])
%-----
%-----
%find the start of stemflow for each storm
    for i=1:numstorms-1
        m=startstorm(i);
        if endstorm (i)+1/timestep<startstorm(i+1)
            n=endstorm(i)+1/timestep; %stemflow must at the latest
start within an hour after the end of the storm
        else
            n=startstorm (i+1)-1;
        end

        for j=m:n
            if Stemflow(j)>0
                startstemflow(i)=j;
                break
            else
                startstemflow(i)=NaN;
            end
        end
    end
%repeat for the last event
    for i=numstorms
        m=startstorm(i);
        if endstorm (i)+1/timestep<numhours
            n=endstorm(i)+1/timestep; %stemflow must at the latest
start within an hour after the end of the storm
        else
            n=numhours;
        end

        for j=m:n
            if Stemflow(j)>0
                startstemflow(i)=j;
                break
            else
                startstemflow(i)=NaN;
            end
        end
    end
    startstemflow=startstemflow';
%-----
%find the end of stemflow for each storm
    for i=1:numstorms-1
        % Find the position in the original data matrix of the start of
        % stemflow
        if startstemflow (i)>0 %only calculate if there is a well
defined start of the stemflow (if there is not start, there is no point
in calculating the end)
            m=startstemflow(i);

```

```

        n=startstorm(i+1)-1; %stemflow must end before the start
of the next storm at the latest
        K=0;
        M=0;
        for j=m:n
            if Stemflow(j)==0
                if (K>=minimumendrain/timestep)
                    endstemflow(i)=j-minimumendrain/timestep;
                    break
                else
                    M=M+1;
                end
                K=K+1;
            else
                endstemflow(i)=n;
                K=0;
            end
        end
    else
        endstemflow(i)=NaN;
    end
end
%repeat for last event
for i=numstorms
    % Find the position in the original data matrix of the start of the
    % event
    if startstemflow (i)>0
        m=startstemflow(i);
        n=numhours;
        K=0;
        M=0;
        for j=m:n
            if Stemflow(j)==0
                if (K>=minimumendrain/timestep)
                    endstemflow(i)=j-minimumendrain/timestep;
                    break
                else
                    M=M+1;
                end
                K=K+1;
            else
                endstemflow(i)=n;
                K=0;
            end
        end
    else
        endstemflow(i)=NaN;
    end
end
endstemflow=endstemflow';
%-----
% Find the total stemflow during a storm
% Find the maximum hourly stemflow intensity during a storm
% Find the average hourly stemflow intensity during a storm including
rain
% free hours

```

```

% Start with the first storm and go to the last storm
for a=1:numstorms
    j=startstemflow(a); % Find the start time of the storm
    k=endstemflow(a); % Find the end of stemflow
    if j>0 && k>0 % Only calculate if there is a well
defined start and end of stemflow response

        % Find the total stemflow in the original data matrix recorded
        % between the start and the end of the stemflow
        totalstemflow(a)= sum(Stemflow(j:k));
        % Find the maximum stemflow intensity in the original data
matrix
        % recorded between the start and the end of stemflow and
        % the time of the peak intensity
        [C,I] = max(Stemflow(j:k));
        % Create a matrix giving the time of the peak stemflow and a
matrix
        % giving the peak stemflow intensity
        timepeakstemflow(a)=I+j-1;
        peakstemflow(a)=C;

        % Find the average stemflow intensity in the original data
matrix
        % between the start and the end of the stemflow
        averagestemflow (a)= mean(Stemflow(j:k));
        else
            totalstemflow(a)=NaN;
            timepeakstemflow(a)=NaN;
            peakstemflow(a)=NaN;
            averagestemflow(a)=NaN;
        end
    end
end

%find when half of the total stemflow occurs
%centroid of stemflow
for a=1:numstorms
    jj=startstemflow(a);
    kk=endstemflow(a);
    x=totalstemflow(a);
    if jj>0 && kk>0 %only do these calculations if there is a
well defined start and end of stemflow
        if (kk-jj)>1/timestep && x>0 %stemflow must last for at
least 1 hour in order to calculate the centroid and total stemflow must
be larger than 0)
            for d=jj:kk
                tt=sum(Stemflow(jj:d));
                if (tt>totalstemflow(a)/2)
                    s50(a)=d;
                    break
                end
            end
        else
            s50(a)=NaN;
        end
    else
end

```

```

        s50(a)=NaN;
    end
end

% Transpose the row matrix into a column matrix
totalstemflow=totalstemflow';
timepeakstemflow=timepeakstemflow';
peakstemflow=peakstemflow';
averagestemflow=averagestemflow';
s50=s50';

%calculate lag times
peaklag=timepeakstemflow-timepeakrain;
startlag=startstemflow-startstorm;
centroidlag=s50-r50;

%plot stemflow data with end and storm times
Y=zeros(numstorms,1);
figure(2)
plot(Counter, Rain, '--b', Counter,Stemflow, '-r')
hold on
plot(startstorm,Y, '*b',endstorm,Y,
'ob',startstemflow,Y, '*r',endstemflow,Y, 'or', s50, Y, 'ys')
hold on
plot(timepeakstemflow,peakstemflow,'sb')
xlabel('Counter')
ylabel('Stemflow (mm/hr)')
xlim([0 numhours])

figure(3)
plot(totalP,totalstemflow,'*r')
xlabel('Total precipitation (mm)')
ylabel('Total stemflow (mm)')

figure(4)
plot(peakrain,peakstemflow,'*g')
xlabel('Peak precipitation (mm/timestep)')
ylabel('Peak stemflow (mm/timestep)')

figure(5)
plot(averagerain,averagestemflow,'*b')
xlabel('Average precipitation intensity(mm/timestep)')
ylabel('Average stemflow intensity(mm/timestep)')

figure(6)
boxplot([startlag,peaklag,centroidlag], 'notch', 'on', 'whisker',1)
ylabel('lagtime (timestep)')

%-----
%calculate coefficient of variation for each event - as a measure of
%peakiness.
for a=1:numstorms
    j=startstorm(a);
    k=endstorm(a);
    if k>0 && j>0

```

```

        meanP(a)=sum(Rain(j:k));
        stdevP(a)=std(Rain(j:k));
        CVP(a)=stdevP(a)/meanP(a);
    else
        meanP(a)=NaN;
        stdevP(a)=NaN;
        CVP(a)=NaN;
    end
end

for a=1:numstorms
    jj=startstemflow(a);
    kk=endstemflow(a);
    stemflowduration(a)=kk-jj;
    if (kk-jj)>1/timestep %stemflow must last for at least 1 hour
in order to calculate the stdev, mean and CV
        meanS(a)=sum(Stemflow(jj:kk));
        stdevS(a)=std(Stemflow(jj:kk));
        CVS(a)=stdevS(a)/meanS(a);
    else
        meanS(a)=NaN;
        stdevS(a)=NaN;
        CVS(a)=NaN;
        meanP(a)=NaN; %replace precip data also to NaN if there
is no corresponding data for stemflow (just so the same number of
datapoints show up in the boxplots)
        stdevP(a)=NaN;
        CVP(a)=NaN;
    end
end
CVratio=CVS./CVP;
figure (7)
boxplot([CVP',CVS'],'notch','on','whisker',1)
ylabel('Coefficient of variation')

figure (8)
boxplot (CVratio)
ylabel('ratio of coefficient of variation')
%-----
% calculate the amount of precip between the start of the storm and the
% start of stemflow
for a=1:numstorms
    j=startstorm(a);
    k=startstemflow(a);
    l=endstemflow(a);
    if j>0 && k>0
        if (l-k)>1/timestep %stemflow must last for at least 1
hour in order to count as a true stemflow event and to calculate precip
before stemflow starts
            Pbeforestemflow(a)=sum(Rain(j:k));
        else
            Pbeforestemflow(a)=NaN;
        end
    else
        Pbeforestemflow(a)=NaN;
    end
end

```



```

        end
    end

    figure (9)
    boxplot (Pbeforestemflow)
    ylabel ('Total precipitation before start of stemflow (mm)')

%-----
% Export the results to excel
    results=[startstorm, totalP, timepeakrain, peakrain, averagerain,
r50, stdevP', CVP', startstemflow, totalstemflow, timepeakstemflow,
peakstemflow, averagestemflow, s50, stdevS', CVS', CVratio', startlag,
peaklag, centroidlag, Pbeforestemflow'];
    xlswrite ('stormresults_110624.xls', results, 'tb301', 'A2');

```

'Cross-correlation script'

```
clear all
% Change the directory
cd 'E:\thesis stuff\Thesis Data\Stemflow_tree Data\stemflow timing\TB2'
% Load the 15 min storm and stemflow data
%load testforcrosscorrelation.txt
%Data = testforcrosscorrelation;
load TB2_storm1_1hr.txt
Data = TB2_storm1_1hr;
time= Data(:,1);      %date and time (counter)
counter= Data(:,2);   %counter
a= Data(:,3);         %first data series - precipitation
b= Data(:,4);         %second dataseries - 4=tree 301; 5=tree xxxx;
maxlag=24;            %maximum positive time shift for cross
correlation - in units of time step thus
                    %number of time steps that stemflow responds

after precip
maxneglag=12;        %maximum negative time shift for cross
correlation - units of time step thus
                    %number of time steps that stemflow responds

before precip
[m,n]=size(a);
[o,p]=size(b);
date = datenum('30-Dec-1899') + time;

figure (1)
plot (counter,a, '-*r',counter,b, '-ob')
grid on
xlabel('Time step')
ylabel('Precipitation or Stemflow (mm/timestep)')

figure (2)
plot (a,b, '-ob')
xlabel('Precipitation (mm/timestep)')
ylabel('Stemflow (mm/timestep)')

%calculate correlation coefficient for negative lag
%stemflow occurs before precip
lengthRR=maxneglag+1;
RR=zeros (lengthRR,1);
negativelag=[0:1:maxneglag]';
i=0;
for i=0:1:maxneglag
    newlengthb=o-i; %change length of b to account for shift in a
    bselect=b(1:newlengthb); %selected part of b to use in correlation
    starta=1+i;
    aselect=a(starta:m);
    j=i+1;
    RR(j)=corr(aselect,bselect,'type','Spearman');
    negativelag (j)=-i;
end

%calculate correlation coefficient for positive lag
lengthR=maxlag+1;
```

```

R=zeros (lengthR,1);
lag=[0:1:maxlag]';
i=0;
for i=0:1:maxlag
    newlengtha=m-i; %change length of a to account for shift in b
    aselect=a(1:newlengtha); %selected part of a to use in correlation
    startb=1+i;
    bselect=b(startb:o);
    j=i+1;
    R(j)=corr(aselect,bselect,'type','Spearman');
    lag (j)=i;
end
CorrelCoef=[RR;R]; %combine negative and positive lag data
Lag=[negativelag;lag]; %combine positive and negative lag data
[Rmax,q] = max(CorrelCoef) ; %find parameter set with max correl coeff
optimumlag=Lag(q) %value of lag that gives largest R value (in units of
time steps)
maxcorrel=Rmax

figure (3)
plot(lag, R, '-r*', negativelag, RR, '--r*')
hold on
plot (optimumlag, Rmax, 'bp', 'markersize',10)
xlabel ('lag (timesteps)')
ylabel ('Spearman correlation coefficient')
title(['Lagg time=', num2str(optimumlag),'timesteps'])

%check correlation for best fit
i=optimumlag;
if i<0
    newlengthb=o-i; %change length of b to account for shift in a
    bselect=b(1:newlengthb); %selected part of b to use in correlation
    starta=1+i;
    aselect=a(starta:m);
else
    newlengtha=m-i; %change length of a to account for shift in b
    aselect=a(1:newlengtha); %selected part of a to use in correlation
    startb=1+i;
    bselect=b(startb:o);
end

figure (4)
plot (aselect,bselect, 'or')
xlabel('Precipitation (mm/timestep)')
ylabel('Stemflow (mm/timestep)')
title(['Lagg time = ', num2str(optimumlag),' timesteps; Spearman rank
corr = ', num2str(maxcorrel)])

```

Appendix B.

Additional stemflow excavation figures

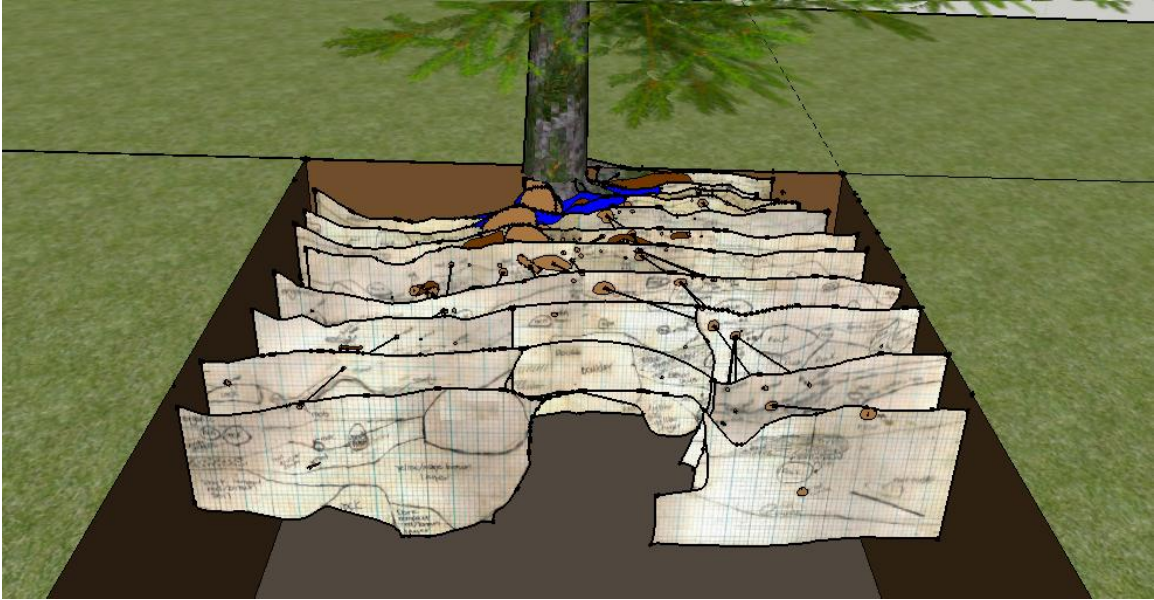


Figure 5.1: Layout of stemflow infiltration experiment 1. Grid on soil profile = 10 cm x 10 cm. Width of excavation is 3 m.

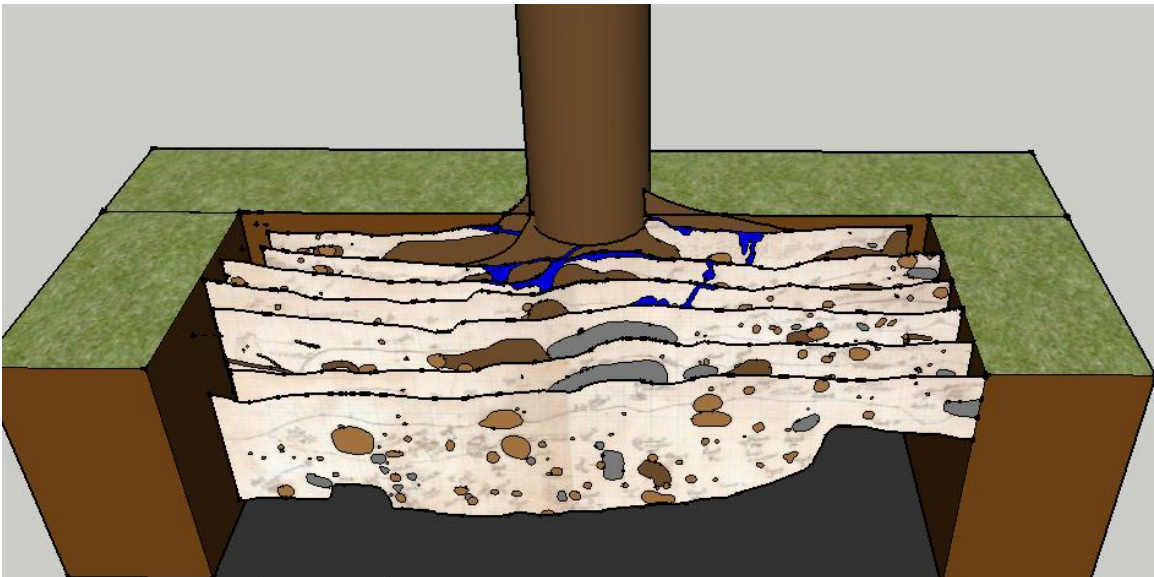


Figure 5.2: Layout of stemflow infiltration experiment 2. Width of excavation is 3 m.

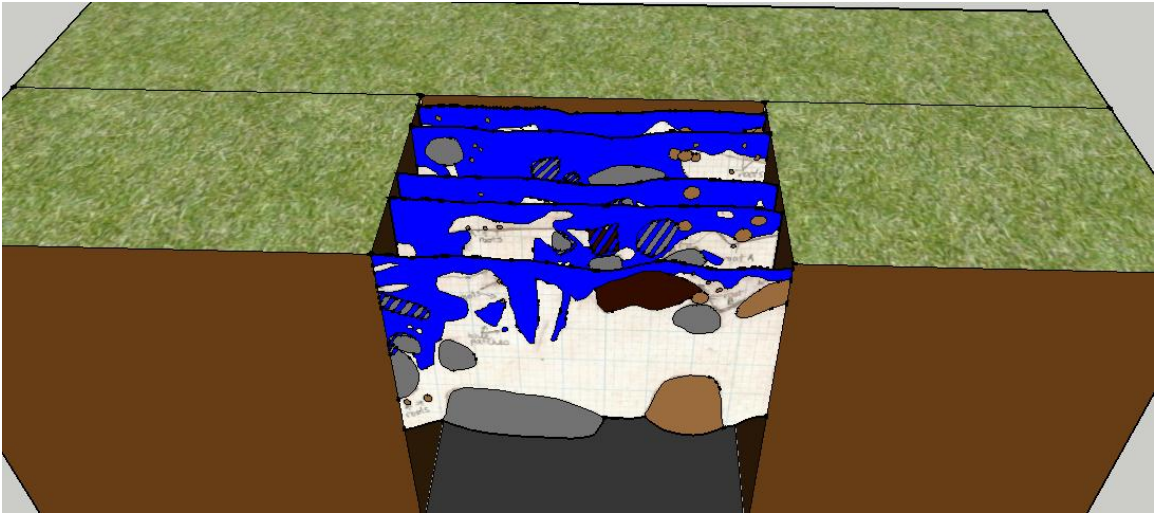


Figure 5.3: Layout of throughfall infiltration experiment. Width of excavation is 0.9 m.

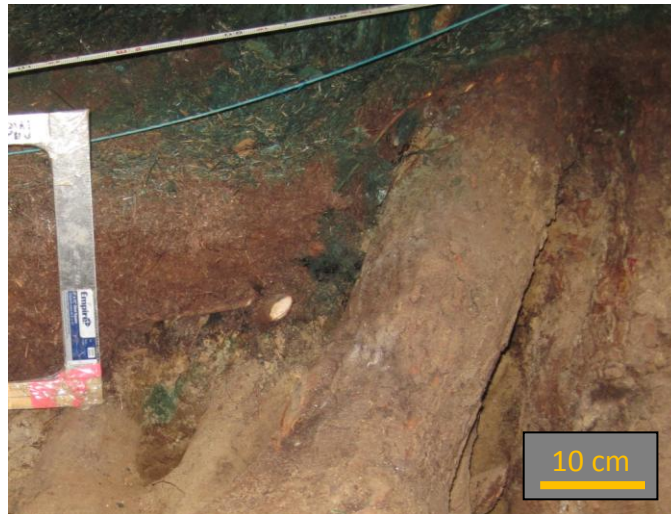


Figure 5.4: Stemflow infiltrating along the large root, in a loose organic layer in SIE 2.



Figure 5.5: Lateral flow along the confining clay layer (yellow arrows) in SIE 1.



Figure 5.6: Confined roots in SIE 2. (note: scale is distorted to right side of photo)



Figure 5.7: Fine roots in blue dye patches in TIE.

Appendix C.

Additional soil moisture figures

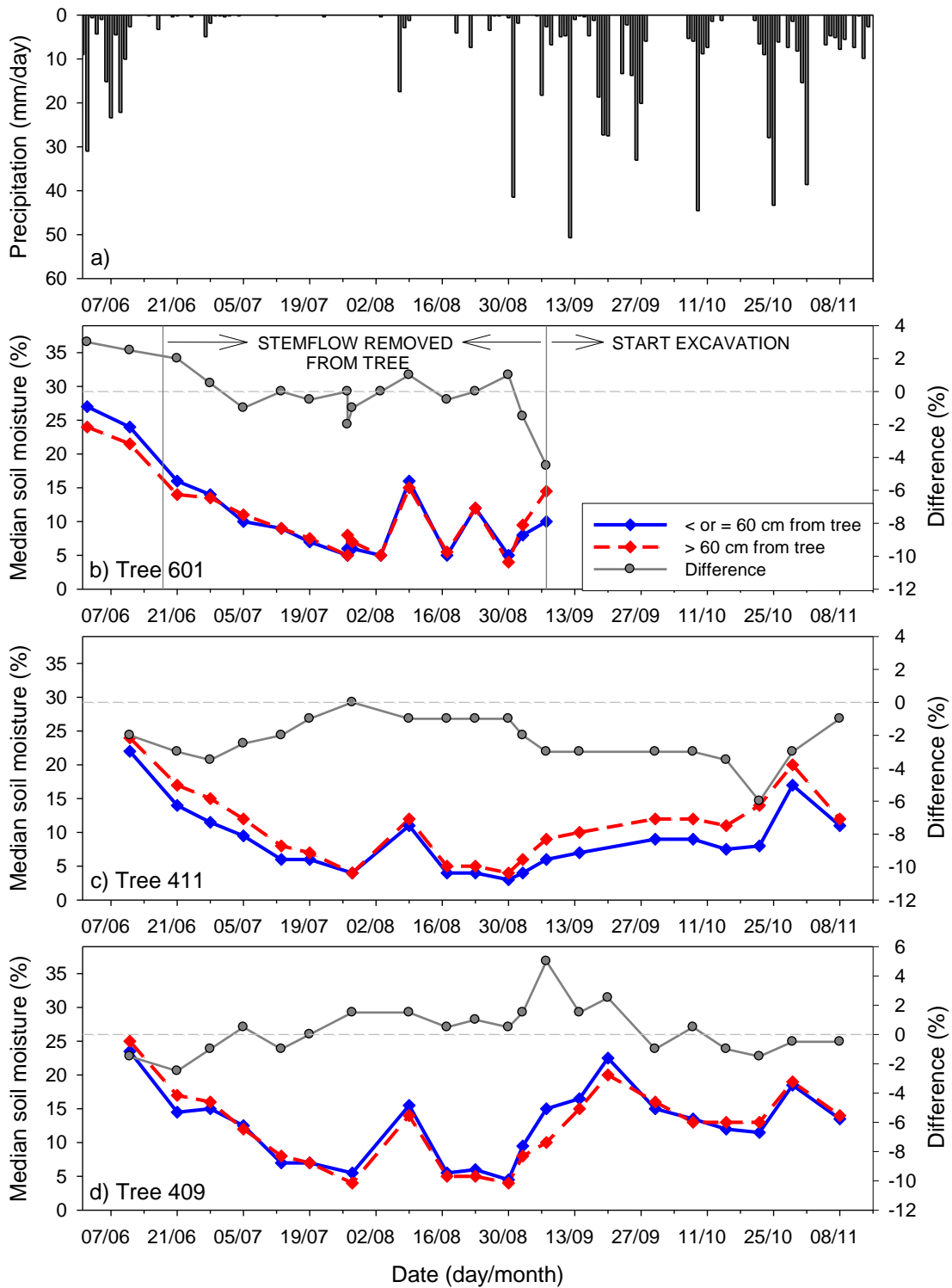


Figure 5.8: Median soil moisture for each tree as a function of time. Blue solid line = soil moisture points within 60 cm of the tree. Red dashed line = soil moisture points more than 60 cm from the tree.

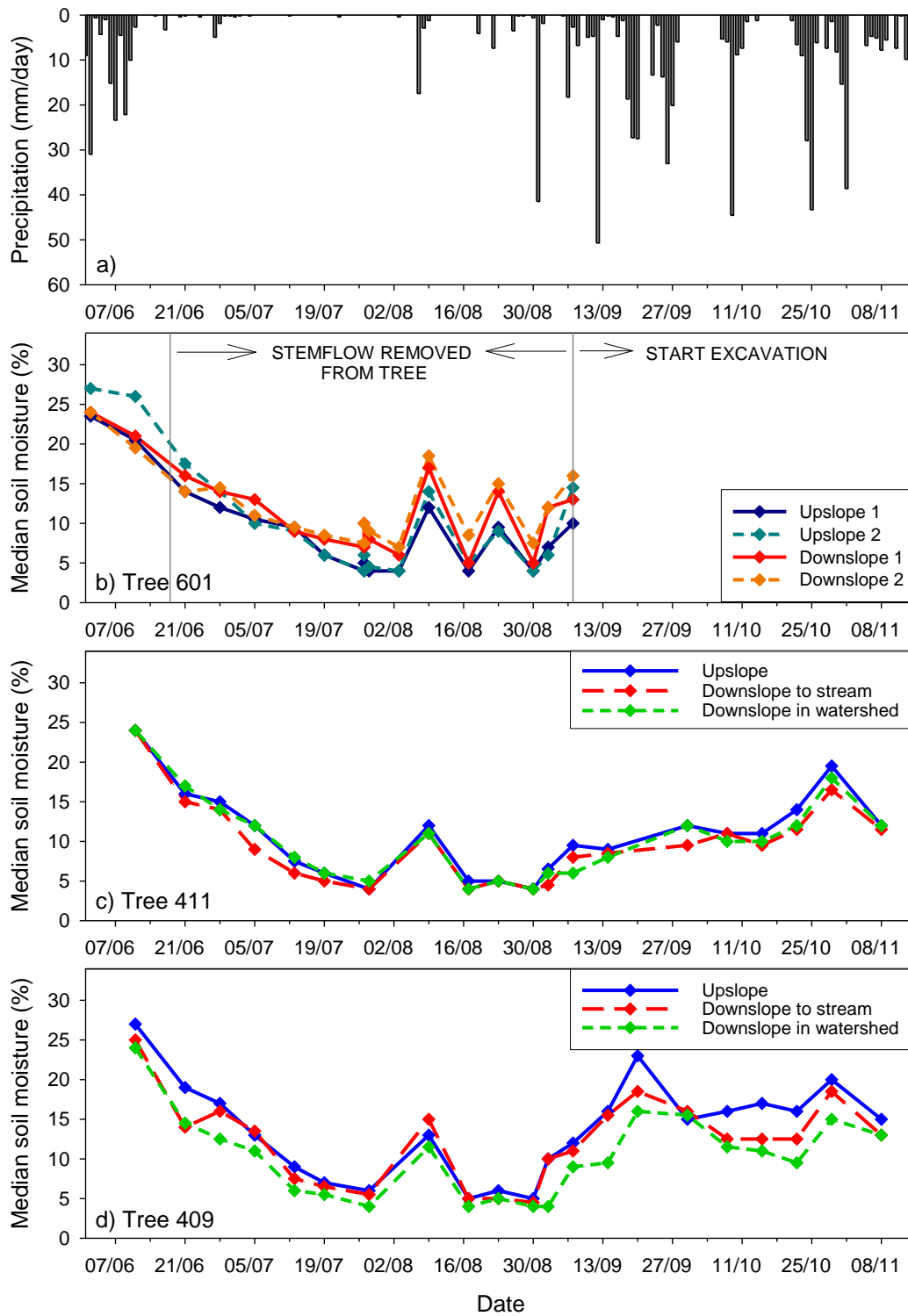


Figure 5.9: Time series of median soil moisture for each tree by slope location. For tree 601, solid blue line is for most upslope oriented transect (UT1) and solid red line is for the most downslope oriented transect (DT1).